

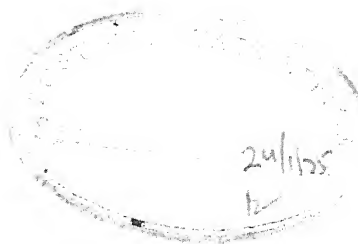
REACTION KINETICS IN THE SYSTEM $\text{Zr (Hf) Cl}_4\text{—NaCl}$

A Thesis Submitted
In Partial Fulfilment of the Requirements
for the Degree of
DOCTOR OF PHILOSOPHY

By
SIBNATH MAJUMDAR

to the

DEPARTMENT OF METALLURGICAL ENGINEERING
INDIAN INSTITUTE OF TECHNOLOGY KANPUR
DECEMBER, 1974



CERTIFICATE

Certified that this work on 'Reaction Kinetics In The System $\text{Zr(Hf)Cl}_4\text{-NaCl}$ ' has been carried out under our supervision and that it has not been submitted elsewhere for a degree.

(H.S. Ray)

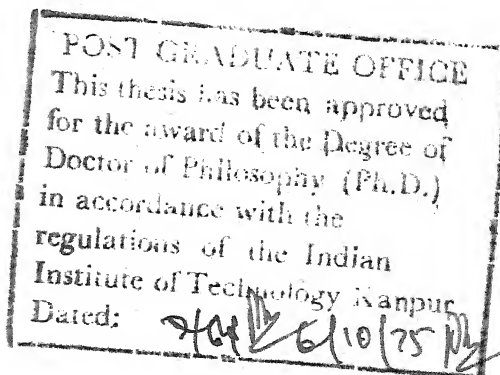
Assistant Professor
Department of Metallurgical
Engineering

Indian Institute of Technology
Kanpur 208016

(P.C. Kapur)

Associate Professor
Department of Metallurgical
Engineering

Indian Institute of Technology
Kanpur 208016



Acknowledgements

I take this opportunity to express my gratitude to Dr. H.S. Ray and Dr. P.C. Kapur for their valuable guidance and constant encouragement at all stages of this work.

I am particularly indebted to my friend Mr. Chandan Roy for his selfless help and cooperation. His assistance has been a source of inspiration at all crucial stages of this work. The valuable assistance provided by the various members of the glass blowing shop is also never to be forgotten. A special mention of Mr. R.K. Rajoria must be made without whose help the whole effort would have been defeating.

I am thankful to Drs. A. Ghosh, T.A. Ramnarayanan and D. Chakraborty for the useful discussions I had with them. I am indeed grateful to Dr. A. Ghosh and Mr. V.N. Sharma for providing me with various materials and instrumental facilities.

I am grateful to my friends Drs. S.P. Mehrotra, K.P. Jagannathan, Messers A. Ali, A. Sengupta, H.S. Maiti, K.L. Luthra and many others for their help in various ways. Finally, I wish to express my thanks to Mr. R.N. Srivastava for his flawless typing.

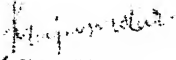

(S. Majumdar)

TABLE OF CONTENTS

LIST OF TABLES	vii
LIST OF FIGURES	viii
LIST OF SYMBOLS	xi
SYNOPSIS	xiv
CHAPTER 1 INTRODUCTION	1
1.1 General introduction	1
1.2 Chlorohafnates and zirconates of alkali metals	5
1.3 Methods for the separation of hafnium from zirconium	9
1.4 Kinetics of formation of chlorohafnates and chlorozirconates	15
1.5 Plan of the work	17
CHAPTER 2 HETEROGENEOUS SOLID-GAS REACTIONS	19
2.1 Introduction	19
2.2 Reaction models	20
2.3 Solid state transport controlled reactions	28
2.3.1 General consideration on solid state transport controlled reactions	29
2.3.2 Role of reaction parameters on reaction mechanism (lattice diffusion)	31
2.3.3 Marker studies	34
2.4 Phase boundary reactions	37

CHAPTER 3	EXPERIMENTAL	40
3.1	Introduction	40
3.2	General principle	40
3.3	Material preparation	42
3.3.1	Preparation of sodium chloride samples	42
3.3.2	Production and purification of the tetrachlorides	44
3.4	Kinetic measurement: apparatus and procedure	47
3.5	Measurement of tetrachloride partial pressure	51
3.5.1	Total pressure measurement	52
3.5.2	Sample collecting apparatus for the measurement of gas phase composition	54
3.6	Measurement of densities of reactants and products	57
CHAPTER 4	EXPERIMENTAL RESULTS AND DISCUSSION - I REACTIONS INVOLVING INDIVIDUAL GASES	58
4.1	Introduction	58
4.2	Swelling parameter, reactant and product density	58
4.3	Results of the kinetic measurements	59
4.4	Marker results	67
4.5	Kinetic models	70
4.6	Effect of reaction parameters on kinetics of reaction	84
4.6.1	Effect of sphere size	84
4.6.2	Effect of temperature	84
4.6.3	Effect of pressure	89

4.7	Diffusion mechanism	93
4.8	Reaction mechanism	99
CHAPTER 5	EXPERIMENTAL RESULTS AND DISCUSSION - II REACTION INVOLVING TETRACHLORIDE GAS MIXTURES	108
5.1	Introduction	108
5.2	Partial pressure of gases in tetrachloride mixture	108
5.3	Swelling parameter, reactant and product density	109
5.4	Results of the kinetic experiments	109
5.5	Outline of the approach to the kinetic analysis	113
5.6	Reaction model: formulation and analysis	115
5.7	Surface reaction	127
CHAPTER 6	CONCLUSIONS	130
	LIST OF REFERENCES	135
APPENDIX I	BASIC KINETIC DATA	141
A.	Formation of Na_2ZrCl_6	141
B.	Formation of Na_2HfCl_6	146
C.	Reaction with gas mixture	151
APPENDIX II	DATA AND CALCULATION: CHANGE IN PORE VOLUME	154

LIST OF TABLES

TABLE		PAGE
I	Important features of the systems $MCl-XCl_4$	4
II	Thermodynamic data for the formation of various hexachlorozirconates and hafnates	10
III	Swelling parameters and density values (formation of Na_2HfCl_6 and Na_2ZrCl_6)	59
IV	Carter-Valensi rate constants for the formation of Na_2ZrCl_6	82
V	Carter-Valensi rate constants for the formation of Na_2HfCl_6	83
VI	Partial pressure of the tetrachloride gas mixture	110
VII	Swelling parameter and product layer density (reaction with gas mixture)	110
VIII	Carter-Valensi rate constants for the formation of Na_2ZrCl_6 - Na_2HfCl_6 solid solution	126
IX	Product layer composition (calculated and measured) under various reaction conditions	128

LIST OF FIGURES

FIGURE		PAGE
1.	Phase diagram of the system NaCl-ZrCl_4	8
2.	Phase diagram of the system NaCl-HfCl_4	8
3.	Schematic representation of different solid-gas reactions	21
4.	Classification of various types of solid-gas reactions	24
5.	Sectional diagrams of moulds for the production of sodium chloride specimens (a. Sphere, b. Marker)	43
6.	Apparatus for the production of tetrachloride from oxide pellets	46
7.	Apparatus for kinetic experiments	48
8.	Apparatus for the measurement of total gas pressure	53
9.	Apparatus for collecting samples of tetrachloride gas mixture for determining the gas composition	55
10.	Effect of Sphere size on the rate of formation of sodium hexachloro zirconate	60
11.	Effect of sphere size on the rate of formation of sodium hexachloro hafnate	61
12.	Effect of pressure on the rate of formation of sodium hexachloro zirconate	63
13.	Effect of pressure on the rate of formation of sodium hexachloro hafnate	64
14.	Effect of temperature on the rate of formation of sodium hexachloro zirconate	65
15.	Effect of temperature on the rate of formation of sodium hexachloro hafnate	66

FIGURE

PAGE

16.	Macro-photograph of partially reacted marker specimen (reaction with zirconium tetrachloride vapour)	68
17.	Macro-photograph of partially reacted marker specimen (reaction with hafnium tetrachloride vapour)	69
18.	Plots of experimental data according to various rate equations (formation of Na_2ZrCl_6)	71
19.	Plots of experimental data according to various rate equations (formation of Na_2HfCl_6)	72
20.	Carter-Valensi plot showing the effect of sphere size on the rate of formation of Na_2ZrCl_6	75
21.	Carter-Valensi plot showing the effect of sphere size on the rate of formation of Na_2HfCl_6	76
22.	Carter-Valensi plot showing the effect of pressure on the formation of Na_2ZrCl_6	77
23.	Carter-Valensi plot showing the effect of pressure on the formation of Na_2HfCl_6	78
24.	Carter-Valensi plot showing the effect of temperature on the formation of Na_2ZrCl_6	79
25.	Carter-Valensi plot showing the effect of temperature on the rate of formation of Na_2HfCl_6	80
26.	Effect of sphere size on the rate constant K_{cv} (formation of Na_2ZrCl_6)	85
27.	Effect of sphere size on rate constant K_{cv} (formation of Na_2HfCl_6)	86
28.	Effect of temperature on rate constant K_{cv} (formation of Na_2ZrCl_6)	87
29.	Effect of temperature on rate constant K_{cv} (formation of Na_2HfCl_6)	88
30.	Effect of pressure on rate constant K_{cv} (formation of Na_2ZrCl_6)	91

FIGURE

PAGE

- | | | |
|-----|---|-----|
| 31. | Effect of pressure on rate constant K_{cv}
(formation of Na_2HfCl_6) | 92 |
| 32. | Schematic representation of outward diffusion
control case (Vacancy and interstitial
mechanism) | 97 |
| 33. | Effect of temperature on the rate of formation
of Na_2ZrCl_6 - Na_2HfCl_6 solid solutions (reaction
with gas mixture) | 111 |
| 34. | Effect of pressure on the formation of
Na_2ZrCl_6 - Na_2HfCl_6 solid solutions (reaction
with gas mixture) | 112 |
| 35. | Carter-Valensi plot showing the effect of
temperature on the rate of formation of
Na_2ZrCl_6 - Na_2HfCl_6 solid solutions | 124 |
| 36. | Carter-Valensi plot showing the effect of
pressure on the rate of formation of
Na_2ZrCl_6 - Na_2HfCl_6 solid solutions | 125 |

LIST OF SYMBOLE

C_j^k	Concentration of species j at interface k, mole/cm ³
c_j^k	Concentration of species j at interface k, number/cm ³
D	Diffusivity, cm ² /hr
D_0	Pre-exponential factor for diffusivity
E_d	Activation energy, kcal/mole
E_{App}	Apparent activation energy, kcal/mole
F	Fraction of solid (reactant) reacted
f	Stoichiometric factor (= 2)
ΔH	Enthalpy change, kcal/mole
J	Flux, number/hr
k_m	Mass transfer coefficient in gas phase, cm/hr
k_r	Specific rate constant for surface reaction, cm/hr
K	Specific rate constant (different cases, cases are defined by subscripts), hr ⁻¹
K_0	Constant (defined in Eq. [4.24])
K'	Equilibrium constant (different cases, cases are defined by subscripts)
K^*	Proportionality constant (Eq. [4.22] and [4.23])
M	Molecular weight

N_0	Avagadro number
P	Total pressure, mm Hg
p_j	Partial pressure of jth species, mm Hg
R_i	Radius of the unreacted core, cm
R_s	Radius of outer solid-gas interface, cm
R_0	Initial radius of solid reactant, cm
r	Radius at any cross-section, cm
ΔS	Entropy change, kcal/mole $^{\circ}K$
T	Temperature, $^{\circ}K$
t	Time, hr
V	Volume, cm^3
V_{Cl}^{\cdot}	Chlorine vacancy
V_{Na}'	Sodium vacancy
W	Weight gain, gm
W_{α}	Weight gain when entire solid has reacted, gm
Z	Swelling parameter (defined in Eq. [2.6])
ϕ	Fraction of reacted sodium chloride which reacts with hafnium tetrachloride (See Eq. [5.1])
σ	Volume of vacancy pair (V_{Cl}^{\cdot} and V_{Na}'), cm^3
ρ	Density, gm/cm^3
μ_s	Molar density of solid reactant, mole/ cm^3
θ	Temperature $^{\circ}C$

Subscripts

A	Species A
a	Adsorption reaction
g	Gas
i	Interstitial
p	Reaction product
r	Solid reactant
s	Surface reaction (Eq. [4.17])
ss	Solid solution forming reaction (Eq. [5.30])
v	Vacancy
vol	Volume

Superscripts

1	Interface 1
2	Interface 2
R_g	Outer solid-gas interface
R_i	Unreacted core-reaction product interface
b	Bulk gas phase
eq	Equilibrium

SYNOPSIS

REACTION KINETICS IN THE SYSTEM $\text{Zr(Hf)Cl}_4\text{-NaCl}$

A Thesis Submitted
In Partial Fulfilment of the Requirements
For the Ph.D. Degree

by
Sibnath Majumdar
to the
Department of Metallurgical Engineering
Indian Institute of Technology, Kanpur
December, 1974.

The kinetics of reaction of vapours of zirconium tetrachloride and hafnium tetrachloride with solid sodium chloride spheres, leading to the formation of sodium hexachloro zirconate (Na_2ZrCl_6) and hafnate (Na_2HfCl_6), respectively, have been studied in a closed system. Individual tetrachloride vapours (ZrCl_4 or HfCl_4) as well as their mixtures were employed as the gaseous reactant. The hexachloro compounds of zirconium and hafnium are important from the point of view of electrolytic extraction of zirconium and hafnium as well as for developing a method for the separation of hafnium from zirconium.

Experimental difficulties associated with handling of the tetrachloride gases precluded the use of conventional open systems and pan balance arrangements. Hence, the kinetic investigations, which forms the core of the present work, were conducted in an all-glass closed apparatus. The course of the reaction was followed by measuring the change in the weight of the reacting sodium chloride spheres by calibrated quartz springs. Inert marker experiments were also conducted to augment the formulation of reaction mechanisms.

The formation of the individual double salts i.e. sodium hexachloro zirconate and sodium hexachloro hafnate was studied as a function of the tetrachloride pressure, reaction temperature and sphere size. Under identical conditions the reaction with hafnium tetrachloride was invariably found to be slower.

In all cases the reaction occurred at a sharp interface. Accordingly, the kinetic data were tested against various appropriate heterogenous solid-gas kinetic models. Of these models, only the Carter-Valensi product phase-transport controlled model gave consistently good fit. The Carter-Valensi rate expression may be expressed as

$$\frac{Z - [1 + (Z-1)F]^{2/3} - (Z-1)(1-F)^{2/3}}{2(Z-1)} = K_{cv} t$$

where Z = Volume of product per unit volume of solid reacted

F = Fraction of solid reactant reacted

t = Reaction time

K_{cv} = Specific reaction rate constant

The failure of the other transport controlled models may be attributed mainly to the swelling of the sphere during the reaction. The swelling is appreciable in these solid-gas reaction systems. The Carter-Valensi specific reaction rate constant, K_{cv} , obtained by fitting the experimental data to the rate expression, has been employed to correlate the effect of the reaction temperature, the pressure and the sphere size with the kinetics on a consistent and comparable basis.

The reaction kinetics for formation of the two hexachloro compounds were studied in the pressure range of 250 to 1000 mm, Hg. The reaction temperature was varied in the range 425-500°C. Sodium chloride spheres of three different sizes, ranging from 3.3 to 6.1 mm radius, were used. The empirical relations representing the effects of various reaction parameters are as follows:

Effect of pressure, P: $K_{cv} \propto P^{1/n}$

where $n = 1.98$ for $ZrCl_4$ reaction, in the range 257 to 1013 mm, Hg and at 450°C.

$n = 2.13$ for $HfCl_4$ reaction, in the range 367 to 945 mm, Hg and at 450°C.

Effect of sphere size, R_o : $K_{cv} \propto \frac{1}{R_o^m}$

where $m = 1.92$ for $ZrCl_4$ reaction at 450°C and 745 mm, Hg pressure

$m = 2.12$ for $HfCl_4$ reaction at 450°C and 945 mm, Hg pressure.

The apparent activation energies for the formation of the two hexachloro compounds are:

Formation of Na_2ZrCl_6 : 7.5 Kcal/mole at 745 mm, Hg pressure and in the range of 425-500°C

Formation of Na_2HfCl_6 : 13 Kcal/mole at 945 mm, Hg pressure and in the range of 440-484°C.

The possible reaction mechanisms have been postulated in the light of the pressure and temperature dependence of the

specific rate constant and the inert marker experiments. On the basis of the experimental evidence, the transport of the chlorine ions from the unreacted core towards the outer product-gas interface appears to be the most likely reaction mechanism. The material transport presumably occurs by vacancy mechanism. In the range of the experimental conditions employed in the present investigation, the formation of both hexachloro zirconate and hexachloro hafnate conforms to the same reaction mechanism. However, there were indications to suggest that the reaction mechanism undergoes a change with change in the polymorphic form of the reaction product.

Some preliminary investigations on simultaneous formation of the hexachloro compounds were also carried out by reacting sodium chloride spheres with vapour mixtures of zirconium tetrachloride and hafnium tetrachloride. In these investigations, additional experiments were performed to ascertain the partial pressure of the reacting gas mixture. This was necessary, since the nature of the solution of the solid tetrachlorides, which produced the reaction vapour mixture, is not known. In order to determine the partial pressures of the two tetrachloride constituents of the reacting gas mixture, the composition of the gas phase and the total pressure were determined by separate experiments.

The kinetic data for the mixed gas reactions could also be fitted to the Carter-Valensi model and presumably is analogous to the reaction involving a single gas. The product

phase involved in this case is a solid solution of the two hexachloro compounds (Na_2ZrCl_6 and Na_2HfCl_6). There was indirect evidence to suggest that the composition remains uniform across the product layer i.e. the composition with respect to zirconium and hafnium does not change with position and time. A direct experimental evidence in this regard, however, could not be obtained. Attempts to conduct electron micro probe analysis across the product layer was foiled presumably due to steady evolution of gases from the specimen surface. Possibility of separation of zirconium from hafnium by kinetic means is also discussed in the light of the mechanism of the simultaneous formation of the two hexachloro compounds.

CHAPTER 1

INTRODUCTION

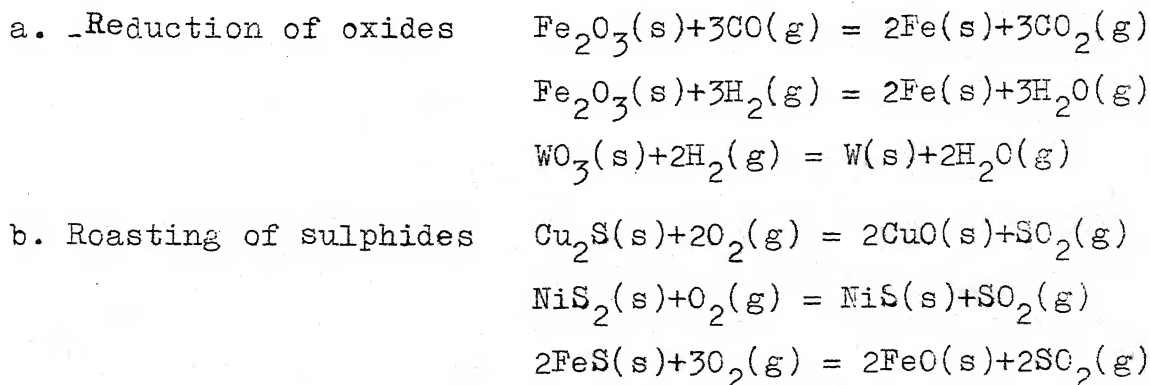
1.1 General introduction

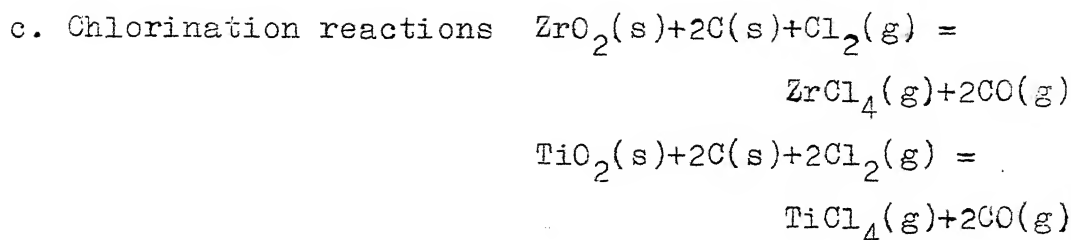
Solid-gas reactions are of great importance from both theoretical as well as practical points of view. These reactions may be classified into following groups.

1. Adsorption (physical and chemical)
2. Solid + Gas (I) = Gas (II)
3. Gas (I) = Solid + Gas (II)
4. Solid (I) + Gas = Solid (II)
5. Solid (I) = Solid(II) + Gas
6. Solid (I) + Gas (I) = Solid (II) + Gas (II)

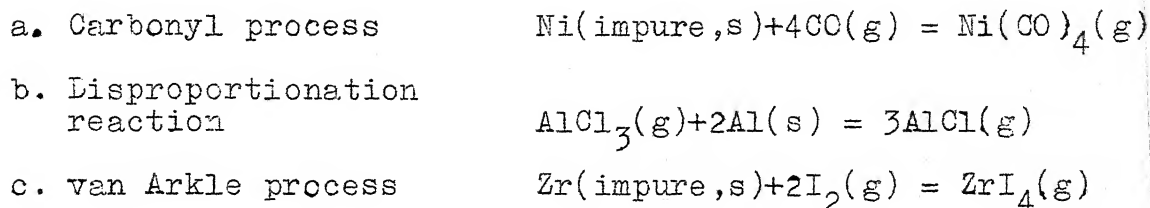
Such reactions are usually known as heterogeneous solid-gas reaction due to distinctive dissimilarities in phases. Heterogeneous solid-gas reactions form the basis of many technological processes. The following are a few examples.

1. Metal extraction:

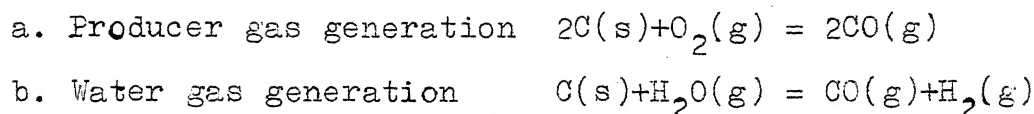




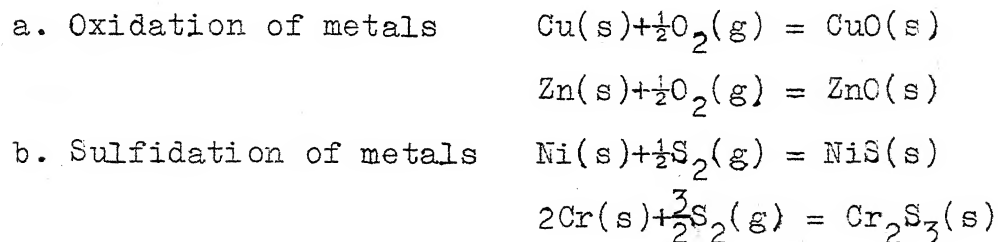
2. Metal refining:



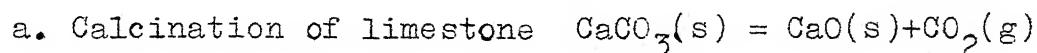
3. Gasification of solid fuels:



4. High temperature gas-metal reactions:



5. High temperature decomposition of compounds:



The scope of heterogeneous solid-gas reactions is obviously very wide and, accordingly, numerous publications are available on various aspects of this subject.

Heterogeneous reactions being studied in the present work are of significance in the extractive metallurgy of zirconium and hafnium. In comparison with usual oxidation-

reduction systems reported in the literature the present systems are considerably more complex. They also present unusual experimental difficulties.

The present study examines kinetic aspects of the formation of sodium hexachloro zirconate (Na_2ZrCl_6) and sodium hexachloro hafnate (Na_2HfCl_6). These ternary compounds form when tetrachloride vapours of zirconium and hafnium, respectively react with sodium chloride.

The hexachloro compounds of sodium as well as those of other alkali metals viz. K, Cs, Li etc., have received considerable attention in recent years in view of considerably lower vapour pressures compared to the pure tetrachlorides. These compounds, thus, represent a greatly stabilised form of the volatile tetrachlorides and, therefore, are of considerable interest as potential electrolytes for the extraction of zirconium and hafnium by fused salt electrolysis.¹

Moreover, for a given alkali metal, the hafnate is generally more stable than the zirconate. Accordingly, the equilibrium pressures of zirconium tetrachloride and hafnium tetrachloride over the double salts are different; the pressure of zirconium tetrachloride being higher. This difference in equilibrium vapour pressure of zirconium tetrachloride and hafnium tetrachloride over the corresponding hexachloro compounds indicates possibility of effecting separation of hafnium from zirconium. It is well known that for nuclear application zirconium should be free of hafnium. The maximum tolerable level

of hafnium is about 200 ppm². Hafnium is undesirable because of its extremely high neutron capture cross-section. This common impurity, however, is difficult to remove in view of the pronounced similarity in the chemical behaviour of these two elements. It may be possible to effect some separation using reaction of tetrachloride vapours with sodium chloride.³, Kinetic data for the formation reaction would also be useful from the point of view of production of these double salts. Moreover, the kinetics of formation of the compounds would be of much theoretical importance as well in view of certain characteristics such as swelling due to reaction, single phase-ternary compound formation etc.

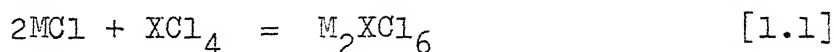
The present work is aimed at studying kinetic aspects of the following three heterogeneous solid-gas reaction systems.

- i) Zirconium tetrachloride (gas) - Sodium chloride (solid)
- ii) Hafnium tetrachloride (gas) - Sodium chloride (solid)
- iii) Mixture of zirconium tetrachloride and hafnium tetrachloride (gas) - Sodium chloride (solid)

The scope of a mechanistic analysis in all the three systems, however, is considerably limited due to total lack of information regarding the defect structures of the reaction products. No direct inferences can be made regarding transport phenomena in these compounds. In all cases, therefore, a conceptual approach has been adopted to analyse the experimental data.

1.2 Chloro-hafnates and zirconates of alkali metals

Hexachloro compounds of zirconium and hafnium of the general chemical formula M_2XCl_6 , where M stands for alkali metals (Li to Cs) and X stands for zirconium or hafnium, have been identified in several phase diagram studies of systems of the type $MCl-XCl_4$.^{1,5-10} Several alkaline earth metal chlorides, namely, $BaCl_2$ and $SrCl_2$ also form similar hexachloro compounds.¹ Reactions leading to the formation of double salts of alkali metals may be written as



The alkaline earth metal chlorides would react similarly.

The systems $NaCl-HfCl_4$, $KCl-ZrCl_4$, $KCl-HfCl_4$, $CsCl-ZrCl_4$ and $CsCl-HfCl_4$ were studied by Morozov and Sun In-Chzhu⁵ in almost the entire composition range. Howell, Sommer and Kellogg⁶ as well as Morozov and Korshunov⁷ have reported phase diagrams for the systems $NaCl-ZrCl_4$. Several additional studies on these systems are also available^{8,9}, which however, are mere exploratory in nature. These systems showed several common characteristics. In all the cases, two eutectics and a congruently melting compound, M_2XCl_6 , were observed. Additional ternary compounds were found in the high $ZrCl_4$ side of the systems $NaCl-ZrCl_4$ ^{6,7,10} and $KCl-ZrCl_4$.¹⁰ A list of the important features of this class of systems is given in Table I. Only those systems for which informations are available in the entire composition range are included in the Table. Phase diagrams of the systems

Table I. Important features of the systems MCl-XCl_4

System	Eutectic 1		Eutectic 2		Congruently melting compound, M_2XCl_6 (all at 66.7 mole percent)		Other compounds		
	Melting point $^{\circ}\text{C}$	Mole percent MCl	Melting point $^{\circ}\text{C}$	Mole percent MCl	Melting point $^{\circ}\text{C}$	Polymorphic transformation $^{\circ}\text{C}$	Compound	Melting point $^{\circ}\text{C}$	Mole percent MCl
NaCl-ZrCl_4 (Ref. 6)	548	72.0	314	37.6	646	-	NaZrCl_5 NaZr_2Cl_9	381 317	50.0 33.3
NaCl-ZrCl_4 (Ref. 7)	539	76.0	311	38.0	695	$\alpha \rightarrow \beta$ 341 $\beta \rightarrow \gamma$ 377	-	-	-
NaCl-ZrCl_4 (Ref. 10)	525 \pm 5	71.5	312 \pm 5	37.0	626 \pm 5	$\beta \rightarrow \alpha$ 382	Na_3ZrCl_7	535 \pm 5	72.0
NaCl-HfCl_4 (Ref. 11)	540	73.4	330	40.6	660	$\alpha \rightarrow \beta$ 384 $\beta \rightarrow \gamma$ 440 $\gamma \rightarrow \delta$ 484	-	-	-
KCl-ZrCl_4 (Ref. 11)	594	75.8	220	42.2	798	-	-	-	-
KCl-ZrCl_4 (Ref. 10)	600 \pm 5	77.0	225 \pm 4	35.0	790 \pm 5	-	$\text{K}_7\text{Zr}_6\text{Cl}_{11}$	565 \pm 5	52.0
KCl-HfCl_4 (Ref. 11)	604	77.6	242	38.0	802	a transformation at 550 $^{\circ}\text{C}$	-	-	-
CsCl-ZrCl_4 (Ref. 11)	572	84.8	286	22.8	805	-	-	-	-
CsCl-HfCl_4 (Ref. 11)	590	81.6	302	34.9	820	-	-	-	-

NaCl-ZrCl_4 and NaCl-HfCl_4 , which may be considered as representatives of this class of systems and eventually are of current interest, are shown in Figs. 1 and 2.

The $\text{MCl-M}_2\text{XCl}_6$ portion of such phase diagrams, in particular, have received considerable attention in recent years because of the technological importance of the compounds, M_2XCl_6 . This region of the phase diagram is characterised by phases with relatively low vapour pressures. The system, therefore, may provide a suitable electrolyte for electrolytic extraction of zirconium and hafnium metal.¹ The hexachloro compounds are also of interest from the point of view of separation of zirconium from hafnium. A suitable technique for separation may be developed based on the difference in the thermal stabilities of the hafnium and zirconium compounds. The thermal stability, which is characterised by the equilibrium vapour pressure of the tetrachloride over these compounds, was first investigated by Morozov and co-workers.¹¹ The vapour pressure data indicated increasing stabilities with increase in the ionic radii of the cations of the reacting metal chlorides. The order of stabilities was found to be: $\text{Cs}_2\text{ZrCl}_6 > \text{K}_2\text{ZrCl}_6 > \text{Na}_2\text{ZrCl}_6$. The same order prevailed for the hafnium compounds also. Dutrizac and Flengas¹ confirmed these findings later. Relative stability of zirconium and hafnium compounds of the same metal chloride was also reported by Morozov and co-workers.¹¹ The hafnium compounds were found to be more stable in all cases. Thermodynamic data pertaining to the formation of these

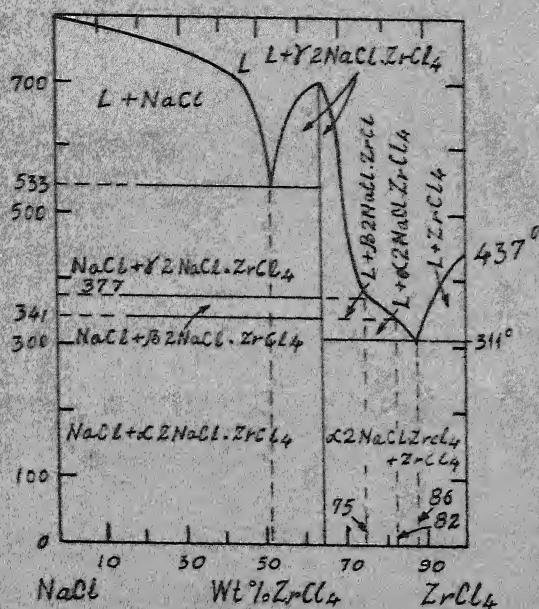


FIG. 1 PHASE DIAGRAM OF THE SYSTEM
NaCl-ZrCl₄ (from reference-7)

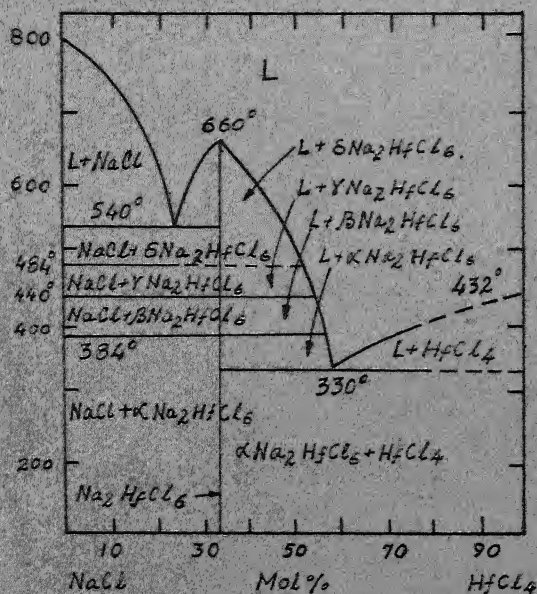


FIG. 2 PHASE DIAGRAM OF THE SYSTEM
NaCl-HfCl₄ (from reference-5)

compounds (solids only), produced by the reaction involving tetrachloride vapours and solid alkali metal chlorides, have been shown in Table II. Only those systems for which data are available for both the zirconium and the hafnium case, have been included in the table. For the sake of completeness, each pair of data (Zr and Hf) has been taken from the same source.

It may be noted that from the point of view of difference in the equilibrium vapour pressures of zirconium tetrachloride and hafnium tetrachloride over the corresponding double compounds cesium chloride should be most suitable for effecting separation. However, these salts would be too stable to allow recovery of zirconium and hafnium tied up in the salt during any process. Moreover, it would not be possible to recover the tied up zirconium and hafnium effectively by applying high temperature and high vacuum due to high vapour pressure of cesium chloride itself.

1.3 Methods for the separation of hafnium from zirconium

Some amount of hafnium, usually 2-3 per cent, is always present in the naturally occurring ores of zirconium. Due to its high thermal neutron capture cross-section, presence of hafnium, even in small amounts, is highly detrimental to zirconium for nuclear applications. The thermal neutron capture cross-section of hafnium is 105 barns^φ/atom compared to only 0.18

φ Barn is unit of area for nuclear cross-section.

1 barn = 10^{-24} cm²

Table II.

Thermodynamic data for the formation of various hexachloro zirconates and hafnates.

Compound	Temperature range, °C	Tetrachloride pressure over the compounds M_2XCl_6 , mm Hg	Free energy of formation cal/mole	Reference
Na_2ZrCl_6	432-630	$\log P = -\frac{5640}{T} + 8.54$	-25800 + 25.9T	Morozov and
Na_2HfCl_6	400-650	$\log P = -\frac{5690}{T} + 8.47$	-26000 + 25.6T	Toptygin ¹²
K_2ZrCl_6	650-790	$\log P = -\frac{11300}{T} + 13.4$	-51750 + 48.1T	Morozov and
K_2HfCl_6	700-790	$\log P = -\frac{11830}{T} + 13.33$	-54100 + 47.8T	Toptygin ¹²
Cs_2ZrCl_6	700-800	$\log P = -\frac{11360}{T} + 11.80$	-51900 + 40.8T	Morozov and
Cs_2HfCl_6	740-820	$\log P = -\frac{11930}{T} + 10.24$	-54500 + 33.7T	Toptygin ¹²
Li_2ZrCl_6	350-496	$\log P = -\frac{3970}{T} + 7.90$	-18200 + 23.0T	Dutrizac and
Li_2HfCl_6	350-500	$\log P = -\frac{3810}{T} + 7.57$	-17400 + 21.5T	Flengas ¹

barns/atom of zirconium.¹³ Consequently, a very high degree of separation is needed. The tolerance limit for nuclear grade zirconium is specified at 200 ppm of hafnium.² Due to pronounced chemical similarity of these two elements, such high degrees of separation can be attained only with special techniques. Extreme similarity in the chemical behaviour of zirconium and hafnium is attributed to the effects of the 'lanthanide contraction' on the ionic radius of hafnium.¹⁴ In fact, no two other elements in the Periodic Table present more difficulty in separation.¹⁴

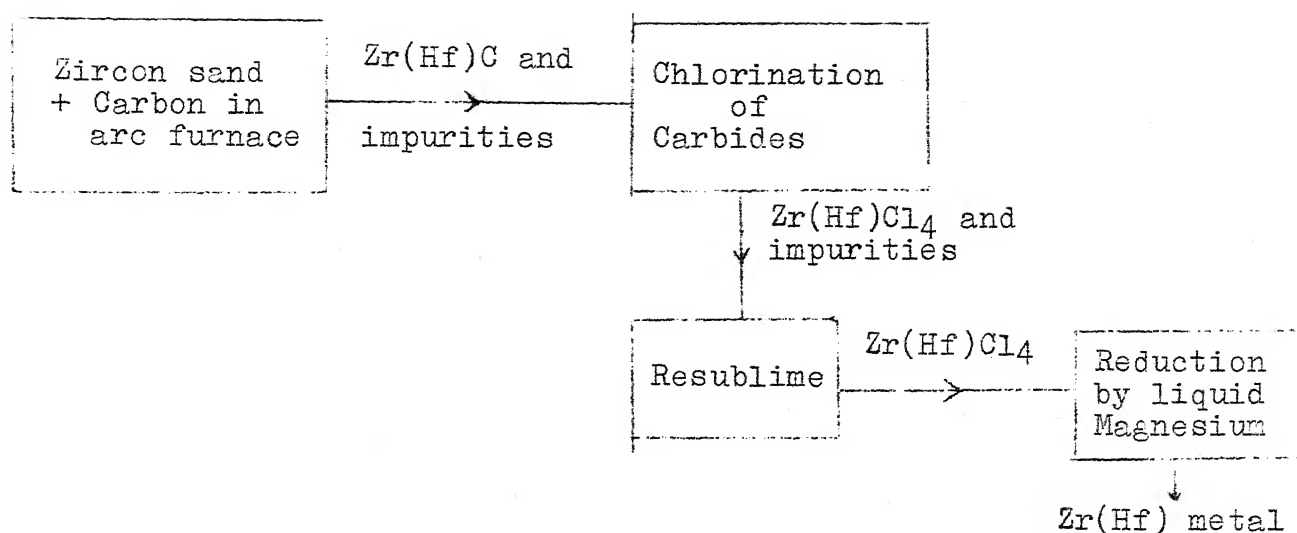
Of the various methods attempted so far, only a few have shown much promise and still fewer could be exploited commercially. A list of the important separation methods are given below:

- 1) Fractional crystallisation from aqueous solutions¹⁵
- 2) Solvent extraction using organic solvents¹⁶⁻¹⁹
- 3) Ion exchange (both cation^{20,21} and anion²²) using commercial resins
- 4) Fractional distillation of tetrachloride mixtures^{14,23,24} and their addition compounds²⁵⁻²⁸
- 5) Differential reduction of tetrachloride mixtures²⁹⁻³⁰
- 6) Vapour phase dechlorination³¹.

Amongst these, the solvent extraction method using tributyl phosphate and methyl isobutyl ketone as solvent has been most widely employed. A fractional crystallisation method based on difference in solubility of K_2ZrF_6 and K_2HfF_6 in water containing hydrochloric acid has also been attempted for

commercial exploitation by Russian workers.¹⁵ The method was found too slow for large scale operation. Besides, too many stages were needed to effect an acceptable separation. After 16 to 18 stages Sajin et. al.¹⁵ obtained potassium fluozirconate containing about 0.003 per cent hafnium. The large number of stages, however, are common to all the methods. In addition to this, most of the methods suffer from various other limitations also such as low separation efficiency, costly chemicals, handling of corrosive compounds, low recovery and throughput etc. Even the solvent extraction method is fairly expensive and difficult to control on account of large number of unit operations involved. These include preparation of extraction feed, liquid-liquid extraction, recovery and recycling of chemicals, precipitation of separated species, calcination of the precipitates etc.

Furthermore, a common difficulty encountered in most methods, including the solvent extraction, is that the methods are generally not compatible to the overall scheme of production of zirconium from ore to hafnium-free metal. Separation processes must be evaluated, not only on their intrinsic merits but also in respect to their compatibility with the total scheme. The well established Kroll's process³² for production of zirconium uses the tetrachloride as the source. The flow chart may be shown as follows:



Clearly this scheme would be best served by a separation process performed on the anhydrous tetrachlorides. But most of the commercial methods need special feed preparation and also leave the product in some form other than the tetrachloride.

It is to be noted, however, that methods which do fit into the overall scheme have had only very limited success. Methods based on fractional distillation of tetrachlorides or their double compounds may be mentioned in this regard. Distillation of tetrachloride mixture under ordinary¹⁴ and high pressure^{23,24} has been attempted. The former resulted in low separation efficiency, while technical difficulties accompanying the required high pressure prevented the latter process from becoming commercially feasible. Distillation of addition compounds of the tetrachlorides with PCl_5 ²⁵ and POCl_3 ²⁶ as well as alkoxides^{27,28} also resulted in low separation factors. Besides, handling of the corrosive compounds involved in these processes posed a major problem. Kim and Spink¹⁴ recently

indicated possibility of low temperature distillation using eutectic melts of Zr(Hf)Cl_4 and mixtures of fused salts like NaCl and KCl .

An alternate class of separation methods, with output and input both in the form of tetrachlorides attempts to fixup hafnium tetrachloride preferentially to a solid phase. Chandler³³ effected separation by reacting HfCl_4 present in the impure gas mixture with ZrO_2 to form ZrCl_4 and HfO_2 . Lutrizac et al.³ worked on the method of preferential reaction between HfCl_4 and NaCl . The method involved reaction between gaseous mixture of ZrCl_4 and HfCl_4 with solid NaCl . Other alkali metal chlorides such as KCl , CsCl , LiCl etc. can also be used instead of NaCl . Applicability of this principle in continuous packed bed reactor has also been demonstrated.⁴ Percentage recovery of zirconium as well as separation efficiency of this method, however, were rather poor.⁴ While the problem of recovery can be overcome by simple vacuum treatment of the reacted solids, any improvement of the separation efficiency would depend on the mechanism of the formation of the two hexachloro compounds. This would require understanding of reaction mechanisms both qualitatively as well as quantitatively. However, these aspects have not been adequately dealt with in the literature. The core of the present investigation is concerned with these kinetic aspects.

1.4 Kinetics of formation of chlorohafnates and chlorozirconates

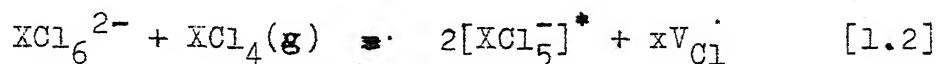
Of the various alkali and alkaline earth metal chloro compounds of zirconium and hafnium, only the kinetics of formation of sodium compounds have been reported.^{34,35}

Dutrizac and Flengas³⁴ studied heterogeneous kinetics of formation of Na_2ZrCl_6 using single crystal plates of sodium chloride. The reaction was said to follow the well-known parabolic law. It was concluded that the reaction kinetics was controlled by diffusion of zirconium tetrachloride through the zirconate layer surrounding the inner core of the unreacted sodium chloride. The temperature coefficient of the process in the range 399–504°C was calculated as 12.3 ± 3 Kcal/mole for reactions conducted at an average tetrachloride pressure of 600 mm of Hg.

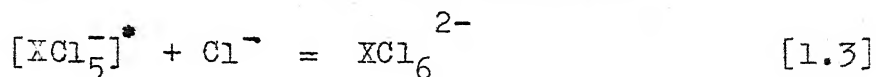
A subsequent study by Pint and Flengas³⁵ on the formation of Na_2ZrCl_6 and Na_2HfCl_6 also reported product phase transport control mechanism. The pressure dependence of the rate constant was studied for both cases at 485°C. For hafnium compound this temperature, incidentally, coincides almost to the polymorphic transformation temperature from γ to δ phase.⁵ The rate constant of the parabolic law was found to be proportional to $1/2.8$ and $1/4.1^{\text{th}}$ power of the ZrCl_4 and HfCl_4 vapour pressure, respectively. Taking into consideration the reported $\pm 2^\circ\text{C}$ fluctuations in the reaction zone temperature, it appears that the observed pressure dependence for the hafnium case

could be an average of the pressure coefficients applicable to the γ and δ phases.

To explain the observed pressure dependence, a reaction mechanism based on probable characteristics of the hexachloro compounds was proposed by Pint and Flengas.³⁵ The reaction was considered to be controlled by diffusion of Cl^- ions from the inner reactant-product interface to the outer solid-gas interface. The compound NaXCl_5 , which has been indicated in several phase studies^{6,7}, was assumed to be present at the outer solid-gas interface. In NaXCl_5 , X stands for zirconium and hafnium both. The reaction considered was



'x' was taken as one for zirconium case and two for hafnium. The chlorine ion vacancy generated in the surface reaction was considered responsible for transport of Cl^- ions from the inner sodium chloride core. The transported Cl^- ions reacted to form the hexachloro compound according to the reaction



The concurrent transport of Na^+ ions were assumed to occur through interstitials in the hexachloro compound lattice. This mechanism apparently explained the observed pressure dependence of the rate constant.

1.5 Plan of the work

In the present study the kinetics of formation of the double compounds, Na_2ZrCl_6 and Na_2HfCl_6 , have been studied using the principle of thermogravimetry in an all glass closed apparatus. Since both the double compounds of zirconium and hafnium as well as their tetrachlorides readily react with air and moisture, the reactions are to be conducted in sealed system. The use of sealed system precludes adoption of conventional pan balances for rate measurements. Transducers also cannot be used because of severe corrosion of metals by tetrachloride vapours. Therefore, calibrated quartz springs seem to be the only device which may be employed in the present system for continuous measurement of the change in weight of the reacting solid.

Experiments were designed to study the effect of parameters such as reaction temperature, gas pressure and sphere size on the rate of formation of the hexachloro compounds. In addition to studying the effect of these parameters on reaction rate, inert marker experiments were also designed to aid the kinetic analysis. In the absence of information regarding transport characteristics of the solids involved, marker experiments serve to give valuable information concerning the reaction mechanism.

Investigations on the kinetics of the mixed gas reactions were also planned along similar lines. In this case, however, partial pressures of the constituent tetrachloride

gases were to be determined separately. Additional experiments, therefore, were designed. The experiments involved measurement of total gas pressure and gas phase composition, separately. Furthermore, to ascertain the compositional relationship between the reacting gas and the solid reaction product, chemical analysis of the product layer was also planned.

Microscopic examinations are of great importance for kinetic studies of this nature. This, however, is not possible in the present case because of the difficulties associated with specimen preparation. Extreme fragile nature of the hexachloro compounds precludes fine polishing. Other valuable supporting experiments such as electron micro probe analysis of the product layer to determine concentration profile (for mixed gas reactions) in the reaction product also cannot be carried out. Preliminary enquiries on the possibility of conducting electron micro probe analysis showed that this technique cannot be applied on these systems. When the beam was projected on the sample surface, the area under the beam was removed in a short time, presumably due to evaporation of chlorides. These vapours would perhaps also damage the apparatus.

CHAPTER 2

HETEROGENEOUS SOLID-GAS REACTIONS

2.1 Introduction

Understanding of the heterogeneous solid-gas reaction kinetics involves identification of the rate controlling step and the pertinent reaction mechanism. While the rate limiting step (s) may be identified through conceptual macro reaction models, elucidation of the mechanism requires knowledge of properties of both the reactant and the product solid at atomic level. Of the various aspects involved in this, understanding of the chemical reaction is most difficult. In fact lack of proper understanding of the solid state properties for defining the concept of reactivity of solids poses major obstacle in the mechanistic evaluation of the overall reactions. On the other hand, solid properties relevant to material transport, at least for binary compounds like oxides, sulfides etc., are adequately known and suitable mechanistic analysis of diffusion through the product phase is generally possible. Obviously, the case of porous product does not require such knowledge, since diffusion in this case depends on the pore structure, porosity and other topological features which are not specific to the chemical nature of the product.

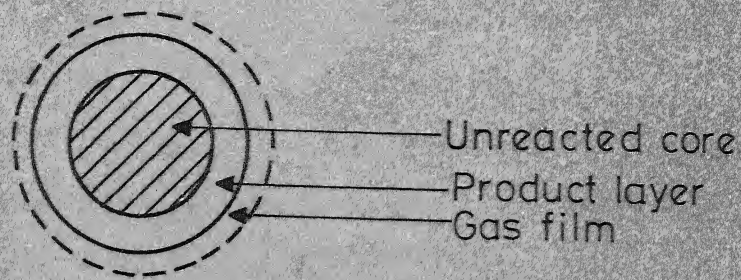
For the ternary compounds Na_2ZrCl_6 and Na_2HfCl_6 , which are of interest in the present investigation, unfortunately, no

information concerning the transport properties is available. Keeping this limitation in mind, the general features of heterogeneous solid-gas reactions are briefly reviewed in the following sections in order to form a basis for subsequent analysis of the rate data obtained in the present investigation. Accordingly, general features of reaction models, mechanisms of solid state transport controlled reactions and general aspects of phase boundary reactions have been discussed in sections 2.2 to 2.4, respectively.

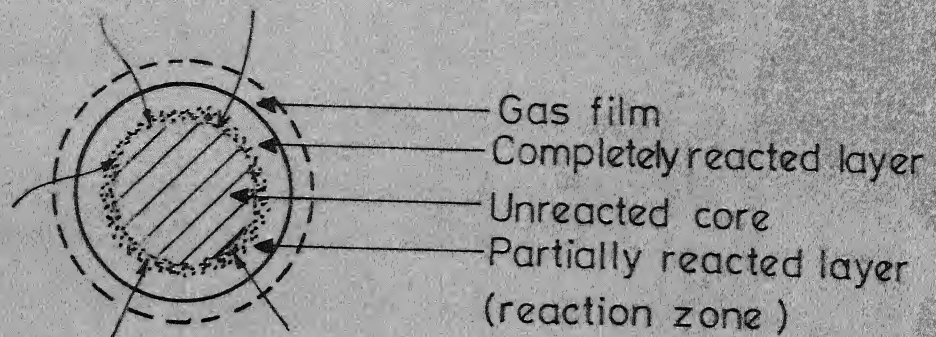
2.2 Reaction models

Solid-gas reaction models essentially are rate equations expressed in terms of parameters which characterise one or more of the reaction steps viz. chemical reaction at the interface, transport through the solid reaction product and the surrounding gas phase. The reactions may be under single or multi step control. The manner in which reaction steps are to be synthesised for building a representative model primarily depends on the nature of both the product and the reactant solid i.e. the extent of porosity.

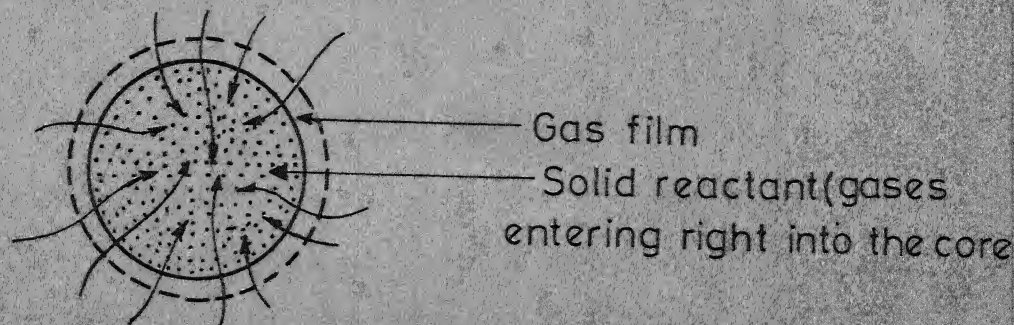
Fig. 3 has been drawn to depict the various situations that may be encountered. A sharp interface may result for both porous and nonporous product layer as shown in Fig. 3a. The sharp interface reaction by far is the most well understood situation. In this case, the reaction steps leading to the product formation occur in series. The step resistances governing



(a) Sharp interface (porous & nonporous product both)



(b) Diffused interface (porous product only)



(c) Homogeneous reaction (porous product only)

FIG.3 SCHEMATIC REPRESENTATION OF DIFFERENT SOLID-GAS REACTIONS

the rate of reaction, therefore, are additive.

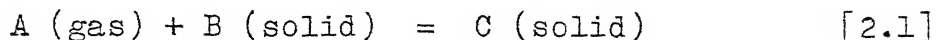
Diffused reaction interface as shown in Fig. 3b is often contended as the most general manner in which heterogeneous solid-gas reaction can take place.^{36,37} It has been argued that for porous reactant and product, and under the condition of mixed control, the reacting gas may diffuse past partially reacted solid particles. In other words, reaction may occur in a diffused zone, where concentration gradients occur both in the solid as well as the gas phase. The diffusion and chemical resistances, therefore, act simultaneously. It is to be noted that in spite of the generality of the diffused interface situation, sharp interface case remains more fundamental. The individual grains which constitute the reaction zone essentially react in accordance with the latter scheme i.e. the consecutive reaction steps.

The third possibility is occurrence of the reaction in virtually homogeneous manner. If the porosity of the reactant solid is very high, the reactant gas may permeate right into the central core. Under such circumstances the reaction takes place in the entire solid simultaneously and the concept of a reaction interface virtually disappears. Fig. 3c shows the features of a homogeneous reaction. This, however, is too drastic a case and is only of limited relevance in solid-gas reactions.

A large number of reaction models have been proposed to quantitatively explain the kinetics of all the three classes of reactions. In recent years, in addition to rate control by mass

transfer and chemical reaction, importance of heat transfer in influencing reaction rate has also been pointed out.³⁸⁻⁴⁰ For reactions involving high enthalpy change, it is essential to incorporate effect of heat transfer in the reaction model. A detailed discussion on these models, however, is beyond the scope and nature of the present work. The following discussion, therefore, is limited only to those sharp interface models which are relevant to the present context. However, a classification of various models, applicable in various situations is shown in Fig. 4.

It was mentioned earlier that the reactions involving sharp interface may be under single or multi step control. Shen and Smith⁴¹ as well as Spitzer, Manning and Philbrook⁴² derived mixed control rate equations for reactions involving formation of both solid and gaseous products. Differential form of the rate equation of reaction of the type



under mixed control is given by^φ

$$\frac{dR_i}{dt} = - \frac{(C_A^b - C_A^{eq})/\mu_s}{\frac{R_i^2}{R_o^2 k_m} + \frac{(R_o - R_i)R_i}{R_o D_A} + \frac{1}{k_r}} \quad [2.2]$$

The various terms in denominator in Eq. [2.2] may be identified, respectively, as the gas film, product layer and chemical step

^φ See nomenclature list in the beginning of the thesis for meaning of symbols.

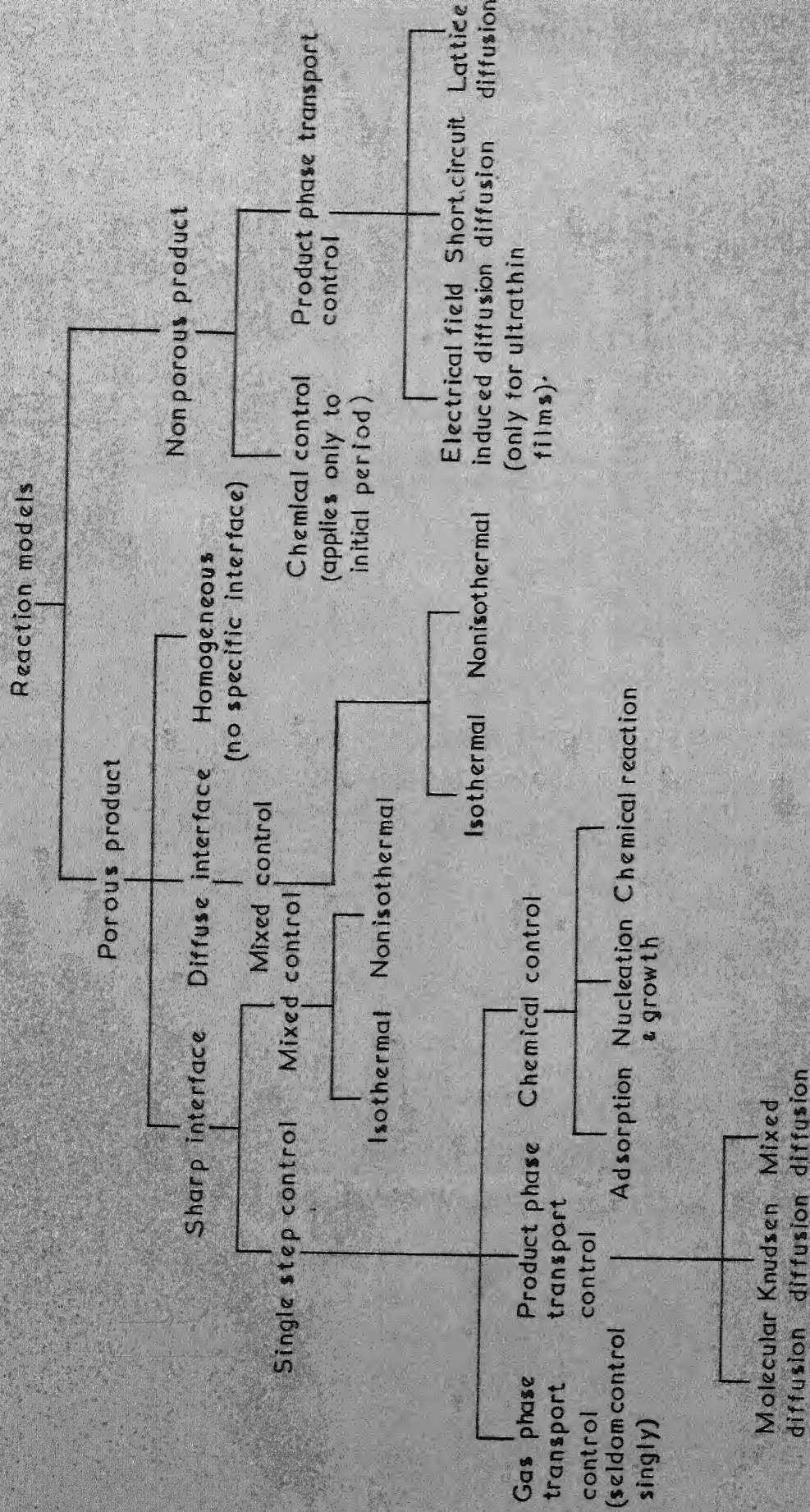


FIG. 4 CLASSIFICATION OF VARIOUS TYPES OF SOLID-GAS REACTIONS

resistances. Single step control models may be derived from Eq. [2.2] by invoking suitable simplifying assumptions. If product phase transport exclusively controls the overall reaction then chemical and gas phase transport resistances may be ignored and the rate equation reduces to

$$\frac{dR_i}{dt} = - \frac{(C_A^b - C_A^{eq})/\mu_s}{(R_o - R_i)R_i/(R_o D_A)} \quad [2.3]$$

Equation [2.3] is the differential form of the rate equation for spherical solids under product phase-transport control. The integrated rate equation may be obtained from this by introducing proper boundary conditions. Similar treatment is applicable for other single step control cases also.

Product phase-transport control models proposed by Carter⁴³ and Valensi⁴⁴ as well as Crank⁴⁵, Ginstling and Brounshtein⁴⁶ follow directly from Eq. [2.3]. The final integrated rate expression for the two models, however, are not the same. Carter-Valensi model in contrast to Crank-Ginstling-Brounshtein model, accounts for change in size of the reactant sphere with the growth of the product layer. The integrated rate equations arrived in the two cases are as follows:

Crank-Ginstling-Brounshtein Equation:

$$1 - \frac{2}{3}F - (1-F)^{2/3} = K_{cgb}t \quad [2.4]$$

Carter-Valensi Equation:

$$\frac{Z - [1 + (Z-1)F]^{2/3} - (Z-1)(1-F)^{2/3}}{2(Z-1)} = K_{cv}t \quad [2.5]$$

The parameter Z , incorporated in Carter-Valensi equation to account for change in sphere size, is defined as

$$Z = \frac{\text{Volume of solid reaction product}}{\text{Volume of solid reactant consumed}} = \frac{R_g^3 - R_i^3}{R_o^3 - R_i^3} = \frac{M_p / \rho_p}{f M_r / \rho_r} \quad [2.6]$$

It has been pointed out that swelling plays an important role only when Z has value more than 2.⁴⁷ For Z values between 1 and 2, Crank⁴⁵-Ginstling and Brounshtein⁴⁶ model fails only at very high percentage of reaction. Obviously then validity of a model may be ascertained adequately only when reaction rate data upto a very high percentage of reaction are available. Testing of the rate data obtained for only a small extent of reaction may result in erroneous rate constant values. The use of frequently applied transport control model of Jander⁴⁸ for reaction over a spherical interface is much more misleading in this respect. The assumption of constant area of reaction front restricts applicability of this model only to a very low percentage of reaction. It is to be noted that in contrast to plane reaction interface, area of spherical reaction interface always decreases with the progress of the reaction. Accordingly, 'parabolic law' which applies to transport control reactions on flat surfaces has quite simplified form.

Jander's model, however, may hold for higher conversion, if the reaction shows appreciable void formation in the reactant core. Void formation has been reported in several oxidation studies.⁴⁹⁻⁵² For reactions occurring by outward diffusion of ions, vacant sites are produced at the product-reactant interface

due to passage of ions in the product lattice. The vacancies thus formed may diffuse into the reactant core and form voids. The void formation prevents shrinking of the reactant core and hence with appreciable void formation Jander's model may stay valid for larger extents of reaction. On the contrary, if such a situation arises, Carter-Valensi as well as Crank-Ginstling and Brounshtein models lose much of their significance. Clearly, shrinking core concept embodied in these models becomes invalid if appreciable void formation occurs. However, void formation is seldom appreciable and these models are generally applicable for transport controlled reactions in spherical geometry.

It is to be noted that testing a model to high percentage of reaction is possible only when reaction mechanism does not change as a function of extent of reaction. A number of cases are known in which reaction mechanisms were found to change with progress of the reaction.^{53,54} Such changes primarily occur due to change in the characteristics of the product layer. Transformation of product layer from nonporous to porous has been reported quite frequently in the literature.^{55,56} Even in such cases testing of a model upto high percentages of reaction is desirable because that would help in identifying changes in the reaction mechanism.

Single step control models, briefly discussed above, adequately explain a reaction provided the magnitude of various reaction resistances differ sufficiently. This is apparent

from the close fit of the rate data to single as well as mixed control models^{39,40} for reactions involving porous product layer. For porous product layer cases, different reaction resistances are often comparable. Under such circumstances, identification of rate controlling steps using reaction models may not be possible. On the other hand, solid state diffusion rates are much slower compared to rates of the other reaction steps and only in this case rate limiting step may be identified unequivocally with the help of rate equations. Even in this case the choice of a truly representative model is subject to the condition that changes in sizes of the reactant be given due consideration.

2.3 Solid state transport controlled reactions

Discussions on the general features of various types of solid state transport controlled reactions form the subject matter of this section. Special emphasis has been given to the case of lattice diffusion controlled reactions. Thus, while in sub-section 2.3.1 a very general discussion on conditions of occurrence of all known types of solid state transport controlled cases is presented, subsequent subsections include discussion on various aspects concerning lattice diffusion only. The role of different reaction parameters as well as that of the marker studies in connection with lattice diffusion controlled reactions are discussed in 2.3.2 and 2.3.3, respectively.

2.3.1 General consideration on solid state transport controlled reactions

In general, the study of the mechanism of the transport control reactions includes identification of the rate controlling species and the manner of its transportation. The migrating species may be ions from either the gaseous or the solid reactant. In the former case, the product forming reaction should occur at the inner product-reactant interface and in the latter case at the outer product-gas interface. In the event of comparable mobilities of species of both types, the reaction may occur in a zone lying between the aforementioned phase boundaries.

Material transport to the reacting phase boundary may involve lattice diffusion, electric field induced diffusion or short circuit diffusion through the grain boundaries and dislocations. The preponderance of one mechanism over others would depend primarily on temperature. In view of the fact that a number of mechanisms are possible, the rate equations should be interpreted cautiously. Contrary to the earlier notion that the parabolic law must necessarily signify material transport by lattice diffusion, it is now known that other solid state diffusion mechanisms also conform to this law. At somewhat lower temperatures (less than Tamman temperature) when recrystallisation and grain growth rates are quite slow, generally short circuit diffusion prevails. Smeltzer et al.^{57,58} advanced a phenomenological description to account for diffusion of this

type. It was shown that the parabolic law will result if microstructure and diffusivity are independent of reaction time.

At still lower temperatures, in the presence of thin product films, electrical field induced diffusion sets in, wherein the space and surface charge fields generate the electrical field.⁵⁹ It has been shown that in the presence of an electrical field, a wide variety of kinetic rate laws, including the parabolic law, may result.⁶⁰ The characteristics of the thin film case, however, are quite distinct from the lattice diffusion case and no confusion should normally arise. Nevertheless, it is worth noting, since the phenomenon giving rise to space charge layer i.e. electron exchange involved in the preceding chemisorption step, is common to high temperature thick product layer case also. However, for thick product layer case the effect of the thin space charge layer is of no consequence since slower transport in the much wider space charge free zone dominates the scene shortly after the start of the reaction.

Yet another source of parabolic law, where the product phase diffusion operates only partly, is the case of simultaneous gas dissolution and scale formation.⁶¹ Oxygen dissolving metals such as zirconium and hafnium are believed to obey this mechanism at certain stages of oxidation.⁶²⁻⁶⁴

From the above discussion it is clear that lattice diffusion mechanism operates only in the formation of thick product layers at high temperatures. Detailed mechanism of this type of reaction is generally well understood because of the

availability of a theory based on the fundamental transport parameters. The theory known as Wagner's theory of oxidation⁶⁵ incorporates the concept of ambipolar diffusion of lattice defects under a chemical potential gradient set by the interfacial equilibrium reactions. Both electronic and ionic defects are considered as the migrating species. The theory has been widely used in numerous investigations pertaining to heterogeneous reaction of metals with oxygen, sulfur, halogens etc. Comprehensive reviews of such studies are available in several monographs.^{59,66,67} However, quite often the theory cannot be used due to the lack of precise information regarding defect characteristics of the solid reaction product.

In spite of the applicability of the theory to most metal-gas reaction systems, the theory is found inadequate for more complex systems e.g. oxidation of alloys. Nevertheless, the concept embodied in it is generally valid and has been successfully developed to explain the kinetic behaviour of such complex reaction system as alloy oxidation leading to the formation of single phase oxide solid solution.⁶⁸ Application of the new theoretical treatment is to be found in recent work of Smeltzer and coworkers.⁶⁹⁻⁷⁰

2.3.2 Role of reaction parameters on reaction mechanism (lattice diffusion)

Detailed analysis of the specific nature of the lattice diffusion mechanism i.e. interstitial or vacancy mechanism involves identification of the defect structure. Since the extent

and type of the lattice defect are directly related to pressure and temperature, investigations on the influence of these two important reaction parameters are necessary for unambiguous establishment of the transport mechanism. Success of such analysis, of course, depends on prior information on the defect structure. Such information may be obtained from extensive study on the extent and type of nonstoichiometry, measurement of partial conductivity, tracer diffusivity etc. However, such extensive and time consuming studies may not always be possible and other qualitative studies like marker experiments may be useful. In the following paragraphs, general features of the dependence of reaction kinetics on pressure and temperature is discussed. A detailed discussion is not undertaken because the nature of dependence varies from system to system.

The effect of pressure on the reaction rate may indicate the validity of a particular defect chemistry, postulated on the basis of certain qualitative informations viz. marker position, effect of impurity etc. For example, if marker studies indicate outward diffusion then the observed pressure dependence of the rate constant can be used to identify the actual mechanism i.e. interstitial or vacancy mechanism. A positive pressure law (rate constant $\propto P^{1/n}$) indicates vacancy mechanism. On the other hand, if the rate constant remains unchanged with pressure then interstitial mechanism is said to operate (for details see Section 4.7). Several oxidation systems reviewed by Hauffe⁵⁹ and Kofstad⁶⁶ exhibit this behaviour. On the contrary, effect of

temperature can be meaningfully interpreted only when specific quantitative informations are available. The Arrhenius type relation, which relates rate constant to reaction temperature, includes enthalpy terms of all the equilibrium steps leading to the formation of the rate limiting defect as well as the activation energy for the diffusion. Determination of activation energy of the rate controlling step, which is often the prime goal of studying temperature effects, therefore, is possible only when all the relevant enthalpy data are available from independent sources. This, however, is seldom the case. In the absence of such detailed data the role of temperature effect is limited to indicating changes in the reaction mechanism only. Pressure effect may also indicate such a change. In the event of a change in the reaction mechanism the pressure coefficient and the temperature coefficient change. A change in reaction mechanism may imply a change in the degree of ionisation of the lattice defects and, in the extreme case, a qualitative transformation of the product layer characteristics.

A change in the pressure law may also be expected with changes in the activity coefficient of the components involved in the defect equilibria.⁷¹ Possible interaction amongst the defects may cause such changes in activity coefficients. However, this may often remain undetected in the absence of any viable method for the estimation of the activity coefficients. Deviations from constant pressure law have often been interpreted in the literature as due to changes in the degree of ionisation

of defects.⁷²⁻⁷⁴ However, this calls for a detailed study. The role of pressure may assume further complexity if the defect character drastically varies across the product layer. Since pressure, or more specifically, chemical potential of the gaseous reactant varies widely across the product layer, significant difference in the defect structure within the product layer is not unlikely. In this connection the example of Ta_2O_5 may be cited. This compound was found to be a p-type semiconductor at oxygen pressures close to one atmosphere and a n-type semiconductor at low oxygen pressures.⁷⁵

2.3.3 Marker studies

It was mentioned earlier that elucidation of the transport controlled reaction mechanism requires identification of the rate controlling species. In those cases where Wagner's theory⁶⁵ applies, this can be predicted provided the required transport data are known. Such data are, however, seldom available. Under such circumstances marker experiments seem to be a valuable practical alternative in spite of its known limitations. Accordingly, this technique has been applied by numerous investigators^{55,76-80} since the pioneering work of Pfeil⁸¹ in 1929.

Inert marker technique involves fixing of markers in the form of thin wire or porous film over the solid surface before reaction. The position of the marker is examined at the end of the reaction. When the product layer is compact and

pore free and the components are transported by lattice diffusion, the final marker position is dependent on the diffusion rates of the components. If the marker is retained at the inner product-reactant interface then it is taken as an evidence of exclusive outward ionic movement (from core to outer solid-gas interface). Similarly, presence of the marker at outer gas-solid interface implies an exclusive inward migration of ions. If migration occurs in both the directions, markers would be found within the product layer itself. All these observations, however, apply to an ideal situation only. Secondary processes may influence and change the marker position in actual cases.

Experimental studies on oxidation of metals show many instances of anomalous marker movement.⁷⁶⁻⁷⁸ In all the investigations, contrary to expectations, the markers were found to be located away from the scale-metal interface. Reported product formation beneath the markers is considered to be the result of partial detachment of the product scale from the reactant and consequent bypassing of the markers.⁷⁷⁻⁸⁰ It has been argued that when the product layer surrounding the metal becomes physically separated from it, markers may be carried off along with the layer. The marker would now stay at the product layer - crack interface. Owing to the loss of contact between the product and the metal, the chemical potential of the metal in the product layer will decrease and the vapour pressure of the non metal will correspondingly increase above the dissociation pressure of the scale. The exposed metal may now

react with the vapour to form new product beneath the marker. Above explanation on the anomalous marker behaviour for gas-metal reaction, however, is quite general and should apply to other systems as well.

Partial loss of adherence between reactant and product responsible for unexpected marker behaviour described above, primarily results from the failure of the product layer to follow the shrinking core. The vacant sites created at the reactant-product interface due to passage of the reactant ions into the product lattice (both to interstices and vacant sites) leads to shrinkage of the reactant volume. Volume shrinkage, however, will not occur if all the vacant sites, created at the interface, diffuse into the reactant core and form voids. Although void formation has been reported in several studies⁴⁹⁻⁵², its extent has always been insufficient to compensate for the loss of the reactant ions. Plastic deformation of the product layer, therefore is necessary to maintain contact between the reactant and the product. But, the required plastic deformation becomes increasingly difficult with increase in the product layer thickness. At some critical thickness product layer may detach itself from the unreacted core.

Meussner and Birchenall⁷⁶ pointed out yet another reason for positioning of the marker within the product layer. They proposed that markers may be displaced from their expected position due to an undercutting action. If markers are too

large, they obstruct the diffusional flow of the migrating ions and thus may be bypassed.

In view of the possibility of misinterpretation of the inert marker experiments, use of isotopes, which themselves are components of the product phase, has been suggested.⁸²⁻⁸⁴ This should obviously be a better technique, particularly when isotopes of both the solid and gaseous reactant are used together, due to the possibility of cross checking. Such experiments have been reported in the literature.⁸⁴ The usual limitation in such work, however, is the nonavailability of suitable isotopes.

2.4 Phase boundary reactions

Mechanistic analysis of phase boundary controlled reactions involved in the heterogeneous solid-gas systems is hindered to a large extent by its dependence on solid characteristics. It has been confirmed in connection with a large number of solid-gas reactions that reactivity of a solid compound is greatly influenced by its history. In fact our inability to characterise the various solid properties that affects solid reactivity is the central stumbling block in comprehending solid-gas reaction kinetics. Presence of multiplicity of phenomena constituting the overall phase boundary process further complicates the situation.

A phase boundary reaction includes steps such as adsorption, product forming reaction and its intermediates, nucleation and growth. Besides, transfer of ions from the

reactant to the product phase, change in charges of the ions upon transfer into the neighbouring phase (for multi layered product) also form part of the overall phase boundary process.

Results reported in the literature, however, are not amenable to interpretation in terms of the ion transfer across the phase interfaces and most attempts to explain phase boundary reactions are based on adsorption, surface reaction, nucleation and growth. In the initial stages of the reaction, particularly for those at low temperatures, the role of adsorption, nucleation and growth in determining the reaction rate is widely recognised, although their detailed mechanisms are still a matter of conjecture. On the basis of some recent experimental evidence, it has been shown that a two dimensional chemisorbed layer forms prior to the formation of the three dimensional product layer.⁸⁵ The two dimensional layer was found to bear a definite relationship with the substrate. As regards the growth of the nuclei, surface diffusion is believed to be the primary mechanism. No definite view, however, is available on such important matters as the dependence of the growth rate on crystal orientation and structure, epitaxial relation between the nuclei and the substrate etc.

In high temperature reactions on the contrary, adsorption and nucleation-growth controlled stages usually remain undetected as they are too fast at this condition. Accordingly, the probability of adsorption or nucleation and growth control is much less in this case, although not impossible. For example,

adsorption might control a reaction at high temperatures and at low gas pressures due to considerable decrease in the number of impinging gas molecules on the solid surface. Hussey et al.⁸⁶ suggested this as the rate controlling step for the formation of magnetite at low pressures and high temperatures. Nucleation and growth control was also suggested for high temperature reaction even after formation of a continuous product film.⁸⁷

The adsorption step plays an important role even when not explicitly rate controlling. A number of kinetic studies⁸⁸⁻⁹¹ on phase boundary control suggest establishment of adsorption equilibrium at the reaction interface and this explains the pressure dependence of the reaction rate. A number of models⁹²⁻⁹⁵ have been proposed based upon the nature of the adsorption species (dissociated or not) and the subsequent slow step controlling the reaction. All these models usually employ Langmuir's approach to determine the time invariant concentration of the adsorbed species on the reaction interface. Validity of these models, however, are hard to check owing to the limited or nonexistent information on the nature of adsorbed species. Thus, the applicability of various models is understood mainly in terms of observed pressure dependence.

CHAPTER 3

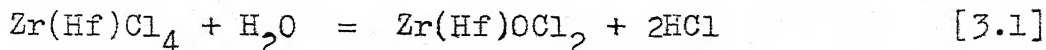
EXPERIMENTAL

3.1 Introduction

All pertinent informations regarding the experiments conducted in the course of the present study have been presented in this chapter. The general precautions and techniques for handling reactive systems such as the present ones are discussed in Section 3.2. The subsequent sections contain detailed information regarding actual experimentation. Sections 3.3 to 3.6 deal with material preparation, kinetic measurement, measurement of tetrachloride partial pressures and densities of the solids.

3.2 General principle

Experimental studies involving zirconium and hafnium tetrachloride vapours require attention to two main factors, namely, volatility and reactivity of these tetrachlorides. These tetrachlorides readily react with moisture to form oxychloride and hydrogen chloride. The reaction may be written as



The oxychlorides may further transform to form oxides. Various hydrated oxychlorides may also form in the presence of moisture. All handling operations of the tetrachlorides, therefore, are to be carried out within a dry box to avoid contact with moisture and air.

The other property, i.e. volatility, of the tetrachlorides appreciably cuts down experimental flexibility. The tetrachlorides are solid compounds with high vapour pressure. However, vapour pressure at room temperature is rather low and the solid tetrachlorides are to be heated to generate necessary gas pressure. In order to attain a pressure of about one atmosphere, the solid zirconium tetrachloride needs heating to about 334°C . Temperature required to attain similar pressure for the hafnium tetrachloride is about 315°C . However, just heating the bulb containing the tetrachloride to a predetermined temperature is not sufficient to ensure a pressure. To avoid condensation and hence to maintain a steady gas pressure all other portions of the apparatus require heating to temperatures higher than that of the bulb producing the vapour. The vapour pressure is necessarily defined by the lowest temperature in the system. Heating of the entire system poses several problems from the experimental point of view. Clearly, open systems can not be used. Also since required temperatures are rather high, it is not possible to use such gas controlling devices as stop cocks. Most metal valves are also not usable due to corrosive nature of the gases.

Another important feature that needs attention is removal of hydrogen chloride and other adsorbed gases from the tetrachlorides. It is very difficult to completely avoid moisture absorption during material handling. Removal of the hydrogen chloride thus formed as well as other adsorbed gases is an absolute necessity for closed cell experimentation.

Residual gases, besides causing uncertainty in gas pressure, may even lead to explosion. Thus, the gases should be removed by prolonged heating of the tetrachloride under vacuum.

3.3 Material preparation

All aspects of material preparation have been discussed in this section. Preparation of the solid reactant as well as the tetrachloride solids which produce the reacting gas have been discussed in Sections 3.3.1 and 3.3.2, respectively.

3.3.1 Preparation of sodium chloride samples

Sodium chloride samples used in the present investigation were in the form of spheres and cylinders. While spheres of various sizes were employed for thermogravimetric experiments, the cylindrical specimens with thin quartz fibres attached on to the surface were used for marker experiments. Both types of samples were prepared by casting molten sodium chloride in hot stainless steel split moulds. The moulds are shown in Fig. 5. The procedure for casting samples are as follows.

a. Making of the spheres

Anhydrous analytical reagent grade sodium chloride was melted in quartz crucibles by flame heating. Prior to pouring, the stainless steel mould was held inside a small furnace and heated to about 500°C . Spheres of nominal diameter 6.6, 9.2 and 12.2 mm were produced using this technique. The spheres were of approximately uniform porosity. From cast to cast the

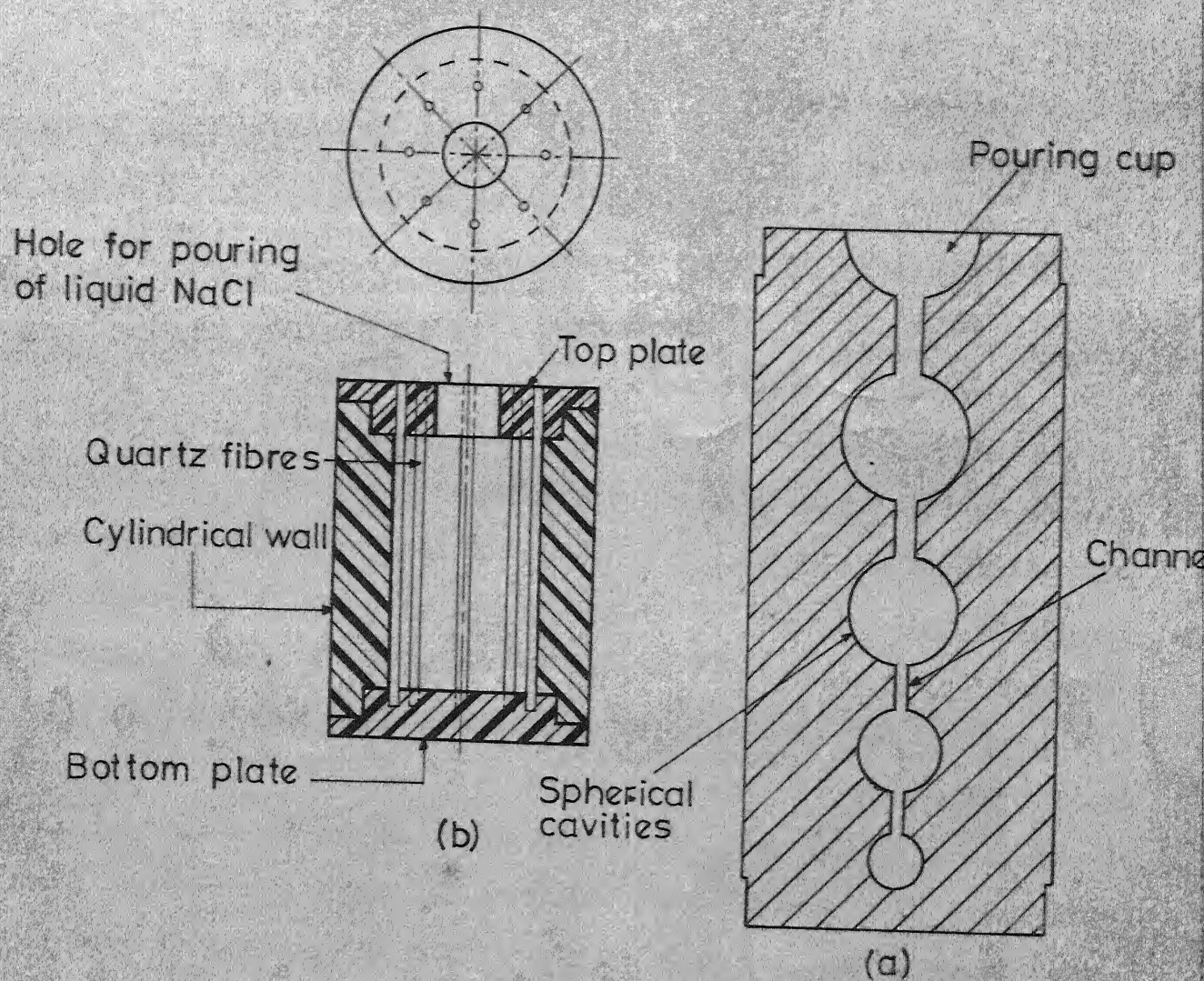


FIG. 5 SECTIONAL DIAGRAMS OF MOULDS FOR THE PRODUCTION OF SODIUM CHLORIDE SPECIMENS (a. Sphere b. Marker)

sphere diameter fluctuated to within ± 0.05 mm while overall porosity varied from 8-12 per cent. The pores, however, were found to be nonuniformly distributed; concentration being somewhat higher in the central regions. The distribution, however, was not too sharp.

b. Preparation of the marker specimens

The cylindrical marker specimens were produced by casting in hot stainless steel split mould shown in Fig. 5b. The thin fibres of quartz of approximate diameter 0.3 mm served as marker. The fibres were attached to the cylindrical surface by inserting them along the periphery of the mould prior to casting. Top and bottom plate of the four piece mould shown in Fig. 5b were designed to hold the fibres along the cylindrical mould surface. The markers were inserted into the mould through small holes made in the top plate. Shallow closed end holes made in the corresponding position in the bottom plate held the markers in position. Molten sodium chloride was poured through a central hole made in the top plate.

3.3.2 Production and purification of the tetrachlorides

The nuclear grade zirconium tetrachloride used in this work was supplied by Nuclear Fuel Complex, Hyderabad. Hafnium tetrachloride used, however, was produced from pure oxides obtained from Bhaba Atomic Research Centre, Trombay. The hafnium oxide used, however, was not much pure. Zirconium content of the supplied HfO_2 was about 5 per cent. Tetrachlorides

of both zirconium and hafnium were purified before use.

Purification was done by vacuum distillation. In all experiments double distilled tetrachloride was used.

a. Production of hafnium tetrachloride

Hafnium tetrachloride was produced by reduction chlorination of the oxide. Carbon was used as the reducing agent. Chlorination was carried out by passing preheated anhydrous chlorine through a packed bed of oxide pellets kept in a furnace at about 700°C . The pellet mixture contained about 15 per cent carbon, 4 per cent dextrene (binder), 3 per cent water and rest hafnium oxide. The packed bed of pellets was preceded by a bed of carbon, which acted as a getter for possible traces of oxygen in the incoming chlorine. A sketch of the apparatus is shown in Fig. 6. Prior to starting the chlorine flow, the entire set up was flushed with argon for about 5-6 hours to remove traces of moisture present in the apparatus and the pellets. Chlorine gas was introduced after moisture elimination. The tetrachloride vapours produced along with oxides of carbon and unreacted chlorine were led to a water cooled condenser through a separately heated connecting tube. The uncondensed gases were allowed to escape through bubbler containing dibutylphthalate as bubbler liquid. After sufficient tetrachloride has been collected, the condenser was detached from the rest of the apparatus by fusing the constrictions at its inlet and outlet.

b. Distillation of tetrachlorides

The distilling apparatus consisted of a long one end

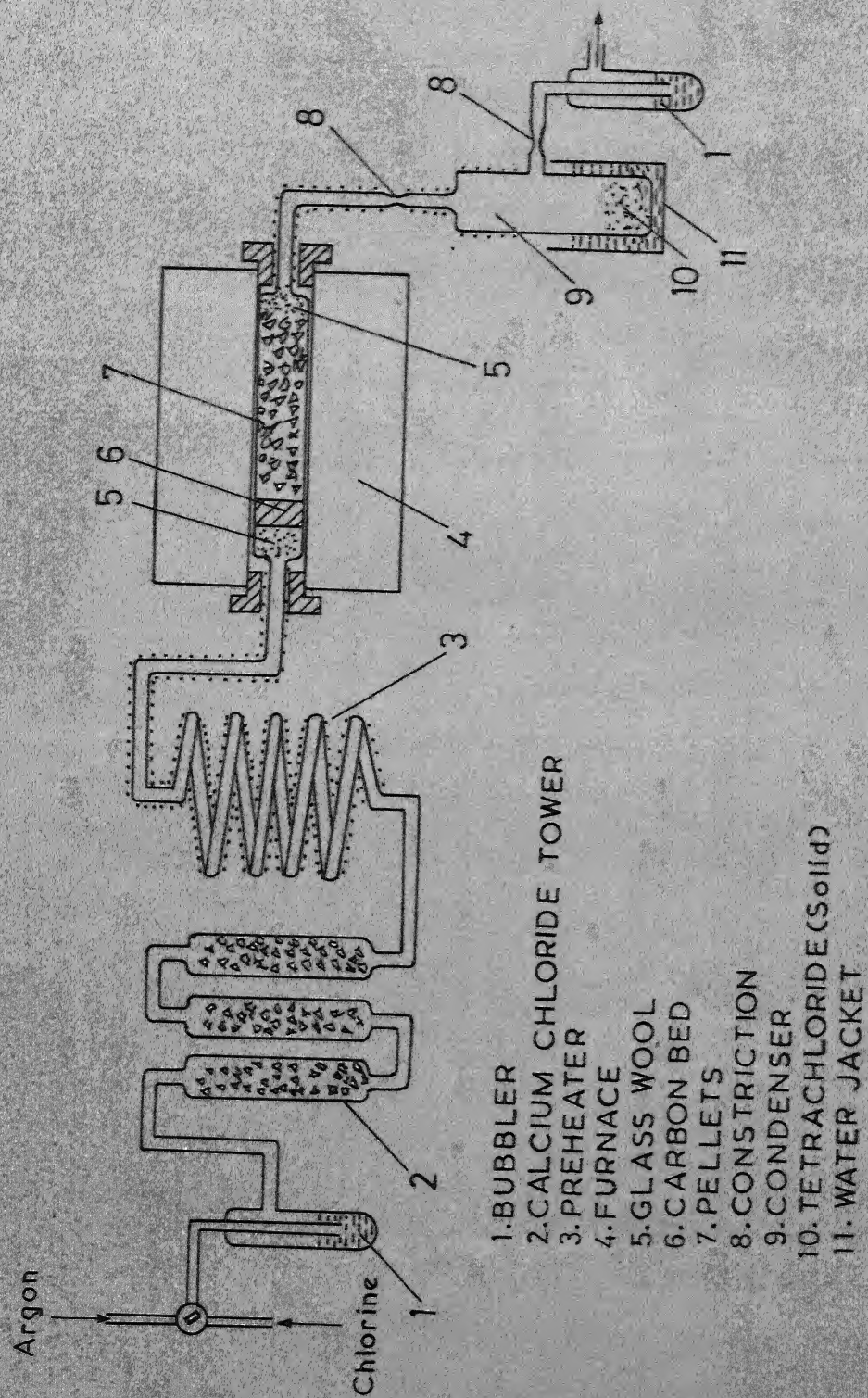


FIG. 6 APPARATUS FOR PRODUCTION OF TETRACHLORIDE FROM
OXIDE PELLETS

closed pyrex tube attached to a vacuum line. After introducing the tetrachloride in the distilling tube, the system was thoroughly evacuated at about 160°C for several hours to remove the gases and then sealed. The closed end of the tube, containing the solid tetrachloride was then heated to about 325°C . The vapours produced condensed at the cooler end of the tube, separated by a thick lump of glass wool. The tube was then broken inside a dry box and distillate redistilled once more.

3.4 Kinetic measurement: apparatus and procedure

Figure 7 shows the all glass apparatus for kinetic experiments. The set up consisted of a vertical reaction chamber connected to a gas generating bulb containing the solid tetrachlorides (ZrCl_4 , HfCl_4 or a mixture of them). The sodium chloride sphere was suspended from a calibrated quartz suspension string into the constant temperature zone of the reaction chamber. The basket containing the sodium chloride ball was also made of quartz. A separately heated connecting tube led the vapours from the heated bulb into the reaction chamber. As shown in the figure, the tetrachloride filled bulb was kept enclosed in an aluminium block placed in the hot zone of a horizontal trolley furnace. With this arrangement the temperature of the bulb could be controlled to within $\pm 1^{\circ}\text{C}$, while the reaction zone temperature could be controlled to within $\pm 2^{\circ}\text{C}$. The bulb temperature was measured by placing a calibrated thermocouple in the well made at the closed end of the bulb, as shown in the

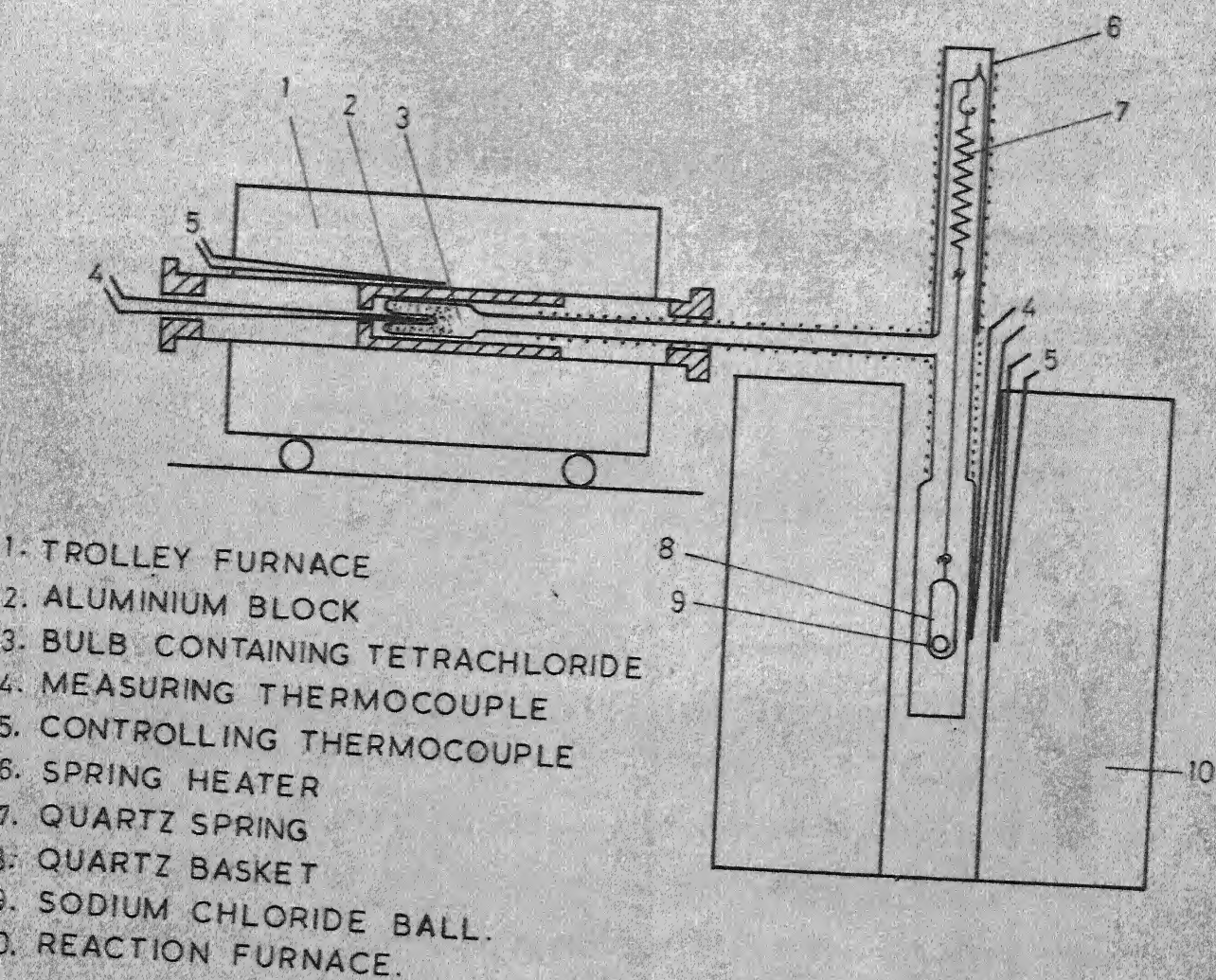


FIG. 7 APPARATUS FOR KINETIC EXPERIMENTS

figure. The thermocouple for measuring reaction zone temperature was tied with the reaction vessel with its tip near the reaction zone.

The vapour pressure of the tetrachloride gas was calculated using published thermodynamic data.⁹⁶ The temperature-vapour pressure relation is given by the following expressions

zirconium tetrachloride:

$$\log P_{\text{mm}} = - \frac{5400}{T} + 11.766 \quad (480-689^{\circ}\text{K}) \quad [3.2]$$

hafnium tetrachloride:

$$\log P_{\text{mm}} = - \frac{5197}{T} + 11.712 \quad (476-681^{\circ}\text{K}) \quad [3.3]$$

The temperature fluctuation ($\pm 1^{\circ}\text{C}$) in the bulb results in pressure fluctuation of about ± 25 mm for both zirconium and hafnium tetrachloride at pressure of 745 mm of Hg. Partial pressure of the reacting gases for mixed tetrachloride reaction, however, was measured separately and is described in the next section.

In order to avoid condensation and thus to ascertain validity of the calculated vapour pressure, it was necessary to heat all portions of the set up to temperatures higher than that of the gas generating bulb. This was done by carefully measuring the temperature distribution along the entire set up including the portions within the furnace. Depending upon the requirement, resistance coils were rewound or auxiliary heaters attached.

To set the apparatus the calibrated quartz spring loaded with the reactant sphere was suspended from a cap with a hook. The cap had a constricted outlet which could be attached to the vacuum line. Constriction was provided to seal the set up after evacuation. The cap was joined to the top vertical portion of the set up by fusing. The top part which enclosed the spring was heated by a separate slip-on heater. The high temperature spring constant was found 4 to 4.25 per cent higher than the room temperature. The exact value was determined for every run. All weight gain measurements were computed from the measured high temperature spring constant. After insertion of the spring and the sodium chloride ball, the temperature of the reaction chamber was raised to actual reaction temperature and evacuated for about 24 hours for removal of traces of adsorbed moisture. The tetrachloride already filled in a bulb inside the dry box was then joined to the system in the minimum possible time and the assembly put under vacuum. The sliding furnace already heated to about 160°C was next pushed over the bulb. The hot evacuation to remove adsorbed gases was continued for an additional period of about 2-3 hours. Finally the system was vacuum sealed from the top.

The apparatus was now ready for a kinetic run. The tetrachloride temperature was brought to the desired level as quickly as possible. The required time varied between 45 to 60 minutes during which a small weight gain could be observed. The reaction time for the initial period of uncertainty was

subsequently determined by back extrapolating the experimental data. Weight change was recorded by measuring the change in spring length viewed through a narrow slit in the refractory casing that surrounded the spring region of the apparatus.

3.5 Measurement of tetrachloride partial pressure

It was necessary to directly measure the partial pressure of the gas for kinetic experiments involving mixtures of the two tetrachloride vapours, since the solid tetrachlorides producing them form solid solution. Niselson⁹⁷ had earlier studied the system $\text{ZrCl}_4\text{-HfCl}_4$ and showed complete solubility of the tetrachlorides. However, nature of the solution is not known.

The partial pressures of zirconium and hafnium tetrachloride at a particular solid composition were determined by two separate experiments. The experiments involved measurement of total gas pressure and estimation of gas composition by chemical analysis of the condensed vapours.

For kinetic as well as pressure measuring runs involving gas mixture, a standard arbitrary mixture of the solid tetrachloride (approximately 75 per cent ZrCl_4 and 25 per cent HfCl_4 , volume basis) was prepared. The mixture was heated in a sealed vessel whose free space was packed with glass wool to the maximum extent. The solution forming heating was done in stages. The stage-heating at low temperatures ($180\text{-}220^\circ\text{C}$), where individual gas pressures were somewhat low (5-10 mm of Hg) FWRs

necessary to avoid composition fluctuation due to the condensation of vapours in relatively cooler portions. Solution formation at lower temperature with minimum possible free space presumably reduces this effect. The heating was continued for about ten days. The entire operation was repeated after remixing the once heated mixture inside a dry box. The standard mixture thus prepared were used for all subsequent experiments i.e. total pressure measurement, gas phase composition determination and kinetic experiments.

3.5.1 Total pressure measurement

The apparatus used for total pressure measurement is shown in Fig. 8. A bulb similar to that used for earlier kinetic experiments, contained the tetrachloride mixture prepared earlier. A quartz U-tube filled with liquid tin was coupled to a mercury manometer to measure pressure. One limb of the U-tube was connected to the gas generating bulb and the other to a vacuum/gas line and the mercury manometer. To read the vapour pressure of the tetrachloride mixture, liquid tin levels in the two limbs of the tin U-tube were brought to the same height by carefully introducing argon or applying partial evacuation on the mercury manometer side. The tetrachloride pressure could now be read directly from the mercury manometer.

To start a run, the tin U-tube was kept filled with pure vacuum cast tin chips and joined to the tetrachloride mixture filled bulb. Immediately after attaching the bulb, the

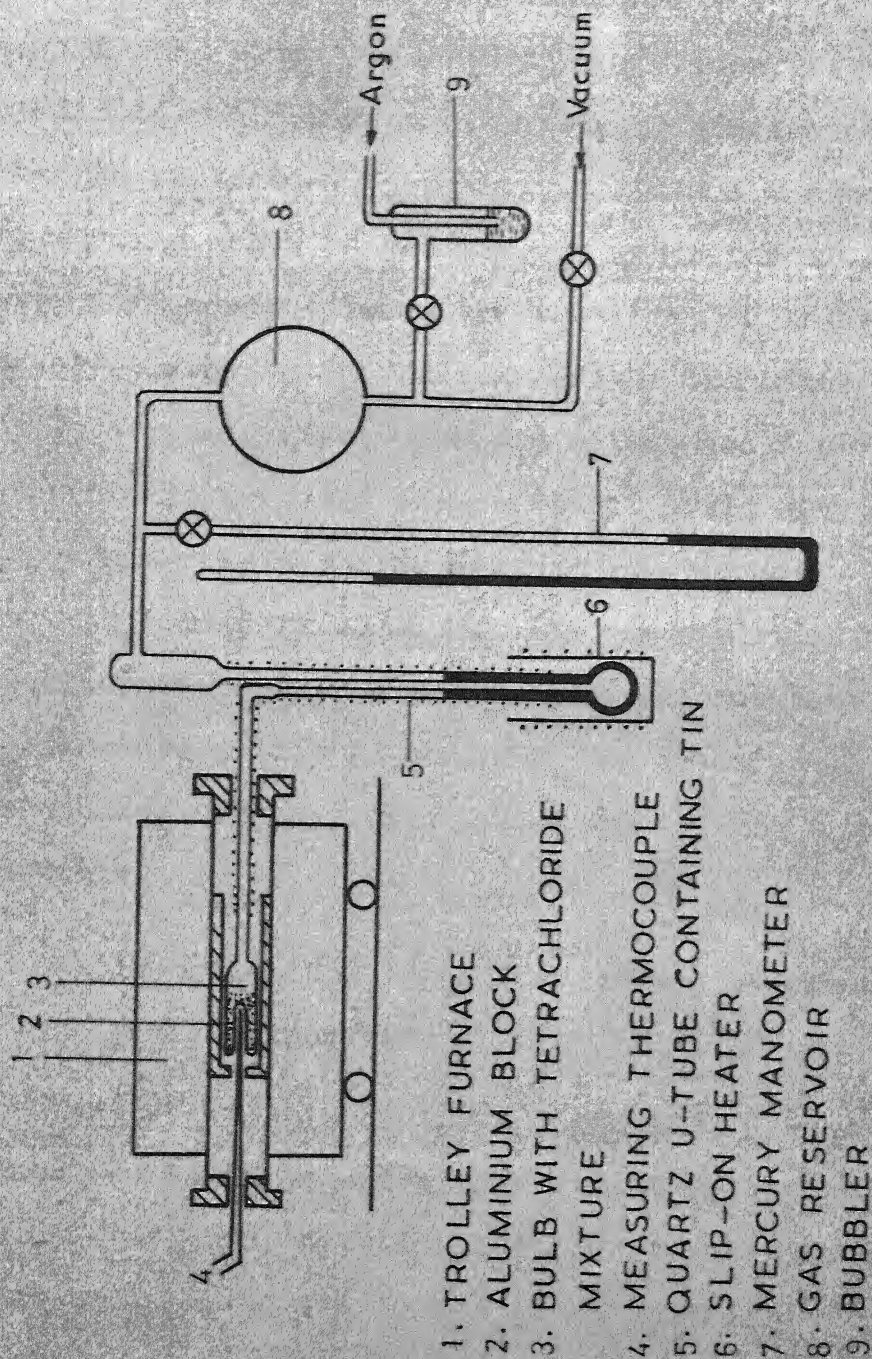


FIG. 8 APPARATUS FOR THE MESEUREMENT OF TOTAL GAS PRESSURE

trolley furnace, already heated to about 160°C , was slowly pushed over the bulb and evacuation started. At the end of evacuation for about 3 hours, tin chips were melted. The liquid tin column now separated tetrachloride side from the rest of the apparatus. A positive pressure was now applied by introducing argon on the mercury manometer side and a pressure difference between the two limbs of the tin filled U-tube established. The bottom part of the U-tube (bent portion) was now frozen. The tin column above this which remained liquid provided the gas-tight seal. The bulb temperature was now raised to the desired level. After stabilisation of the bulb temperature, the frozen tin was remelted and vapour pressure read from the mercury manometer by bringing molten tin levels to same height. The measured pressure remained almost constant for long period (≈ 6 hours) and was reproducible.

3.5.2 Sample-collecting apparatus for the measurement of gas phase composition

The apparatus used for this purpose was similar to that used for total pressure measurement and is shown in Fig. 9. In this the U-tube containing liquid tin was replaced by a liquid tin filled quartz bubbler and a condenser. The bubbler had separate heaters for heating separately the bottom and top regions. In this case also, tin was introduced in the form of chips and melted only after hot evacuation of

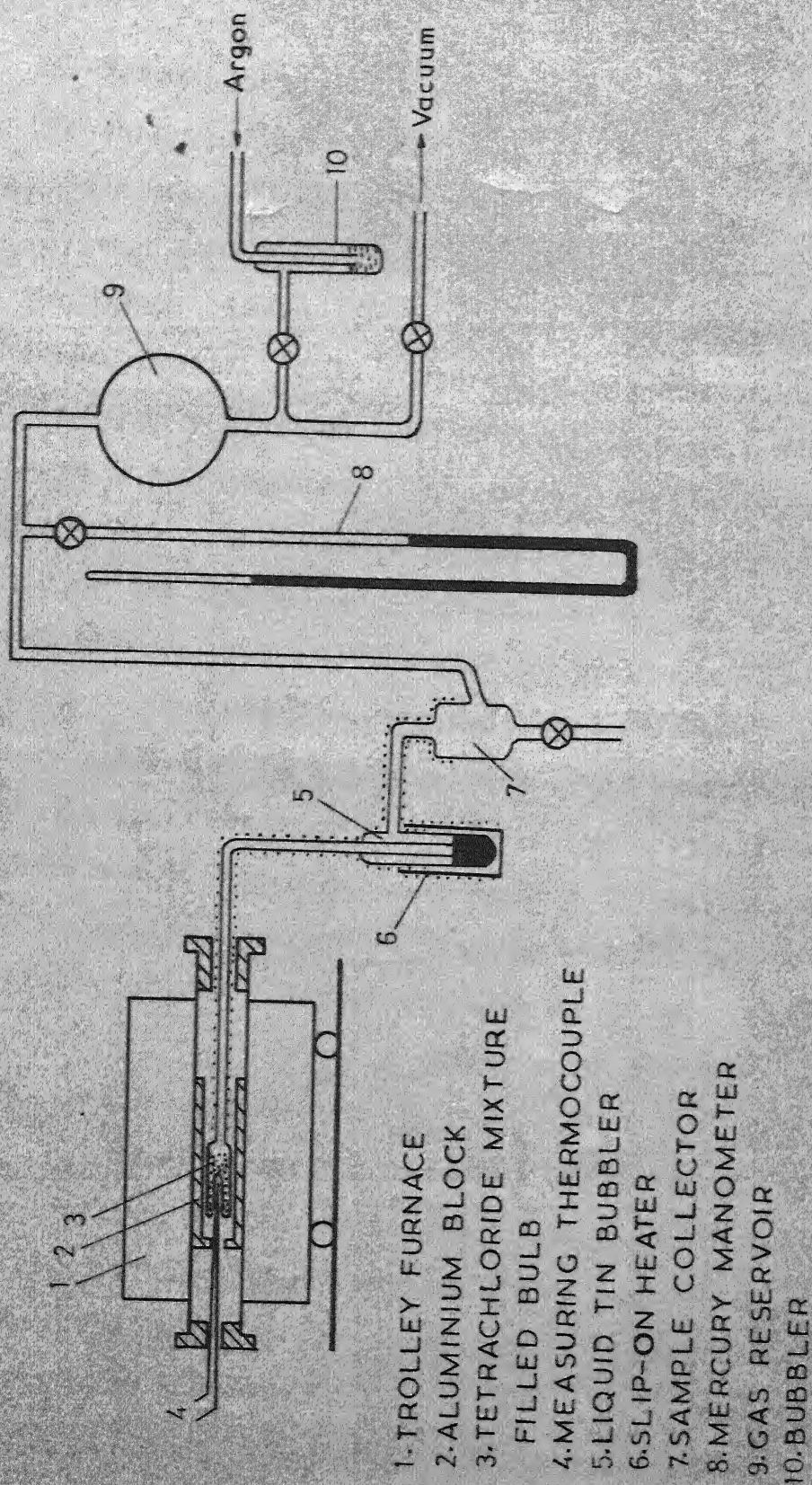


FIG. 9 APPRATUS FOR COLLECTING SAMPLES OF TETRACHLORIDE GAS MIXTURE
 FOR DETERMINING THE GAS COMPOSITION

the tetrachloride bulb was complete. After melting, as before, pressure was applied from the tin manometer side to raise molten tin column in the inner bubbler tube. The bottom heater, was then switched off to freeze the bottom portion of tin in the bubbler while tin in contact with tetrachloride vapour stayed molten. Bulb temperature was now raised to the desired level and a pressure just few millimeters less than the already known total pressure of the tetrachloride mixture at this temperature established on mercury manometer side. Slowly, the frozen tin was melted. Slight excess pressure of the tetrachloride vapours allowed the gas to bubble through liquid tin. The vapours released were collected in the condenser. Vapours were collected only intermittently to avoid change in composition of the gas that came out. These two precautions i.e., intermittent collection and maintenance of small pressure difference between the two sides of the tin bubbler are necessary, since release of gas disturbs equilibrium in the tetrachloride bulb. The collected solid tetrachloride mixture was subsequently chemically analysed for hafnium content.

The samples for chemical analysis were prepared in the following way. The total condensate was first dissolved in distilled water. Ammonium hydroxide was then added to the aqueous solution to precipitate out dissolved zirconium and hafnium in the form of hydroxides. The precipitate was now filtered, dried and fired at 900°C for about 4 hours. The

oxide sample thus obtained was chemically analysed by the method of neutron activation analysis.^φ

3.6 Measurement of densities of reactants and products

The densities of the sodium chloride spheres used were determined from the measurement of their weight and diameter. The densities of the reaction products were measured using glass pycnometer. Pure ortho xylene was used as the fluid. All the density data reported in the next chapter pertain to room temperature ($\approx 34^{\circ}\text{C}$).

^φ The neutron activation analysis was carried out by Bhaba Atomic Research Centre, Trombay.

CHAPTER 4

EXPERIMENTAL RESULTS AND DISCUSSION - I

REACTIONS INVOLVING INDIVIDUAL GASES

4.1 Introduction

The experimental results and discussion on the kinetics of formation of sodium hexachloro zirconate and sodium hexachloro hafnate are the subject matter of this chapter. Here formation of only the individual compounds are discussed. Simultaneous formation of both zirconate and hafnate is discussed in the next chapter.

The experimental results presented in Section 4.2 to 4.4 include density values, kinetic data and results of marker studies. Most data are presented graphically. The basic experimental data may be obtained from relevant Tables in Appendix I. The kinetic data are analysed in terms of possible reaction mechanisms and kinetic models in Sections 4.5 to 4.7.

4.2 Swelling parameter, reactant and product density

Calculated values of the swelling parameter and the density values used in the calculation are shown in Table III. The calculation was made using the expression given in Eq. [2.6]. Average of the measured density values were used for the purpose. For the sake of accuracy, average density of the reacted sodium chloride layers rather than that of the spheres as a whole has

Table III. Swelling parameters and density values.

Average density gm./cc			Swelling parameter, Z	
Reacted NaCl layer	Na_2ZrCl_6	Na_2HfCl_6	Formation of Na_2ZrCl_6	Formation of Na_2HfCl_6
2.107	2.43	3.06	2.595	2.571

been used. Density of the outer sodium chloride layer, which reacted, could be estimated from the dimension and weight of the residual spherical core. Dimension and weight of this residual sphere could be directly measured after stripping the product layer. Since, the hexachloro reaction products (both hafnium and zirconium) were extremely fragile at room temperature and became even more so on storage, the product layer could be readily stripped from the unreacted core.

4.3 Results of the kinetic measurements

The kinetic data on the formation of hexachloro compounds of zirconium and hafnium were obtained from thermogravimetric experiments conducted under various reaction conditions. The effects of various reaction parameters on the rate of formation of the hexachloro compounds are presented in Figs. 10 to 15.

The time-conversion plots for the formation of sodium hexachloro zirconate and hafnate showing the influence of sphere size, are depicted in Figs. 10 and 11, respectively. The nominal

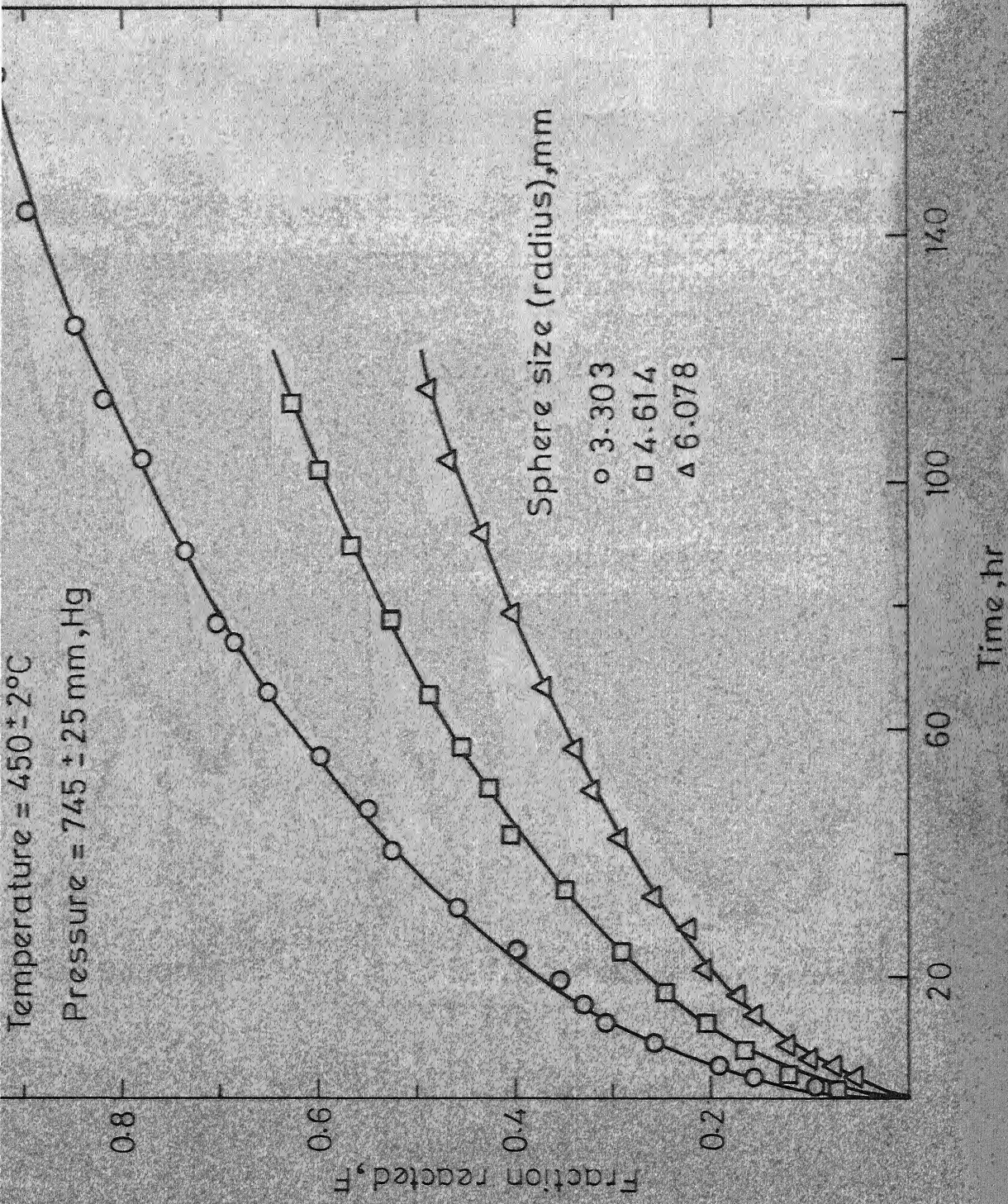


FIG. 10 EFFECT OF SPHERE SIZE ON THE RATE OF FORMATION OF SODIUM HEXACHLORO ZIRCONATE

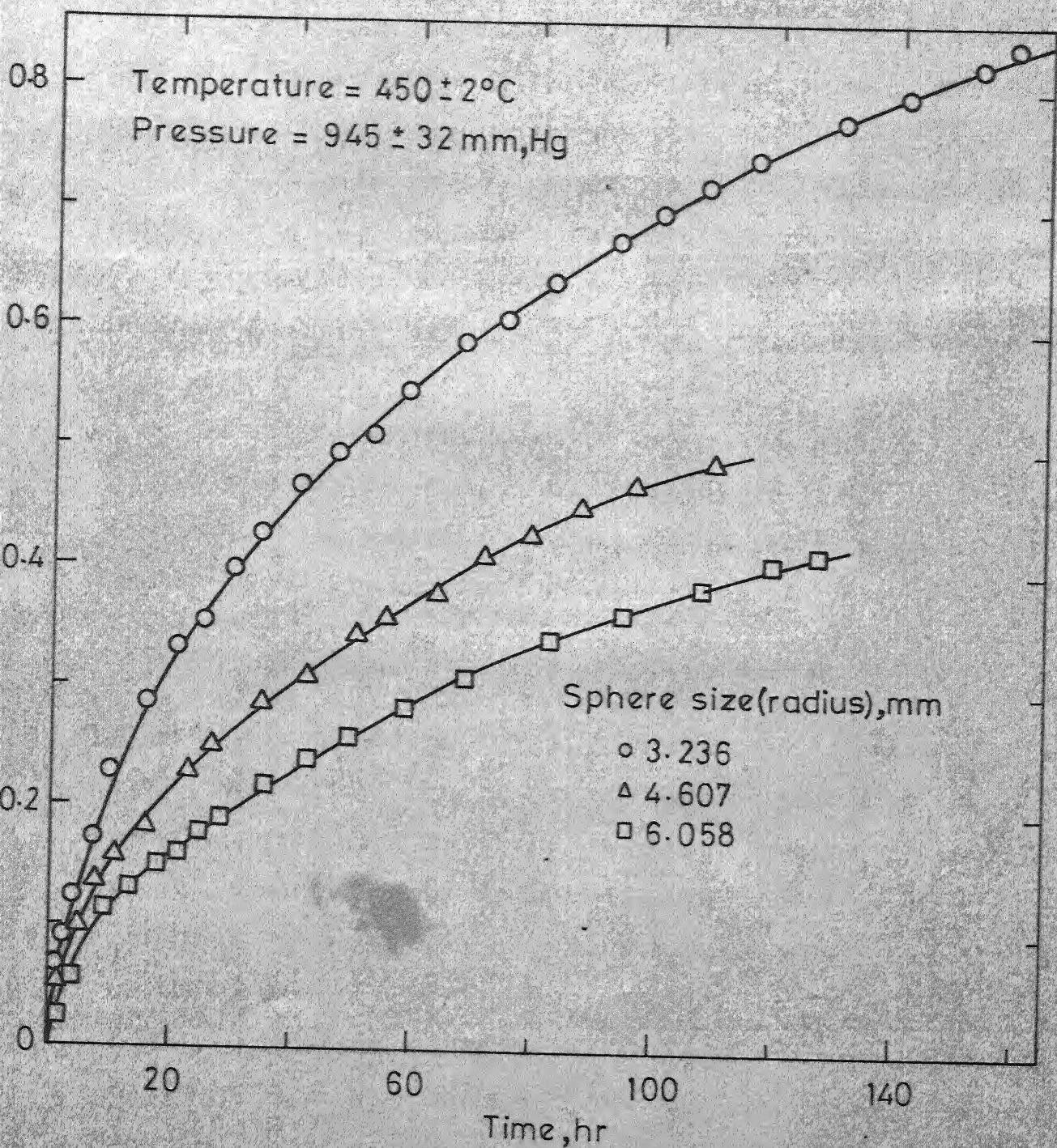


FIG. 11 EFFECT OF SPHERE SIZE ON THE RATE OF FORMATION OF SODIUM HEXACHLORO HAFNATE

diameters of the spheres used in these runs were 6.6, 9.2 and 12.2 mm. The figures show that the rate of reaction increases rapidly with decreasing sphere size.

Figures 12 and 13, respectively, show the effect of the vapour pressure of zirconium and hafnium tetrachlorides on the formation of corresponding sodium hexachloro compounds. The rate enhancing influence of the gas pressure is evident from both the figures.

As expected, the reaction temperature also had similar influence on the reaction rate. The rate of formation of both the zirconium and hafnium compounds increased with temperature. Figures 14 and 15 show the time-conversion plots for the formation of zirconate and hafnate, respectively.

It is to be noted that in most cases reactions have not been carried out to very high percentages. Various experimental difficulties arising out of the slow nature of the reactions, prevented conduction of reactions upto very high extents. Reactions were so slow that even under favourable kinetic conditions, conversion of 50 per cent of the reactant solid to hexachloro zirconate took about 120 hours (at 745 mm, Hg and 450.5°C). The time needed to attain similar conversion for the hafnium reaction was even more. For the same reason, composite runs were taken in which step changes in the reaction condition were introduced in a continuing run. The kinks in some of the conversion-time plots as well as corresponding model fitting plots are due to the adoption of this procedure of step change

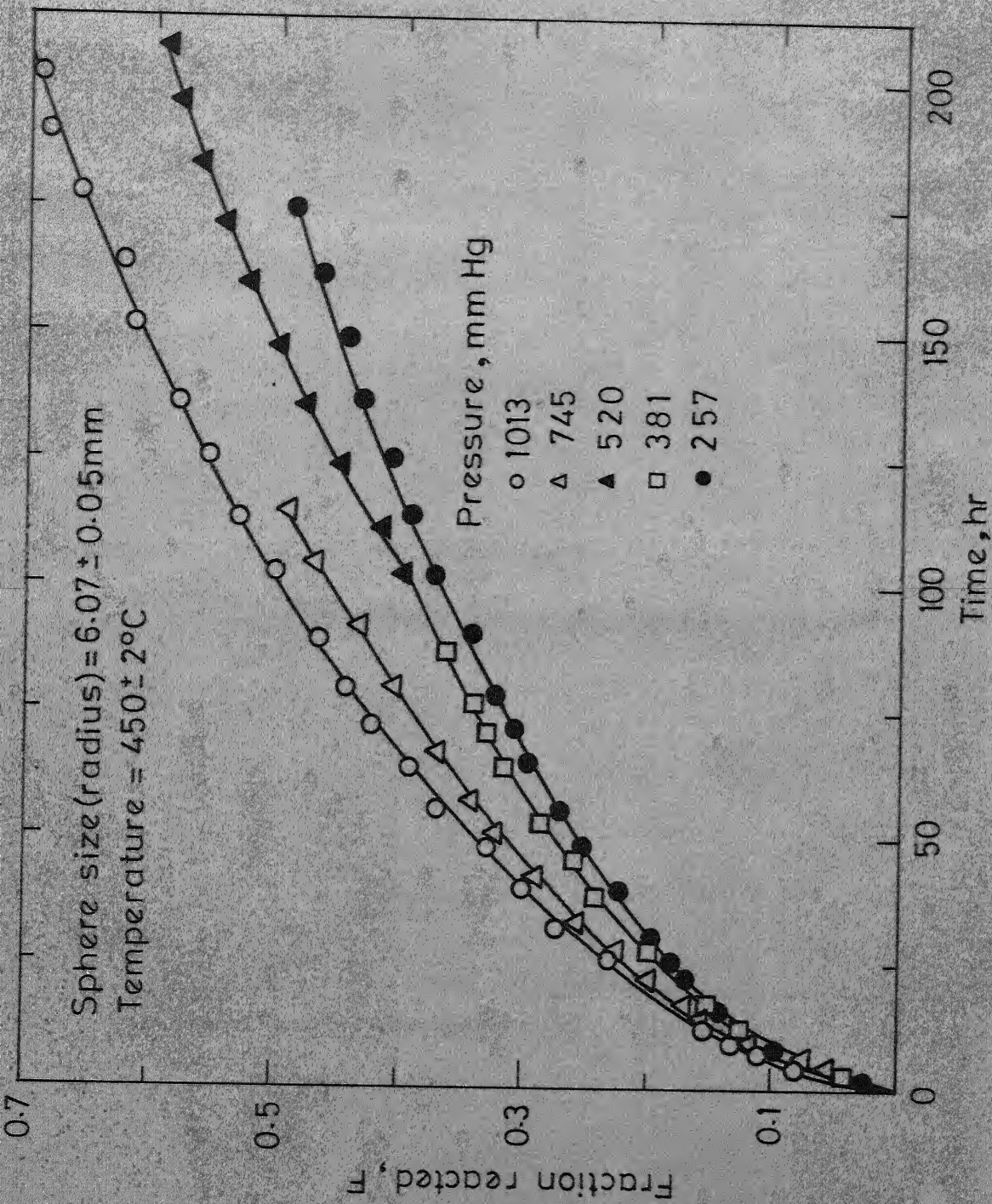


FIG. 12 EFFECT OF PRESSURE ON THE RATE OF FORMATION OF SODIUM HEXACHLORO ZIRCONATE

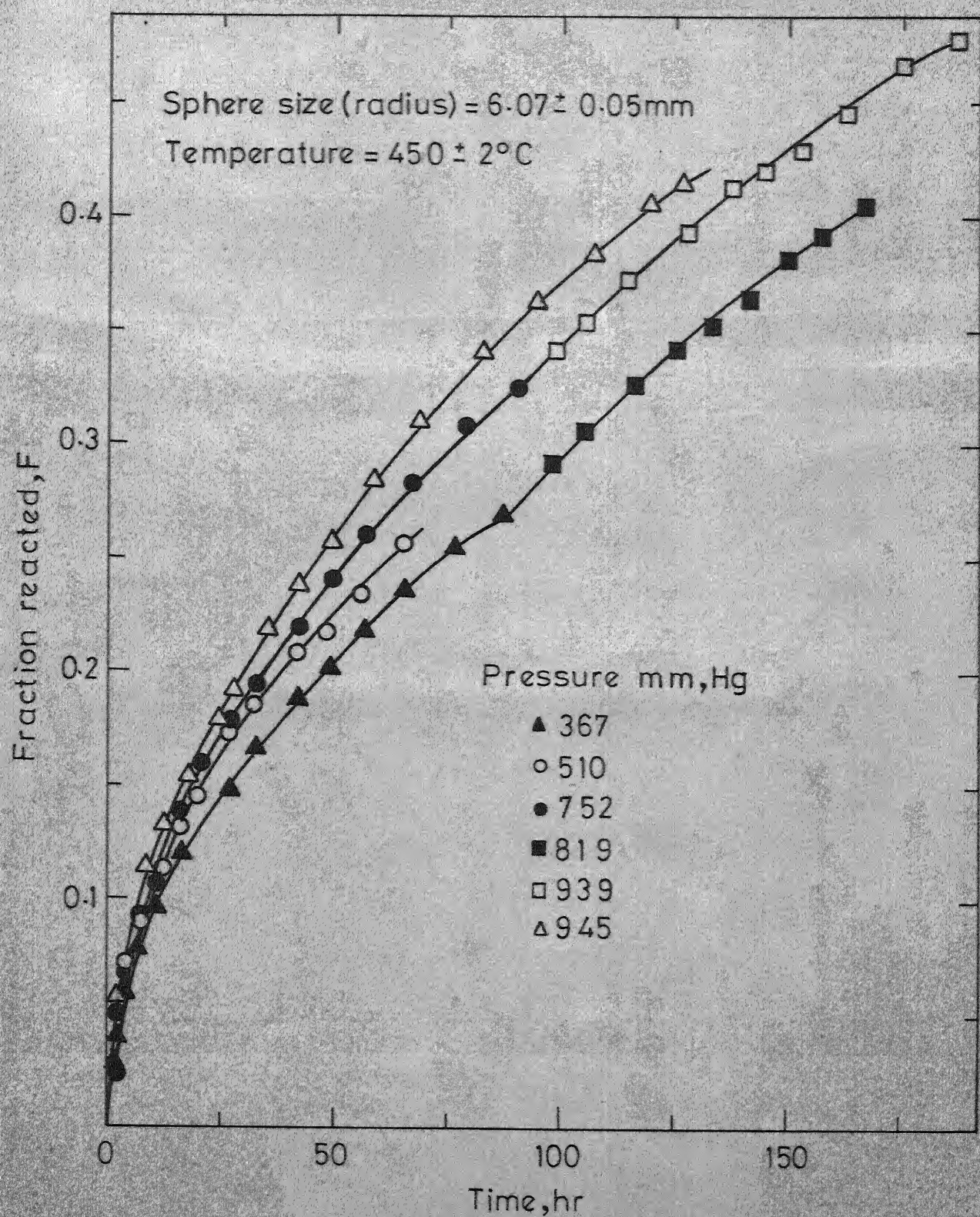


FIG. 13 EFFECT OF PRESSURE ON THE RATE OF FORMATION OF SODIUM HEXACHLORO HAFNATE

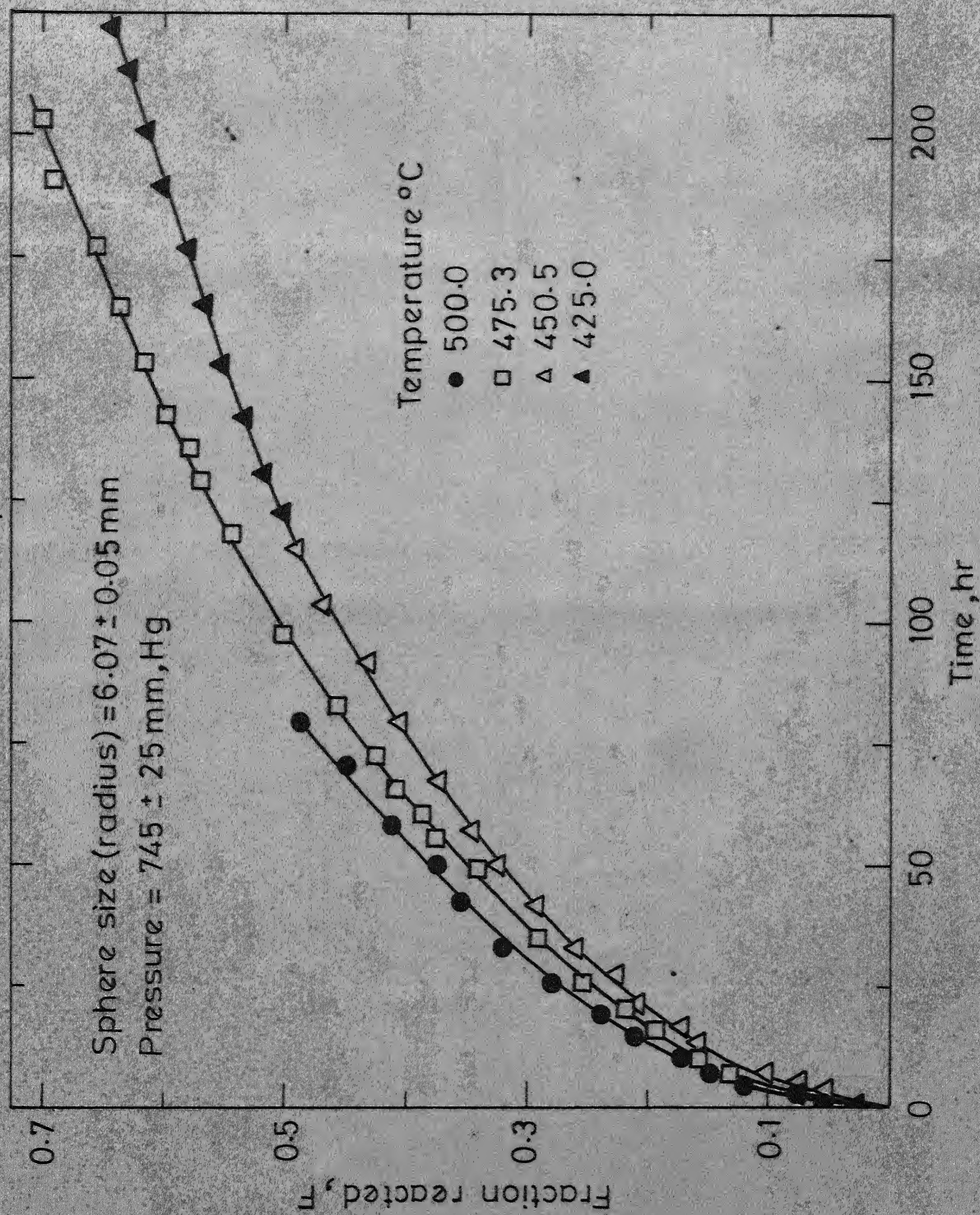


FIG. 14 EFFECT OF TEMPERATURE ON THE RATE OF FORMATION OF SODIUM HEXACHLORO ZIRCONATE

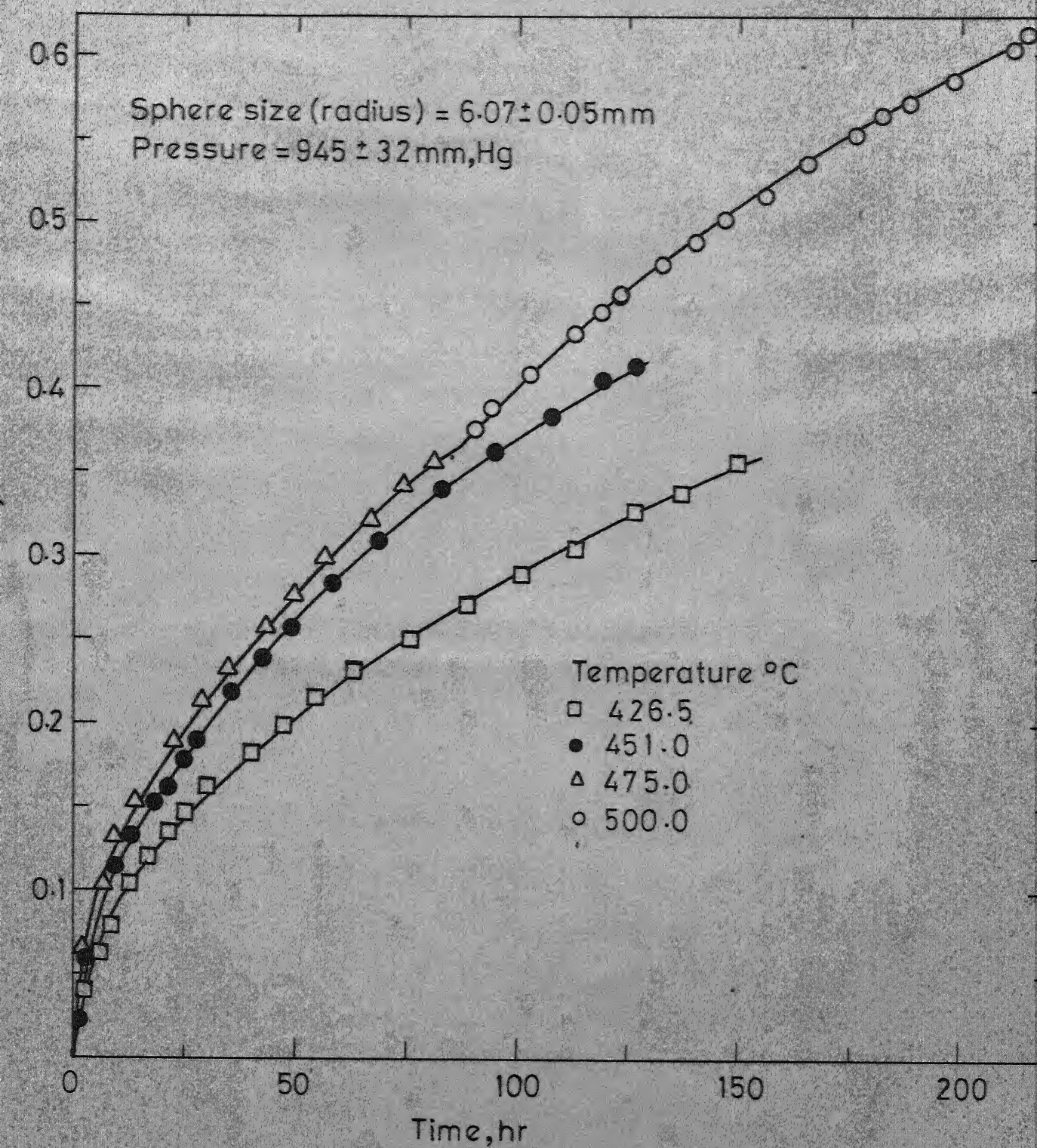


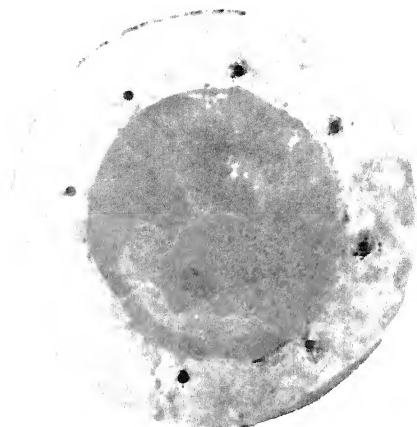
FIG. 15 EFFECT OF TEMPERATURE ON THE RATE OF FORMATION OF SODIUM HEXACHLORO HAFNATE

in the reaction condition. The rate constant calculated from the second part of such a run remains true representative of the reaction under the changed condition provided the reaction mechanism is not a function of the extent of reaction. That the reaction mechanism did not change with conversion was verified from the excellent fit of the kinetic data to the Carter⁴³-Valensi⁴⁴ model for conversion as high as 90 per cent (Figs. 18 and 19, to be discussed). Moreover, when an experiment conducted with a new sodium chloride sample was repeated after effecting step change in a continuing run to same pressure and temperature condition, nearly identical rate constant value was obtained. This further confirms the validity of the composite runs in the present systems.

4.4 Marker results

Figs. 16 and 17 show macro photographs of two reacted marker specimens. The photographs show the sharp interface between the product layer and the unreacted core. The black dots around the unreacted core-product interface are heads of the inert quartz markers.

Although the markers stayed embedded within the product layer, they were found to be displaced from their original positions. In the case of reaction of sodium chloride with the vapour of zirconium tetrachloride as shown in Fig. 16, the average marker movement recorded was 0.75 mm. The experimental conditions were 450°C, 257 mm. Hg and 174.5 hours reaction time.

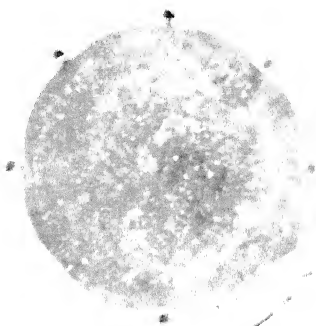


mdar, Sibnath

action kinetics in the system
 (f) $Cl_2 - NaCl$. Supervised by
 ay and P.C. Kapur. Kampus,
 1974.

Ap.
 thesis: (Ph.D) H.T. Kampus

ed marker
 tetrachloride
 x.)



Reaction conditions:

Temperature = 450.5°C

Gas pressure = 939 mm, Hg

Time of reaction = 109.5 hr

Fig. 17 Macro-photograph of partially reacted marker specimen (reaction with hafnium tetrachloride vapour); Magnification - 3.5 (approx.)

The markers were found to have moved towards the sodium chloride core. In the case of reaction with hafnium tetrachloride also, the markers moved in the same direction. The average inward marker movement for reaction at 450.5°C and 939 mm pressure and for 109.5 hours of reaction was 0.42 mm. The direction of the marker movement indicates that, in all likelihood, the matter transport occurs from the inner reactant-product interface to outer gas-solid interface by lattice diffusion mechanism.

4.5 Kinetic models

In view of the sharp reaction interface shown in Figs. 16 and 17 for the formation of Na_2ZrCl_6 and Na_2HfCl_6 , respectively, only those reaction models which are specific to this situation were tested against the conversion-time data. Figs. 18 and 19 show rate curves plotted according to several single step controlled rate equations for the zirconium and hafnium runs, respectively. In order to obtain an unambiguous discrimination, the models were tested against data from those runs which were carried to about 90 per cent reaction. The different rate equations tested are listed below.

Phase boundary control⁹⁸: $1 - (1-F)^{1/3} = K_p t$ [4.1]

Product phase transport control:

Jander's equation⁴⁸ $[1 - (1-F)^{1/3}]^2 = K_j t$ [4.2]

Crank⁴⁵-Ginstling and Brounshtein⁴⁶ equation

$$1 - \frac{2}{3} F - (1-F)^{2/3} = K_{cgb} t$$
 [4.3]

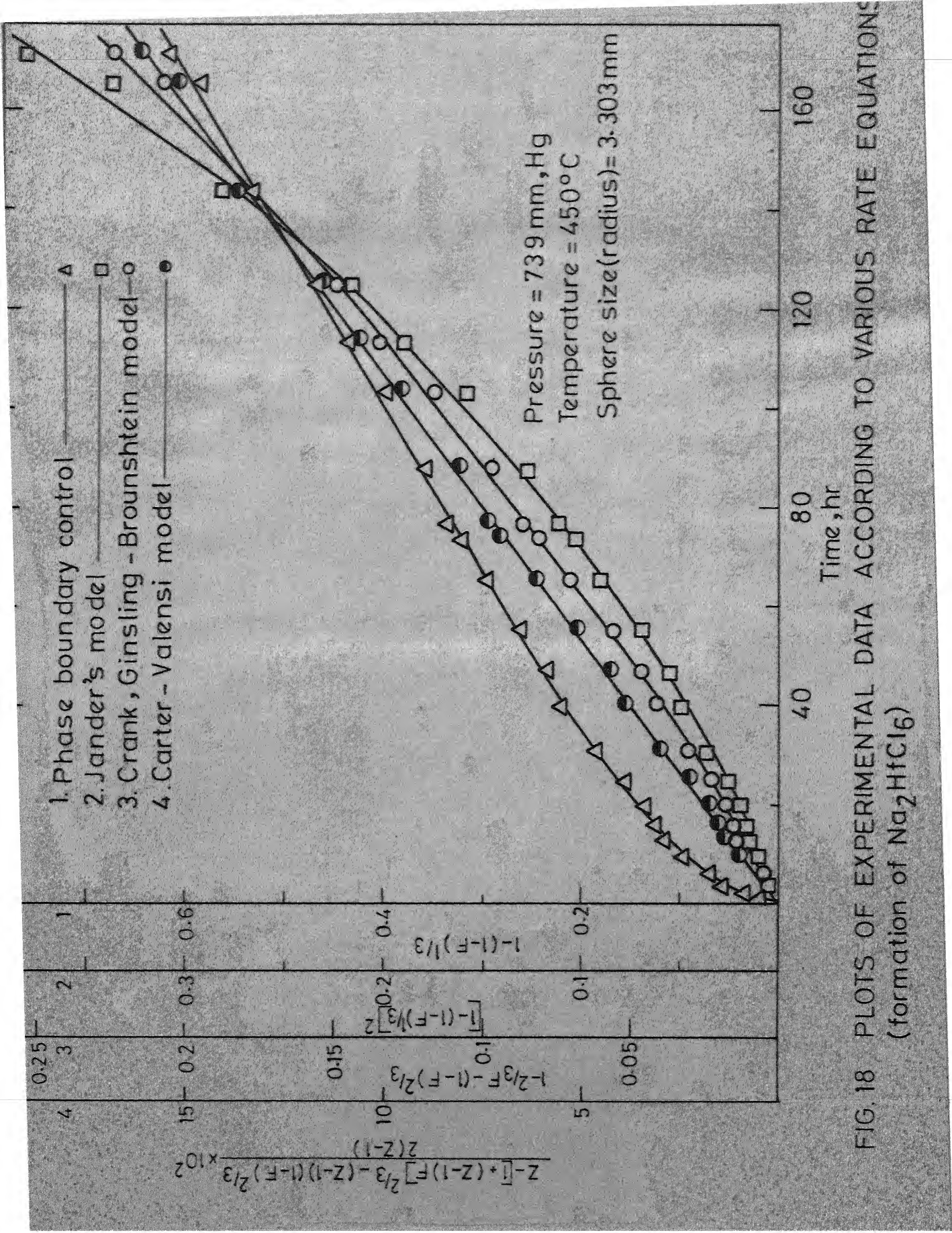


FIG. 18 PLOTS OF EXPERIMENTAL DATA ACCORDING TO VARIOUS RATE EQUATIONS
(formation of Na_2HfCl_6)

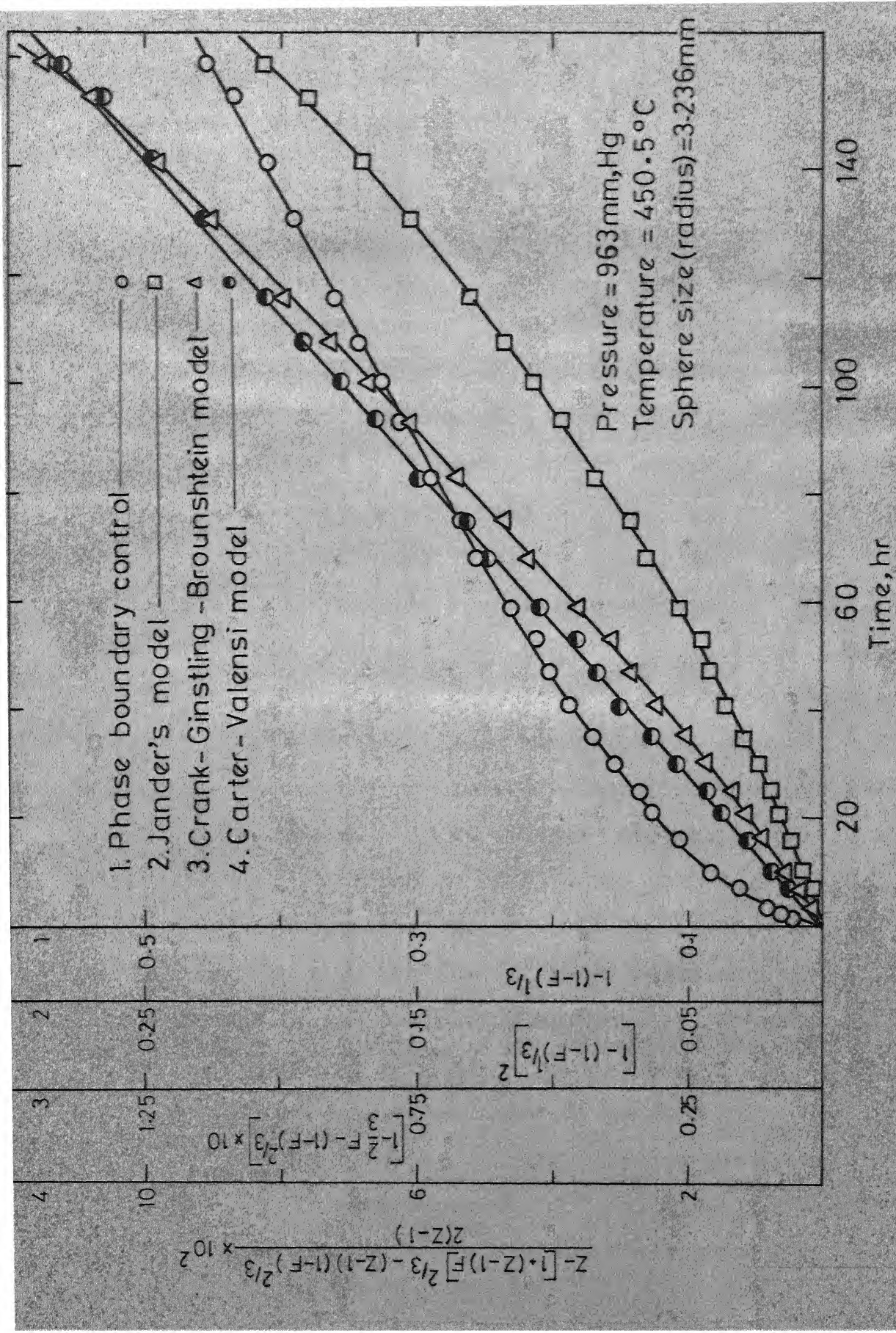


FIG. 19 PLOTS OF EXPERIMENTAL DATA ACCORDING TO VARIOUS RATE EQUATIONS (formation of Na_2HfCl_6)

Carter⁴³-Valensi⁴⁴ equation

$$\frac{Z - [1 + (Z-1)F]^{2/3} - (Z-1)(1-F)^{2/3}}{2(Z-1)} = K_{cv}t \quad [4.4]$$

The figures show excellent fit only to Carter⁴³-Valensi⁴⁴ product phase transport control model. Phase boundary control rate equations as well as other transport control rate expressions failed to represent the rate data over the full range.

Of special significance is the failure of the phase boundary reaction controlled rate equation almost right from the start of the reaction. This may be contrasted with the experiences in the case of reactions resulting in porous product layer. For these cases, it has been stated in several recent publications^{40,42} that the rate data pertaining to product phase transport or mixed control case may follow the pattern predicted by chemical reaction control till a fairly high percentage of reaction is completed. In our system this phenomenon is almost totally absent. This may be seen in the context of much slower solid state diffusion that prevails in the present systems. On the contrary for reaction systems with porous reaction products, where much faster gaseous diffusion prevails, comparability of gaseous diffusion and rate of chemical reaction presumably leads to confusion regarding broad controlling mechanism.

Of further importance in the present systems is the failure of all transport controlled models except the Carter⁴³-Valensi⁴⁴ model, which. for both hafnium and zirconium hexachloro

compound formation, could be fitted to the experimental data over almost the complete range of reaction. Transport control models due to Crank⁴⁵-Ginstling and Brounshtein⁴⁶ as well as Jander⁴⁸ failed to conform to the reaction behaviour even during the early stages. This is quite expected, since, unlike Carter-Valensi model, the models due to Jander, Crank-Ginstling and Brounshtein were derived on the assumption of constant sphere size, which is invalid in the present case. Earlier, Carter⁴⁷ had pointed out the prominent role of swelling in determining the reaction pattern, especially if Z value exceeds 2. It may be seen that the performance of the Jander's model is poorer compared to that due to Crank - Ginstling and Brounshtein. This is because of the additional assumption made in Jander's model regarding area of product-reactant interface. Jander assumed reactant-product interface area also to remain constant. This assumption, though is approximately valid in the initial stages of the reaction, particularly for reactions involving large spheres, is not generally true for reactions in spherical geometry.

All the experimental data for the formation of Na_2ZrCl_6 and Na_2HfCl_6 are plotted in Figs. 20 to 25 according to the Carter-Valensi rate expression. These figures also show the effect of variations in the different reaction parameters on the slopes of the plots. Consistently good fit to the Carter-Valensi rate expression was obtained in all the plots. Carter-Valensi rate constant, which is given by the slope of these plots, is expressed as

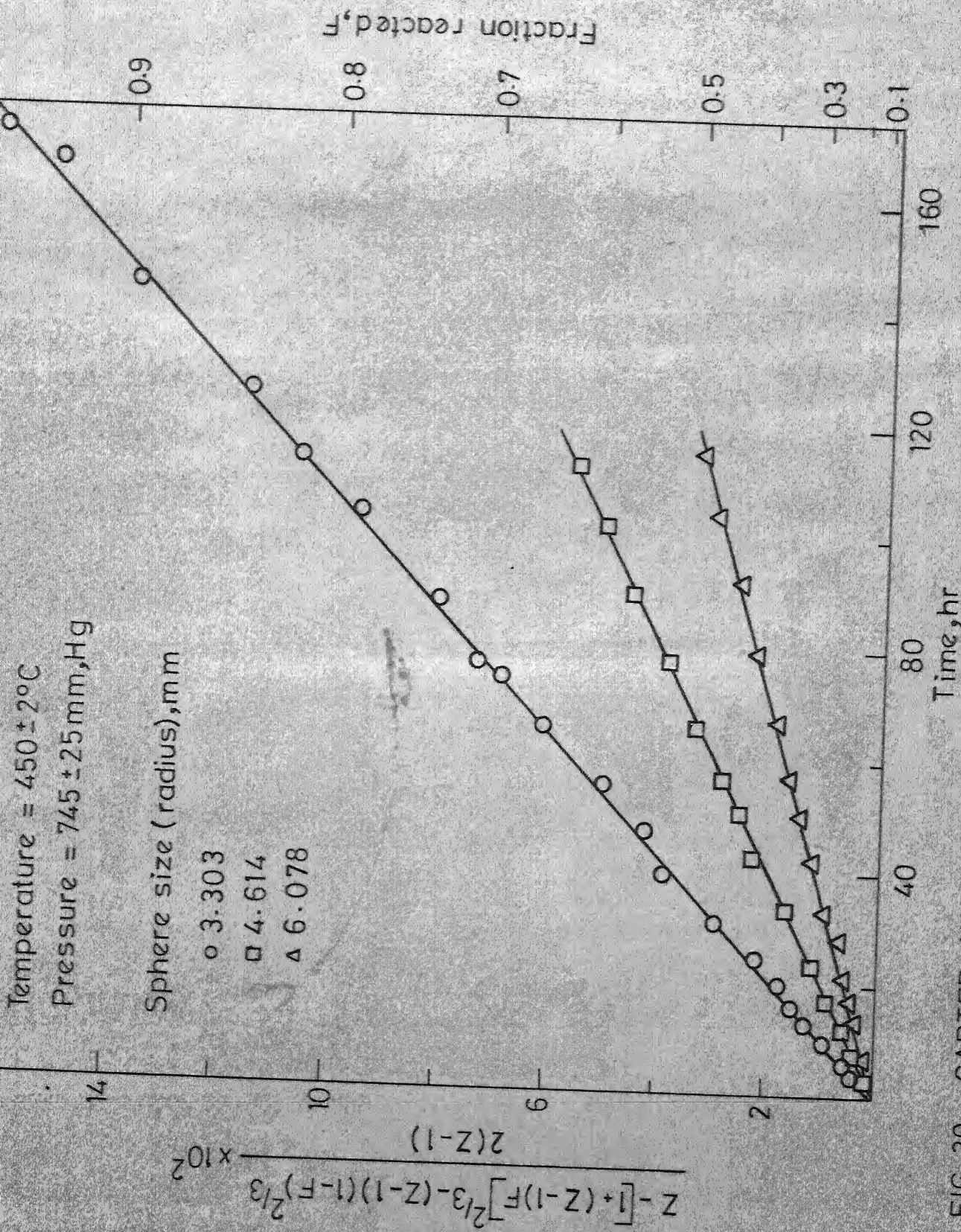
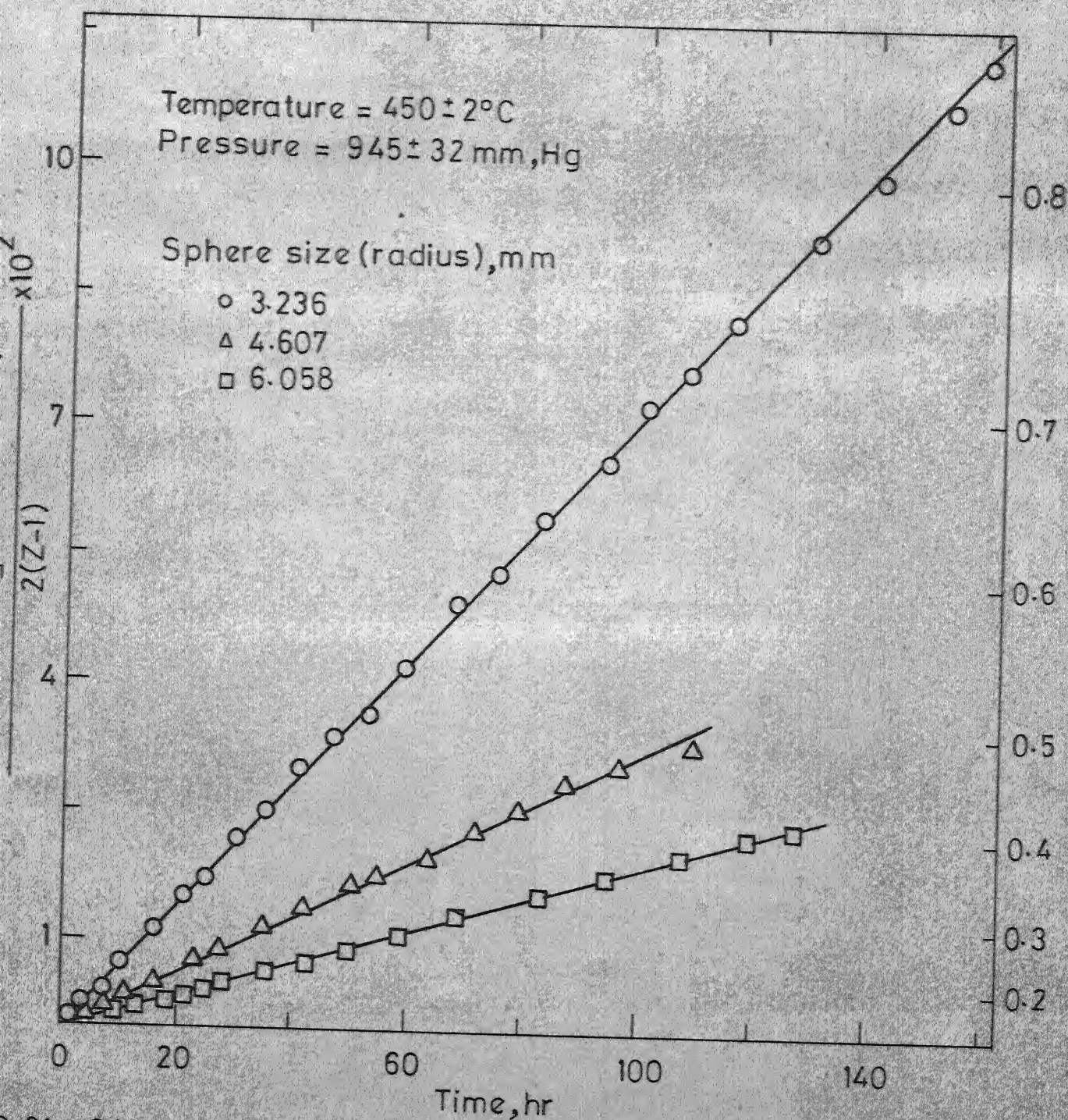


FIG. 20 CARTER-VALENSI PLOT SHOWING THE EFFECT OF SPHERE SIZE ON THE RATE OF FORMATION OF NO₂



6.21 CARTER-VALENSI PLOT SHOWING THE EFFECT OF SPHERE SIZE ON THE RATE OF FORMATION OF Na_2HfCl_6

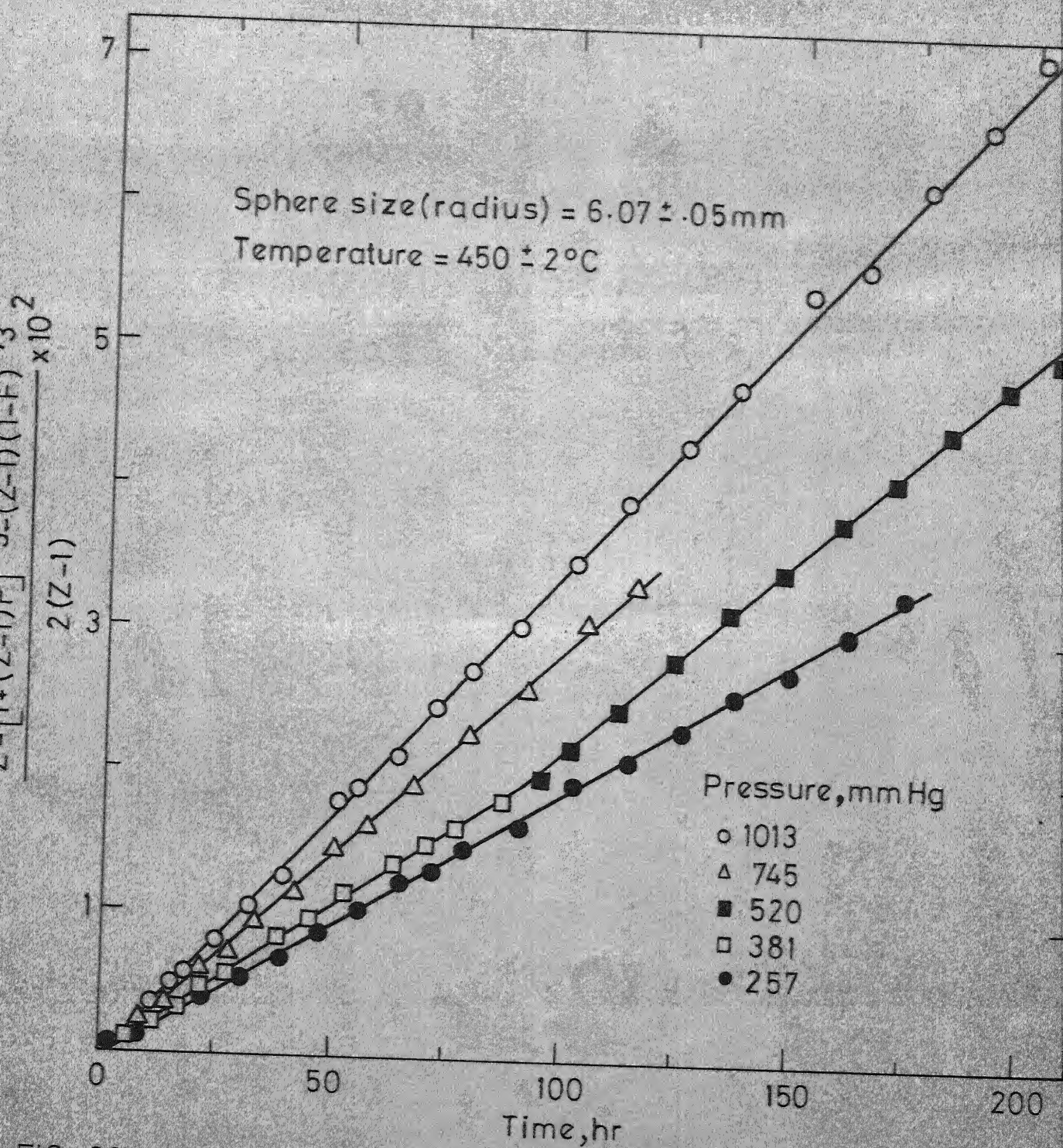
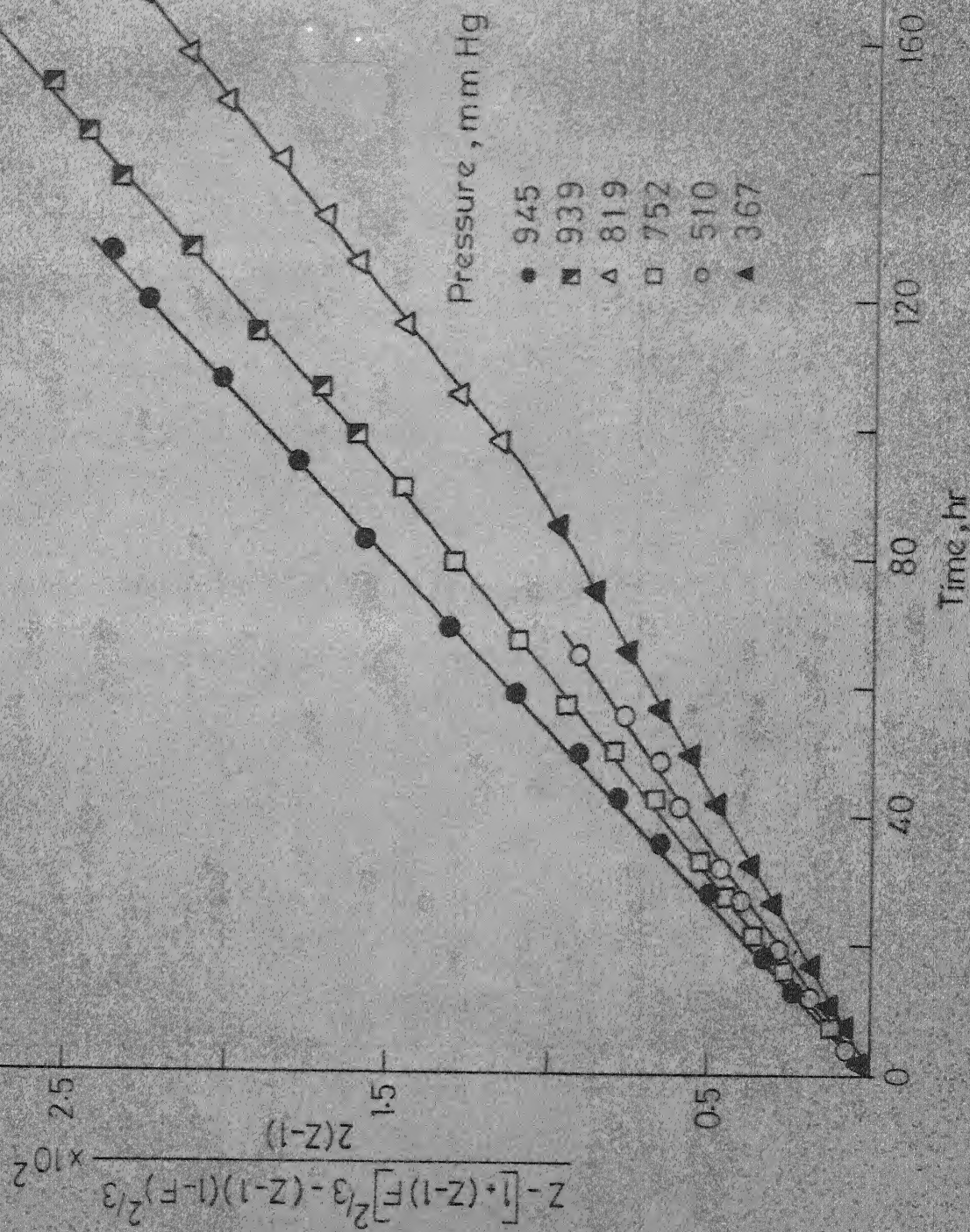


FIG. 22 CARTER-VALENSI PLOT SHOWING THE EFFECT OF PRESSURE ON THE FORMATION OF Na_2ZrCl_6

Sphere size (radius) = 6.07 ± 0.05 mm
 Temperature = $450 \pm 2^\circ\text{C}$



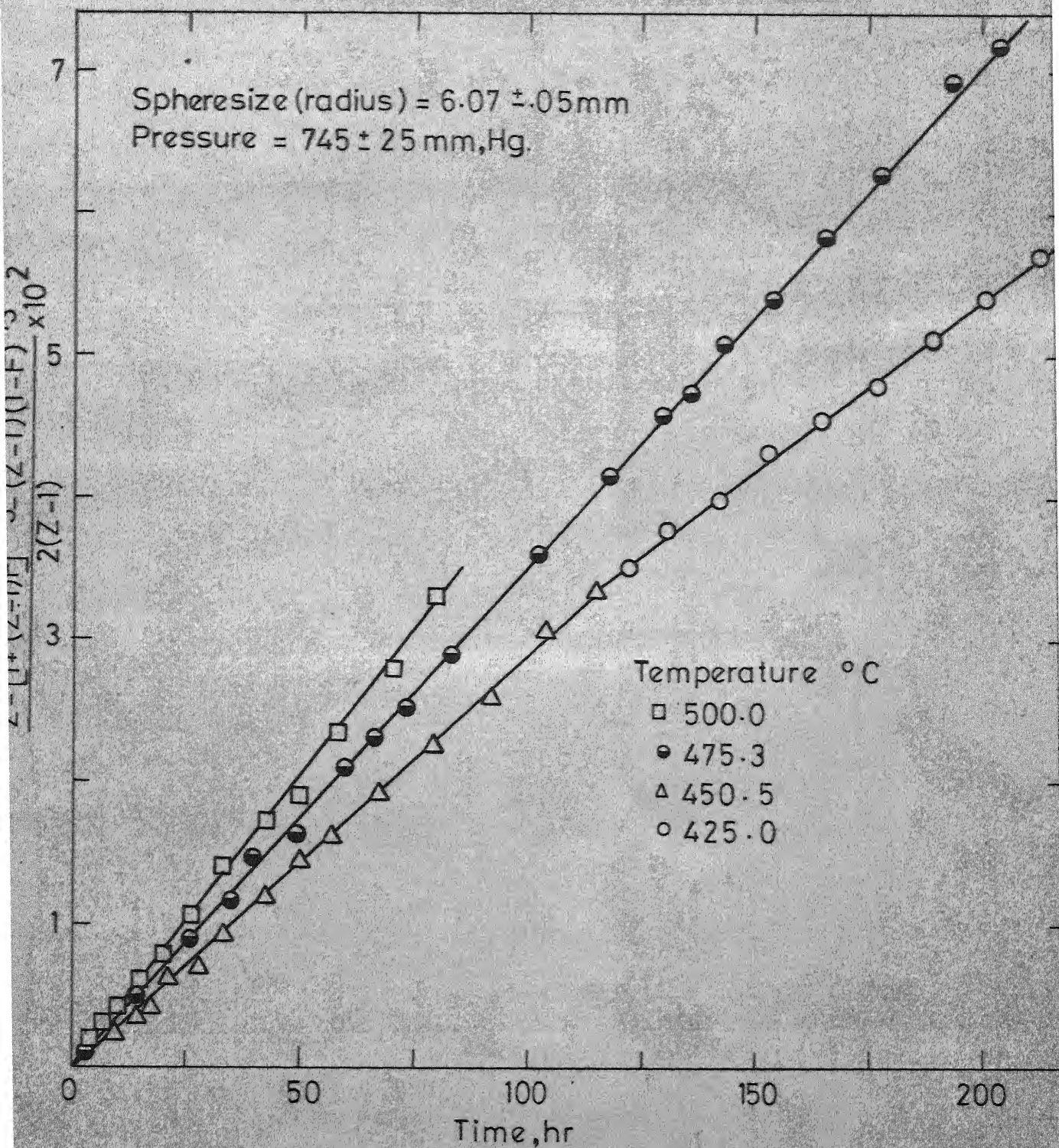


FIG. 24 CARTER-VALENSI PLOT SHOWING THE EFFECT OF TEMPERATURE ON THE FORMATION OF Na_2ZrCl_6

$$K_{cv} = \frac{K}{R_o^2} = \frac{D_v M_r C_v^g}{r R_o^2} \quad [4.5]$$

The rate constants so obtained are used in further kinetic analysis. The values of the rate constants obtained by least squares fit to the reaction data are given in Tables IV and V. A major advantage of fitting the kinetic data to the reaction model is that the specific rate constant, K_{cv} , can be used for evaluation of the effect of reaction parameters on a consistent basis which is explicitly independent of the extent of reaction or the reaction time.

It is to be noted that the Carter-Valensi equation was originally derived for matter transport from the outer solid-gas interface to the inner product-reactant interface. On the other hand, there is sufficient indication to show that in both systems under investigation, matter transport occurred in the opposite direction. This, however, does not affect the applicability of the Carter-Valensi equation, since the same mass flux equation applies to transport in either direction. That this indeed is the case is shown in Section 5.6 by rederiving the Carter-Valensi rate equation using vacancy flux. In Section 4.7, it is discussed that the product phase transport in the present systems involves simultaneous migration of vacancies towards the unreacted core. Thus the surface concentration C_v^g and diffusivity D_v in Eq. [4.5] refer to the slowest moving vacancy migrating inwards.

Table IV. Carter-Valensi rate constants for the formation of
 Na_2ZrCl_6

Effect of	Sphere size (radius) R_0 mm	Temperature $^{\circ}\text{C}$	Pressure P_{ZrCl_4} mm, Hg	Rate constant $K_{\text{cv}} \times 10^4, \text{hr}^{-1}$
Pressure	6.041	450.0	257	1.757
	6.089	451.0	381	2.158
	6.089	451.0	520	2.630
	6.078	450.5	745	2.968
	6.087	450.5	1013	3.560
Temperature	6.078	425.0	745	2.375
	6.078	450.5	745	2.968
	6.075	475.3	753	3.456
	6.089	500.0	734	4.031
Sphere size	3.303	450.0	739	9.575
	4.614	451.0	753	5.027
	6.078	450.5	745	2.968

Table V. Carter-Valensi rate constants for the formation of
 Na_2HfCl_6

Effect of	Sphere size (radius) R_0 mm	Temperature $^{\circ}\text{C}$	Pressure P_{HfCl_4} mm, Hg	Rate constant $K_{\text{cv}} \times 10^4, \text{hr}^{-1}$
Pressure	6.085	450.5	367	1.145
	6.090	450.0	510	1.337
	6.059	450.5	752	1.622
	6.085	450.5	819	1.668
	6.059	450.5	939	1.788
	6.058	451.0	945	1.804
Temperature	6.075	426.5	933	1.204
	6.058	451.0	945	1.804
	6.059	450.5	939	1.788
	6.044	475.0	954	2.431
	6.044	500.0	954	2.713
Sphere size	3.236	450.5	963	7.043
	4.607	450.5	939	3.223
	6.059	450.5	939	1.788
	6.058	451.0	945	1.804

4.6 Effect of reaction parameters on kinetics of reaction

4.6.1 Effect of sphere size

Figs. 26 and 27 show the effect of the size of the sodium chloride sphere on the rate constant. The computed slope values 1.92 and 2.12 for the zirconium and the hafnium cases, respectively, compares well with the value of 2 expected from Eq. [4.5]. These results are, therefore, consistent with the Carter-Valensi model.

4.6.2 Effect of temperature

The effect of temperature on the specific rate constant is shown in Figs. 28 and 29, where Arrhenius type of equation relating the rate constant to the temperature of reaction is plotted. In the case of the formation of hexachloro compound of hafnium, shown in Fig. 29, the overall plot shows a distinct deviation from linearity. Apart from the failure of the Arrhenius equation, the deviation may be attributed to various polymorphic transformations of the reaction product in the temperature range studied. The phase diagram of the NaCl-HfCl_4 system⁵ reproduced in Fig. 2, show polymorphic transformations of Na_2HfCl_6 at 384° , 440° and 484°C ; these being $\alpha \rightarrow \beta$, $\beta \rightarrow \gamma$ and $\gamma \rightarrow \delta$, respectively. Stability range of the three polymorphic forms are also shown in Fig. 29. On the other hand, the zirconium compound does not show any transformation in the temperature interval ($425\text{--}500^\circ\text{C}$) investigated in the present work.

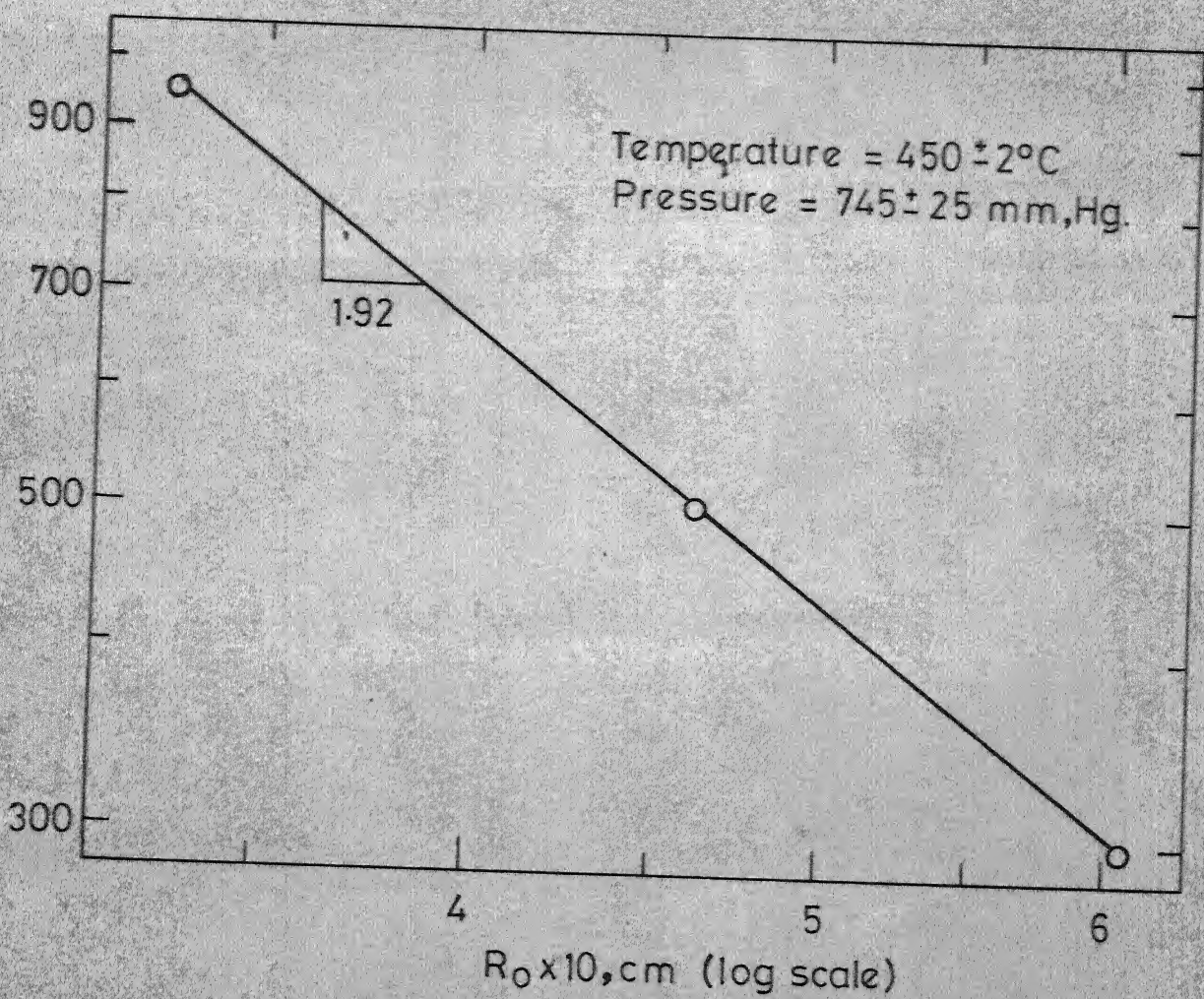


FIG. 26 EFFECT OF SPHERE SIZE ON THE RATE CONSTANT K_{ev} (formation of Na_2ZrCl_6)

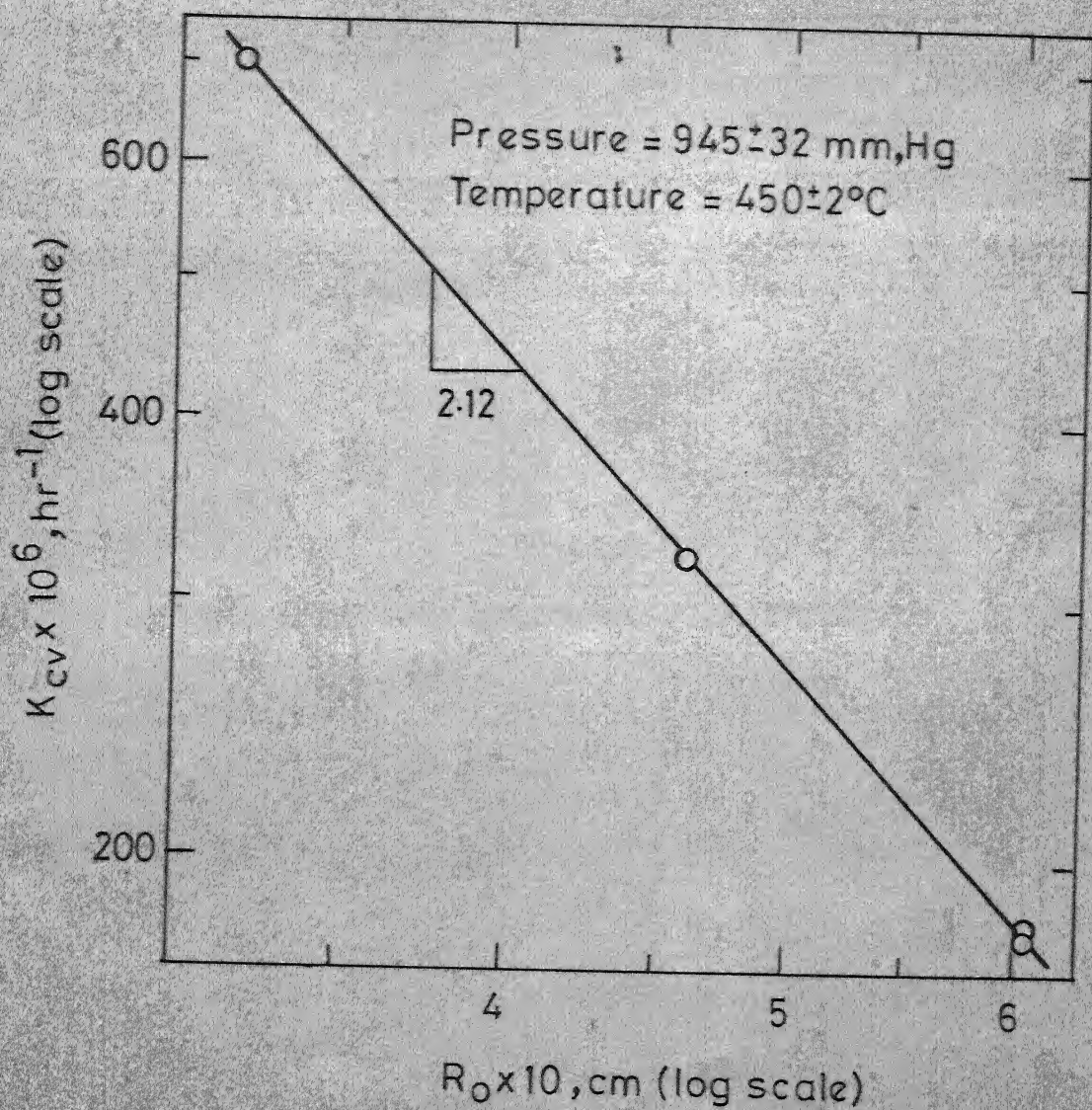


FIG. 27 EFFECT OF SPHERE SIZE ON RATE CONSTANT K_{cv}
(formation of Na_2HfCl_6)

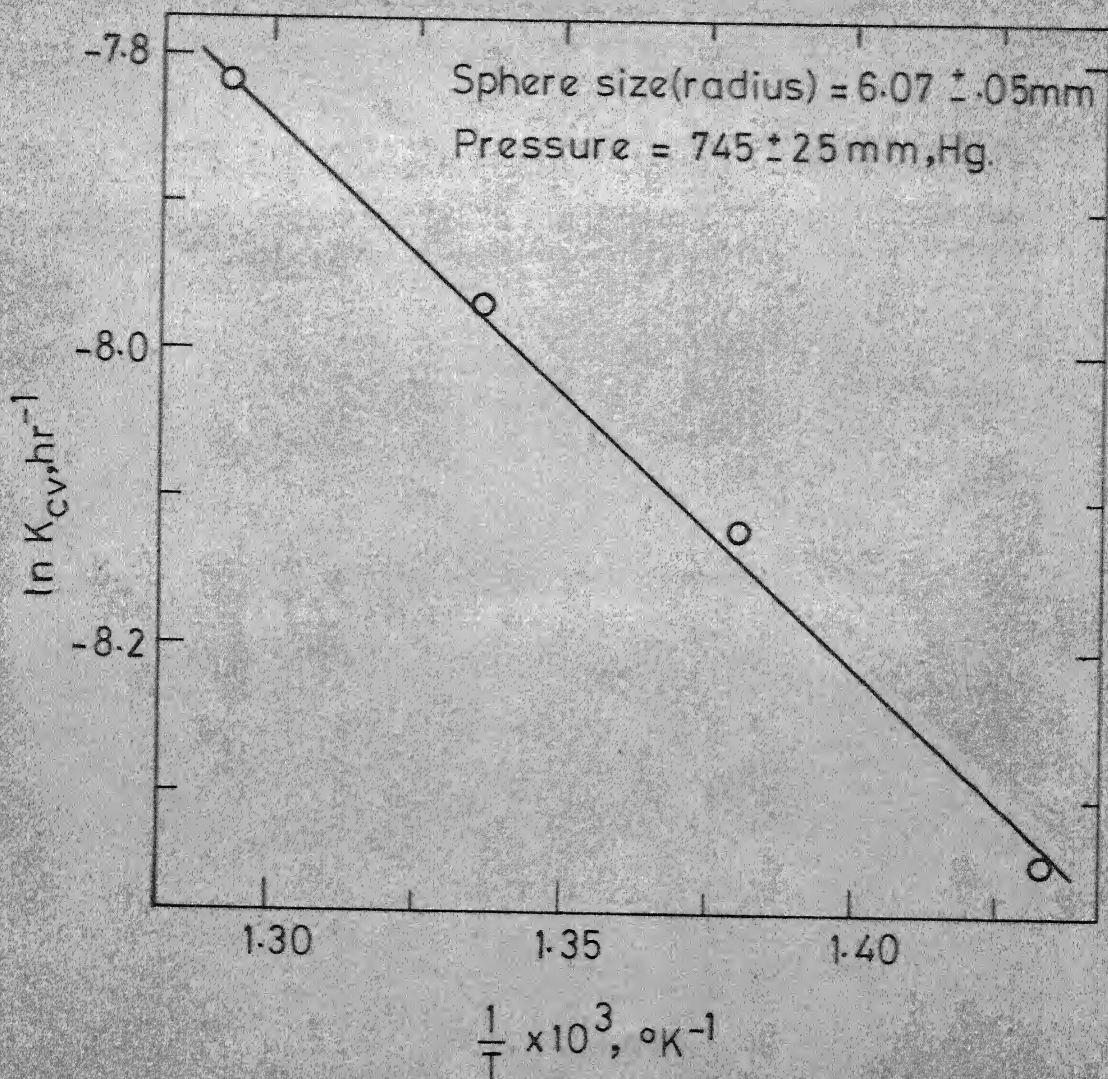


FIG. 28 EFFECT OF TEMPERATURE ON RATE CONSTANT K_{cv} (formation of Na_2ZrCl_6)

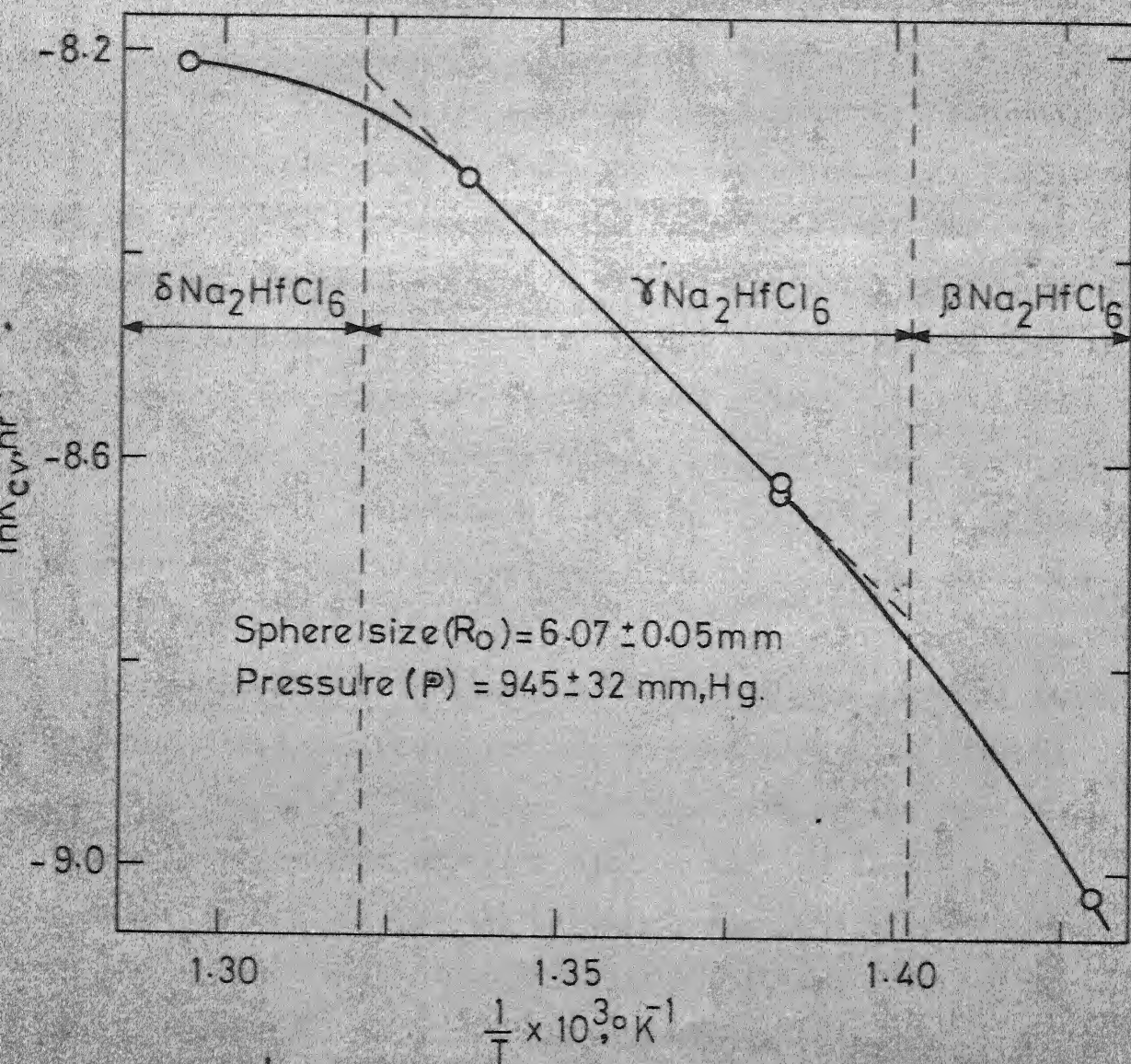


FIG. 29 EFFECT OF TEMPERATURE ON RATE CONSTANT K_{cv}
 (formation of Na_2HfCl_6)

However, Na_2ZrCl_6 undergoes polymorphic transformation at 341 and 377°C (cf. Fig. 1), which are well below the lowest temperature used.

From the measured slope of the linear plot shown in Fig. 28, the temperature coefficient (apparent activation energy) of the ZrCl_4 -NaCl reaction in the range 425-500°C was computed. Because of the nonlinearity, similar calculation for the HfCl_4 -NaCl reaction was possible only in the γ -phase region i.e. in the temperature range 440 to 484°C. The temperature coefficients for the zirconium and the hafnium reactions in the temperature range stipulated above, were estimated to be 7.5 and 13 kcal/mole, respectively. The reaction pressures in these two cases were 745 and 945 mm, Hg, respectively. Earlier, Luthra⁹⁹ using the same experimental technique but at 1033 mm, Hg pressure obtained a value of 9.9 kcal/mole for the zirconium case in the same temperature range. The other investigation in the zirconium tetrachloride-sodium chloride system resulted in a value of 12.3 kcal/mole³⁴ in the temperature range 399 to 504°C and under 600 mm, Hg pressure. This value, however, was obtained for a single crystal plate of sodium chloride in contrast to the polycrystalline solids used in the Luthra's⁹⁹ and the present work. No earlier work has been reported on the temperature effect for the hafnium system.

4.6.3 Effect of pressure

The effect of tetrachloride pressure on the rate of

formation of Na_2ZrCl_6 and Na_2HfCl_6 , both at 450°C , are shown in the log-log plot depicted in Figs. 30 and 31, respectively. The straight line plot in both cases suggest a power relationship between the gas pressure and the rate constants. Empirically the pressure effect can be represented by

$$K_{cv} \propto P^{1/n} \quad [4.6]$$

where the pressure coefficient n , for zirconium and hafnium case, respectively, have values 1.98 and 2.13. Values of n were obtained from the slopes of the plots given in Figs. 30 and 31. Earlier Pint and Flengas³⁵ had studied the pressure effect for both zirconium and hafnium tetrachloride reactions. The zirconium reactions were reported to follow $1/2.8^{\text{th}}$ power of the tetrachloride pressure at 485°C . For the same reaction at 500°C Luthra⁹⁹ found n to be equal to 2.4. These values may be compared to the present value of 1.98.

For the reaction involving hafnium tetrachloride, however, pressure coefficient at 485°C reported by Pint and Flengas³⁵ is much different than that obtained in our investigation. While we found that n equals 2.13, Pint et. al.³⁵ reported a value of 4.1. This discrepancy presumably arises from different polymorphic forms of the reaction product Na_2HfCl_6 , encountered in the two investigations. Phase diagram of the system NaCl-HfCl_4 ⁵ shows $\gamma \rightarrow \delta$ transformation at 484°C . It is to be noted that while in the present work pressure effect

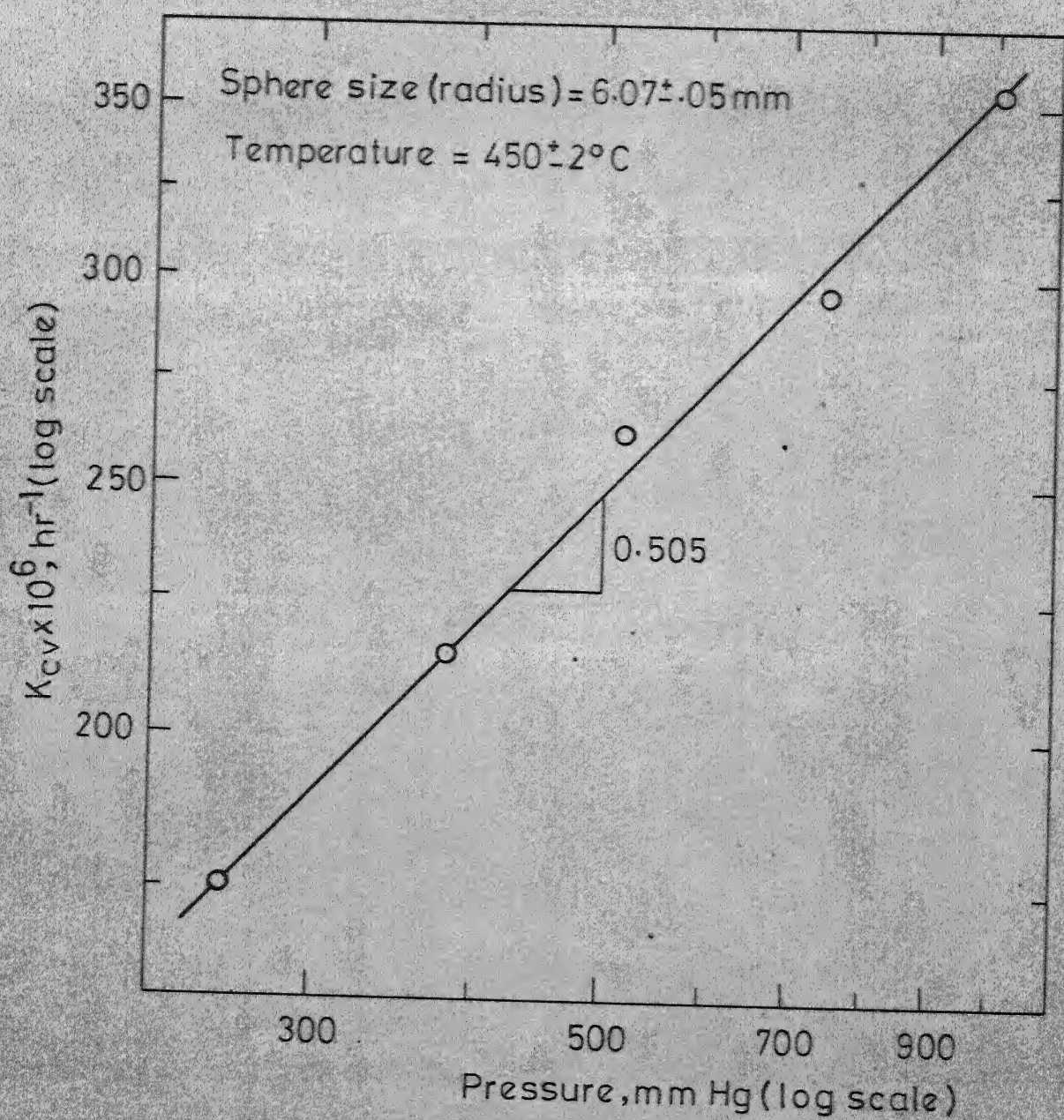


FIG. 30 EFFECT OF PRESSURE ON RATE CONSTANT K_{cv}
(formation of Na_2ZrCl_6)

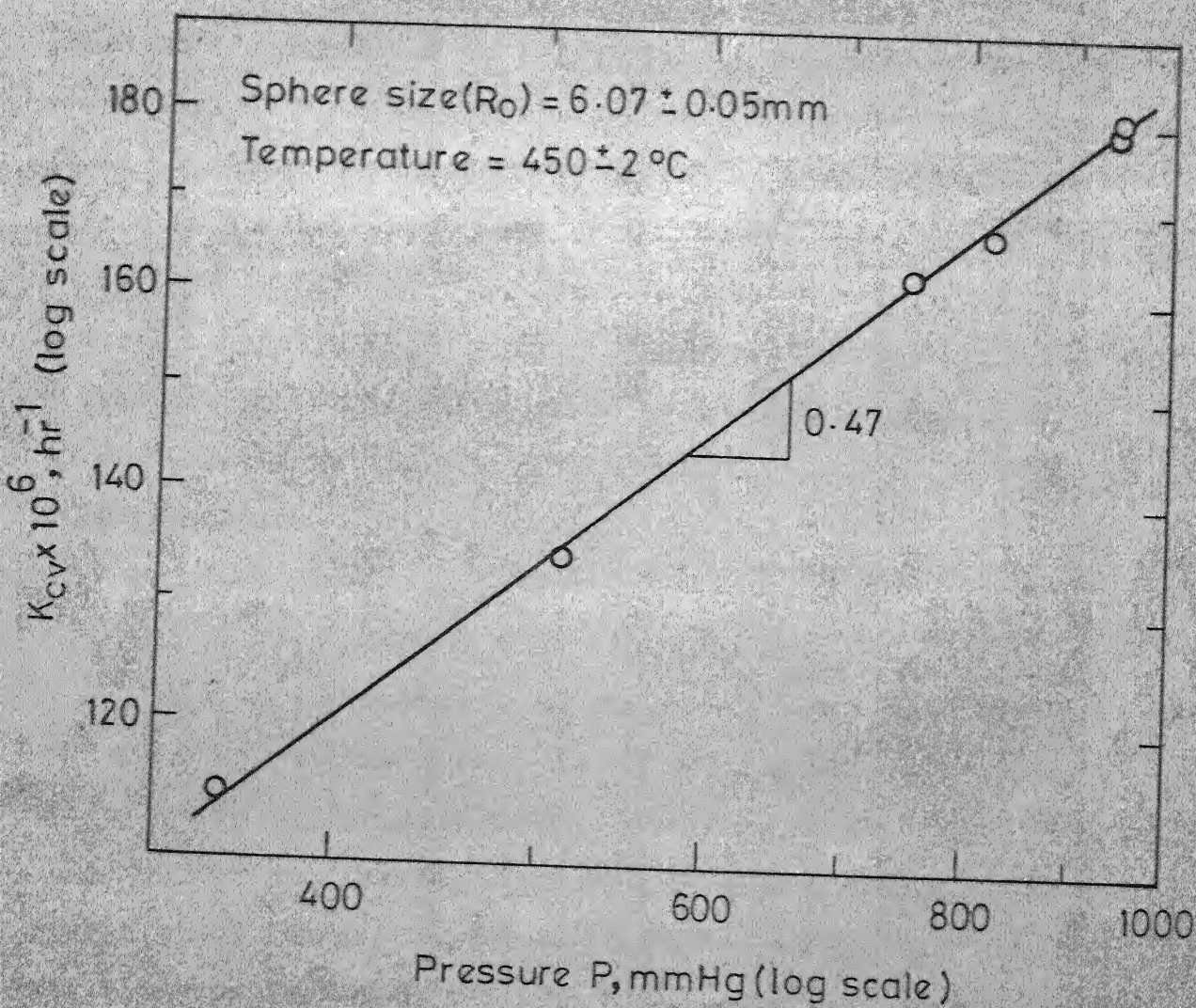


FIG. 31 EFFECT OF PRESSURE ON RATE CONSTANT K_{cv}
(formation of Na_2HfCl_6)

Next it is necessary to ascertain whether the outward diffusion occurs by interstitial or vacancy mechanism. In view of the nature of the pressure dependence of the reaction, it is more likely that the vacancy mechanism prevails for both the systems. Since, pressure effect on the rate constant is manifested through the concentration difference of the rate controlling species across the product layer, which in turn is dependent on gas pressure prevailing at the respective interfaces, the nature of diffusion mechanism may be understood from the behaviour of the rate constant with the change in the gas pressure. This may be explained with the help of a schematic representation of the concentration profile shown in Fig. 32. The dotted and the firm lines shown in the sketch, respectively, show concentration profiles of interstitials and vacancies under the condition of control by outward diffusion of matter. As diffusion through the product layer is rate determining, reactions at phase boundaries are rapid and thermodynamic equilibrium prevails at both the phase boundaries (interface 1 and 2). The partial pressure of the reacting gas at interface 1 is equal to the equilibrium dissociation pressure of the product in contact with the solid reactant, p_g^1 , while that at interface 2 is equal to the ambient gas pressure, p_g^2 . For diffusion to occur by interstitial mechanism concentration of the diffusing interstitial species, C_i , should be higher at interface 1 i.e. $C_i^1 > C_i^2$. Since, decomposition pressure, p_g^1 , is less than

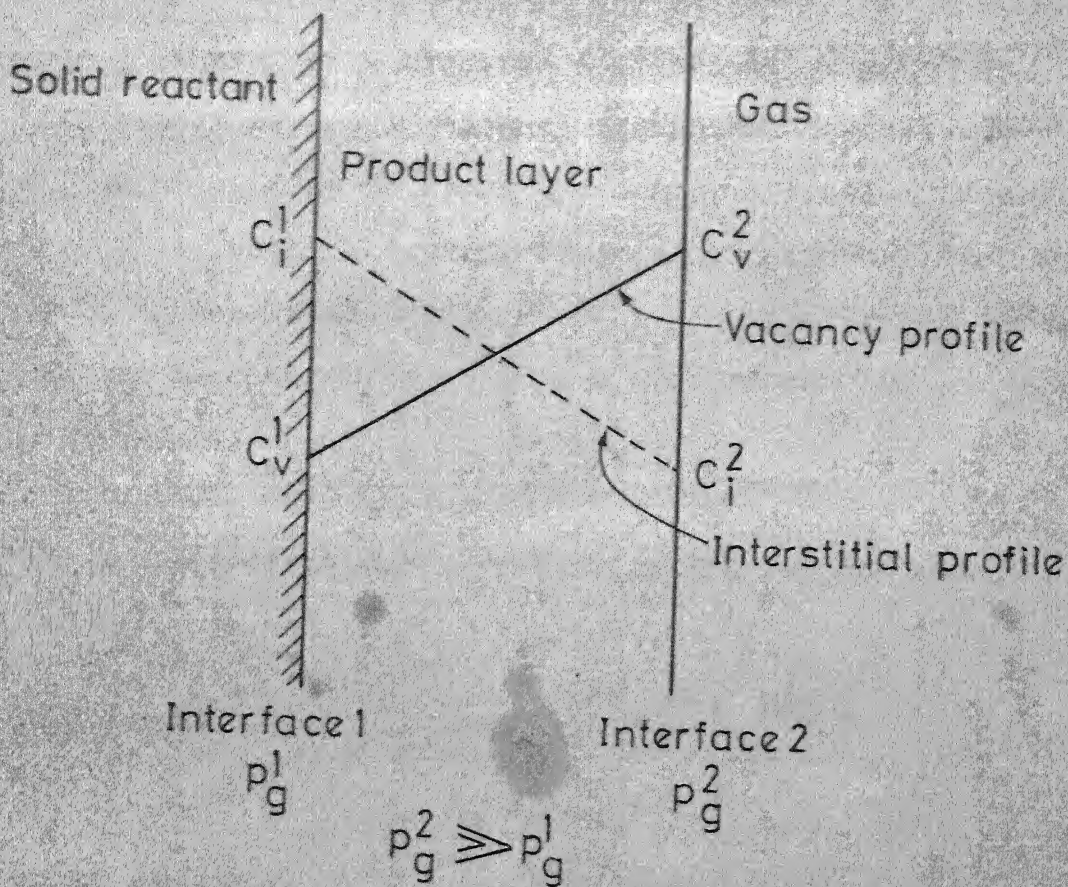


FIG. 32 SCHEMATIC REPRESENTATION OF OUTWARD DIFFUSION CONTROL CASE (Vacancy and interstitial mechanism)

ambient gas pressure, p_g^2 , this implies a higher interstitial concentration in equilibrium with lower gas pressure as shown in the figure. Thus

$$C_i \propto p_g^{-1/n} \quad [4.7]$$

where n = pressure coefficient

Situation reverses if vacancy mechanism operates. For outward diffusion of ions to occur by vacancy migration in the opposite direction, vacancy concentration at interface 2 need be higher. Again from similar argument this essentially implies higher vacancy concentration at higher gas pressure i.e.

$$C_v \propto p_g^{1/n} \quad [4.8]$$

Now rate constant for interstitial and vacancy case, respectively, may be expressed as

$$K_i = K_i^* (C_i^1 - C_i^2) \quad [4.9]$$

$$\text{and} \quad K_v = K_v^* (C_v^2 - C_v^1) \quad [4.10]$$

where K_i^* and K_v^* represent appropriate proportionality constants.

Substituting for concentration terms in Eq. [4.9] and [4.10]

$$K_i = K_i^* [(p_g^1)^{-1/n} - (p_g^2)^{-1/n}] \quad [4.11]$$

$$\text{and} \quad K_v = K_v^* [(p_g^2)^{1/n} - (p_g^1)^{1/n}] \quad [4.12]$$

Since $p_g^2 \gg p_g^1$, K_i reduces to

$$K_i = K_i^* (p_g^1)^{-1/n} \quad [4.13]$$

while K_v becomes

$$K_v = K_v^* (p_g^2)^{1/n} \quad [4.14]$$

It is thus evident from Eq. [4.14] that when vacancy mechanism operates, rate constant would result in a positive pressure coefficient. On the other hand, if interstitial mechanism prevails, rate constant would remain independent of ambient gas pressure, since p_g^1 which governs the rate constant depends on reaction temperature only.

Observation on the variation of rate constant with gas pressure in the present case, is consistent with the formulation on vacancy mechanism. Therefore, for both the hafnium and zirconium cases being studied presently, vacancy mechanism appears more probable.

4.8 Reaction mechanism

From foregoing discussion the formation of both Na_2ZrCl_6 and Na_2HfCl_6 appears to occur by outward diffusion of ions by vacancy mechanism. The vacancies needed for matter transport are likely to be produced by a surface reaction involving the transported ions and tetrachloride vapours at the outer gas-solid interface. The transport of matter obviously involves both the cation and the anion comprising the solid reactant, sodium chloride, as both these species are constituents of reaction products Na_2ZrCl_6 and Na_2HfCl_6 . Since equal moles of these two ions constitute the product lattice, the surface

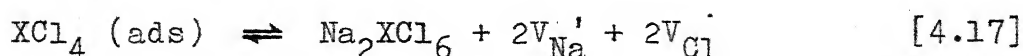
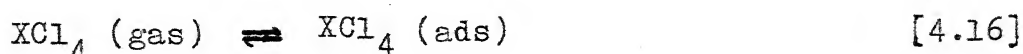
reaction between the transported sodium and chlorine ions and the reacting tetrachloride vapour would generate equal number of vacancies of both types.

Furthermore, in view of the observed effect of pressure on temperature coefficient, it seems necessary to include the adsorption step that normally precedes a heterogeneous solid-gas reaction. It was stated earlier that the temperature coefficient for the zirconium reaction resulted in different values at different reaction pressures. The observed variation of the apparent activation energy with pressure, although small (≈ 13 per cent), perhaps does not arise simply from experimental errors. Such behaviour is expected when adsorption is one of the reaction steps, even if an equilibrium state prevails. The temperature coefficient, which accommodates all the preceding equilibrium heat terms, may depend on pressure, since, the heat of adsorption term included in it is dependent on surface heterogeneity.¹⁰¹ The surface sites are not equally reactive; more active sites are covered at low gas pressure while lesser active sites start participating in the adsorption reaction with increase in gas pressure. Khalafalla et. al.¹⁰² have described the role of heat of adsorption in determining the true activation energy for the reduction of iron oxides. Widely different values of the activation energy have been reported for the reduction reaction such as

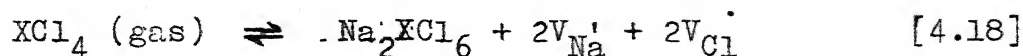


where the oxides reduced were in different forms of subdivision.¹⁰² The discrepancy were shown to virtually disappear, when the heat of adsorption was duly accounted for. The role of adsorption has also been recognised for solid-gas reactions under phase boundary reaction control.⁹¹⁻⁹⁵ For these cases pressure dependence of the reaction rate, could be adequately explained by taking adsorption equilibrium into account.

It is to be noted that of the two systems being considered here data for the zirconium tetrachloride case only is available to substantiate the role of adsorption. However, in view of the close similarity in the reaction behaviour of zirconium and hafnium tetrachlorides, inclusion of adsorption step in the case of hafnium reaction also, seems quite appropriate. In the light of the above discussion, the surface reaction may be formulated as below -



Combining Eqs. [4.16] and [4.17]



where, X stands for Zr and Hf. V_{Na}' and V_{Cl}' , respectively, represent singly charged sodium and chlorine ion vacancies. Assuming ideal behaviour for the vacancies, equilibrium constant for the overall vacancy generating reaction, Eq. [4.18] can be written as

$$K'_e = K'_s K'_a = \frac{[V_{Na}']^2 [V_{Cl}']^2}{P} \quad [4.19]$$

where K'_e , K'_a and K'_s represent, respectively, equilibrium constants for the overall, adsorption and surface reaction. It may be noted that in writing the above equilibrium relation, concentration of adsorbed XCl_4 is assumed to be

$$XCl_4 (ads) = K'_a P \quad [4.20]$$

Eq. [4.20] represents the limiting form of Langmuir's adsorption isotherm when $K'_a P \ll 1$.

The pressure dependence of the rate constant K_{cv} , defined in Eq. [4.5], can now be explained using the aforementioned defect equilibrium relation. However, since the defect structure of the product layer Na_2ZrCl_6 as well as Na_2HfCl_6 is not known, various possibilities are considered. The following possibilities exist.

Case I Product layer contains Schottky defects i.e. V_{Na}' and V_{Cl}' . Therefore,

$$V_{Na}' = V_{Cl}'$$

From Eq. [4.19],

$$[V_{Na}'] = [V_{Cl}'] = (K'_e P)^{1/4} \quad [4.21]$$

Case II Product layer contains Frenkel defects with imperfections in the sodium lattice i.e. V_{Na}' and Na_i' . Since, lattice defects originally present are relatively more

product scale. Formation of Cr_2O_3 , as reported by Caplan et al.¹⁰⁰, may be cited as an example in this regard. Such irregularities would have been quite prominent in the present case in view of the large swelling that accompanies the formation of Na_2ZrCl_6 and Na_2HfCl_6 . However, in none of the experimental runs these phenomena were observed. Hence, in the following discussion diffusional transport is considered to occur only in the outward direction.

Further evidence of outward lattice diffusion is obtainable from the consideration of change in the density of the residual core. Under outward diffusion control either by vacancy or interstitial mechanism, the vacant sites left at the product-reactant interface may diffuse into the residual core and form voids. Void formation, however, would not occur if vacancies get annihilated in suitable vacancy sinks such as grain boundary, dislocation etc. In the present investigation, comparison of the original total pore volume of the sphere as a whole with the sum of the calculated pore volume in the unreacted core and the reacted layer showed a small but consistent increase at the end of the reaction. The increment varied between 0.01 to 0.3 per cent. Detailed calculation regarding this is shown in Appendix II. This small increase in porosity, however, is too small to affect the kinetic analysis presented before and may be considered an evidence in favour of occurrence of outward diffusion.

was studied at 450°C (γ -phase region), Pint and Flengas³⁵ conducted their experiments at 485°C (δ -phase region). The dissimilar pressure dependence of the reaction rate in the two phase fields, seemingly is indicative of a change in the reaction mechanism with polymorphic transformation in the product phase. It is difficult to discuss the nature of such changes. This aspect is further emphasised by the changes in slope in the $\ln K_{cv}$ against $1/T$ plot as shown in Fig. 29. From the figure, a sharp change in slope with polymorphic transformation appears a distinct possibility, as shown by the dotted lines. This, however, could not be adequately confirmed due to lack of sufficient data.

4.7 Diffusion mechanism

In the preceding sections it was shown that the kinetics of both the reaction systems being studied are controlled by diffusion in the product layer. Analysis of the reaction model, although not conclusive, further indicated possibility of the operation of lattice diffusion mechanism as the mode of transportation in the product layer. Results of the marker experiments seem to confirm this. In both systems the inert markers attached to the surface of the solid reactants registered inward movement when examined at the end of the reaction. This is a clear indication of lattice diffusion. However, the markers were found seated within the product layer near the unreacted core boundary. Implications of such marker behaviour have been discussed in

Section 2.3.3. Accordingly, this might mean diffusion of reactant ions from the shrinking core to outer solid-gas interface (outward diffusion) or simultaneous outward and inward diffusion of ions. Of course, ideally such a situation indicates matter transport in both directions. The former interpretation seems more appropriate in the present systems. Numerous instances⁷⁶⁻⁷⁸ are known where markers were found within the product layer although diffusion occurred only in the outward direction. In spite of outward ionic diffusion markers may remain embedded in the product layer, if at certain stage of reaction, the reaction product partially loses its adherence to the shrinking core. Product layer may lose adherence to its substrate, if plastic deformation necessary to maintain firm reactant-product contact is prevented. Since, the ease with which reaction product undergoes plastic deformation is directly related to product layer thickness, partial detachment of the product layer appears quite possible in the present case, especially because an unusually high product layer thickness is produced due to excessive swelling associated with the formation of Na_2ZrCl_6 and Na_2HfCl_6 .

Again, in view of the swelling, simultaneous inward and outward diffusion mechanism does not seem likely. This is because if diffusion occurs in both directions, the product forming reaction occurring within the product layer would be accompanied by very high stresses. This should ordinarily lead to nonuniform product formation exhibiting nonuniform growth, blistering, wrinkling and even peeling or detachment of the

$$\text{Case I} \quad K_{cv} = K_o D_v (K_e' P)^{1/4}; V_{Na}' \text{ or } V_{Cl}' \text{ rate controlling} \quad [4.25]$$

$$\text{Case II} \quad K_{cv} = K_o D_v \left(\frac{K_e'}{K^*} P \right)^{1/2}; V_{Cl}' \text{ rate controlling} \quad [4.26]$$

$$\text{Case III} \quad K_{cv} = K_o D_v \left(\frac{K_e'}{K^*} P \right)^{1/2}; V_{Na}' \text{ rate controlling} \quad [4.27]$$

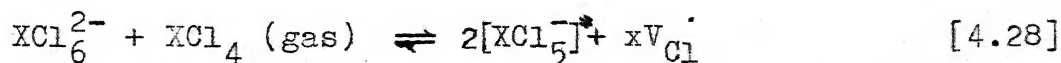
It is seen that the square root dependence of K_{cv} on the reacting gas pressure, expected for both Case II and III, is in reasonable agreement with experimentally observed pressure effect as shown in Figs. 30 and 31. These figures show that rate constant K_{cv} follows $1/1.98$ and $1/2.13^{\text{th}}$ power of the tetrachloride pressure for the zirconium and the hafnium reaction, respectively.

Although both Case II and III explain the observed pressure effect, Case II seems more appropriate from the consideration of ionic size. Since, the chlorine ion is much bigger in size than the sodium ion, it is more probable that sodium ions would go to the interstices. Therefore, migration of Cl^- ion vacancies formed in accordance with the scheme presented as Case II appears to be the rate controlling mechanism. Although the mechanism postulated above, explains pressure dependence observed in the present work, it fails to explain similar data obtained by Pint and Flengas.³⁵ It was mentioned earlier that Pint and Flengas found that the rate constant follows $1/2.8^{\text{th}}$ and $1/4.1^{\text{th}}$ power of the zirconium and the hafnium tetrachloride

pressure, respectively. The discrepancy in the case of hafnium obviously is too wide to be attributed to experimental errors. For hafnium case, the discrepancy has already been shown to possibly arise from the different polymorphic forms of the products encountered in the two investigations (see Section 4.6.3). While in the present case $\gamma\text{-Na}_2\text{HfCl}_6$ formed, Pint et al.'s experiment presumably dealt with $\delta\text{-Na}_2\text{HfCl}_6$.

It is interesting to note that the observed change in the pressure dependence and, hence, reaction mechanism presumably due to the polymorphic transformation of the reaction product, may imply transformation from Frenkel defect structure to Schottky defect structure i.e. shift from Case II to I. If that be the case, pressure effect observed by Pint and Flengas conforms to the basic reaction scheme postulated above through Eq. [4.18].

It is to be noted that Pint and Flengas³⁵ also postulated a vacancy generating surface reaction. This was mentioned earlier in Section 1.4. The reaction was considered to occur in steps, involving formation of an intermediate, NaXCl_5 . In NaXCl_5 , X stands for both zirconium and hafnium. The reactions considered were



In Eq. [4.29], x was considered 1 for zirconium case and 2 for hafnium case. Incorporation of such arbitrariness in the defect equation certainly is not justified and the representation

above seems is incomplete. However, there is broad agreement in the two postulations (i.e. present one and that due to Pint and Flengas³⁵) as far as diffusion mechanism is concerned. In both the postulates, migration of chlorine ion by vacancy mechanism is considered to be rate limiting.

Equation [4.26] may be further used to evaluate temperature dependence of the reaction rate constant. On substitution of the appropriate Arrhenius relationship for D , K'_a and K'_s , Eq. [4.26] transforms to

$$K_{cv} = \frac{K_o D_o}{\sqrt{K^*}} \sqrt{P} \exp\left(-\frac{2E_d - \Delta H_s - \Delta H_a}{2RT}\right) \exp\left(\frac{\Delta S_a + \Delta S_s}{2R}\right) \quad [4.30]$$

where ΔH_a , ΔH_s and E_d are heat of adsorption, heat of reaction (Eq. [4.17]) and activation energy for diffusion, respectively. ΔS_s and ΔS_a represent corresponding entropy changes and D_o is the preexponential term of temperature dependence relationship for D . Temperature coefficient or apparent activation energy E_{App} , therefore, is represented as

$$E_{App} = E_d + \frac{1}{2} \Delta H_s + \frac{1}{2} \Delta H_a \quad [4.31]$$

If Eq. [4.31] has a mechanistic basis then our analysis shows that a number of temperature dependent steps are composited in the overall specific rate constant K_{cv} and no definite conclusion can be drawn from the apparent activation energy obtained therefrom. However, the justification of inclusion of the adsorption step may be seen from Eq. [4.31]. In general, ΔH_a is known to become less negative with increasing surface coverage

and, hence, the reaction pressure. The effect of such a change in the value of ΔH_a will be to reduce the apparent activation energy as described in Eq. [4.31] at lower pressure although this effect may be quite small. This may be noted in the light of the present temperature coefficient values obtained at different reaction pressures. Apparent activation energy for Na_2ZrCl_6 formation in the temperature range 425 to 500°C is 7.5 and 9.9 kcal/mole at 745 and 1033 mm pressures, respectively. Clearly the temperature coefficient values obey the trend discussed above. For the hafnium reaction, however, such an analysis could not be carried out due to nonavailability of data.

CHAPTER 5

EXPERIMENTAL RESULTS AND DISCUSSION - II
REACTION INVOLVING TETRACHLORIDE GAS MIXTURES

5.1 Introduction

Results and discussion on the reaction of sodium chloride with mixtures of zirconium and hafnium tetrachloride vapours are presented in this chapter. Experimental results are presented in Sections 5.2 to 5.4. These include partial pressure and density values as well as results of the kinetic experiments. Keeping in view the complexity of the mixed gas reaction leading to the simultaneous formation of several compounds, an outline of the approach adopted in the succeeding kinetic analysis is presented in Section 5.5. Subsequently, experimental results are analysed in terms of kinetic model and product layer composition in Sections 5.6 and 5.7. The role of kinetics in enhancing separation of hafnium from zirconium by the method involving reaction between sodium chloride and gas mixture containing zirconium and hafnium tetrachloride is also discussed in Section 5.7. .

5.2 Partial pressure of gases in tetrachloride mixture

The partial pressure of the two tetrachloride gases constituting the reacting gas mixture was estimated from experimentally obtained total pressure and the gas phase

composition data. The details of the measurement techniques have been discussed in Section 3.5. In all the measurements, the same mixture of solid tetrachlorides was used. Different pressures were achieved by heating the tetrachloride mixture containing bulb to different temperatures. The results obtained are given in Table VI.

5.3 Swelling parameter, reactant and product density

Swelling parameter Z as defined in Eq. [2.6] was calculated using the densities of the reactant and the product. As before, average density of the reacted sodium chloride layer rather than that of the sodium chloride sphere as a whole has been used. However, due to the variation in the product layer density with variation in the reaction conditions, no unique value for swelling parameter Z , could be obtained. Estimated Z values and corresponding product layer density values are shown in Table VII.

5.4 Results of the kinetic experiments

Results of the thermogravimetric experiments under different conditions of reaction temperature and pressure are shown in Figs. 33 and 34, respectively. The plots show an increase in the reaction rate with increase in temperature and total pressure. In these two figures, total weight gain per unit weight of solid has been plotted rather than the fraction of sodium chloride reacted. Since, sodium chloride reacts to

Table VI. Partial pressure of the tetrachloride gas mixture
Solid tetrachloride composition - 25% HfCl_4 , 75% ZrCl_4
(approx., volume basis)

Temperature of the solid tetrachloride mixture $^{\circ}\text{C}$	Total pressure (p_{ZrCl_4} + p_{HfCl_4}) mm, Hg	Gas phase composition (chemical analysis of collected samples) % Hf	Mole fraction of HfCl_4 in gas phase	Partial pressure mm, Hg	
				p_{ZrCl_4}	p_{HfCl_4}
333.375	980	21	0.1611	822	158
330.75	908	-	-	-	-
326.00	787	24	0.1876	640	147
321.25	674	26	0.2051	536	138
312.00	507	-	-	-	-

Table VII. Swelling parameter and product layer density

Density of reacted sodium chloride layer (average) gm/c.c.	Reaction Temper- ature $^{\circ}\text{C}$	Partial pressure mm, Hg		Product layer density gm/c.c.	Swelling parameter Z
		p_{ZrCl_4}	p_{HfCl_4}		
2.107	450.5	822	158	2.398	2.786
	450.0	536	138	2.347	2.791
	424.8	822	158	2.243	2.930
	450.0	640	147	2.393	2.794
	490.0	822	158	2.422	2.789

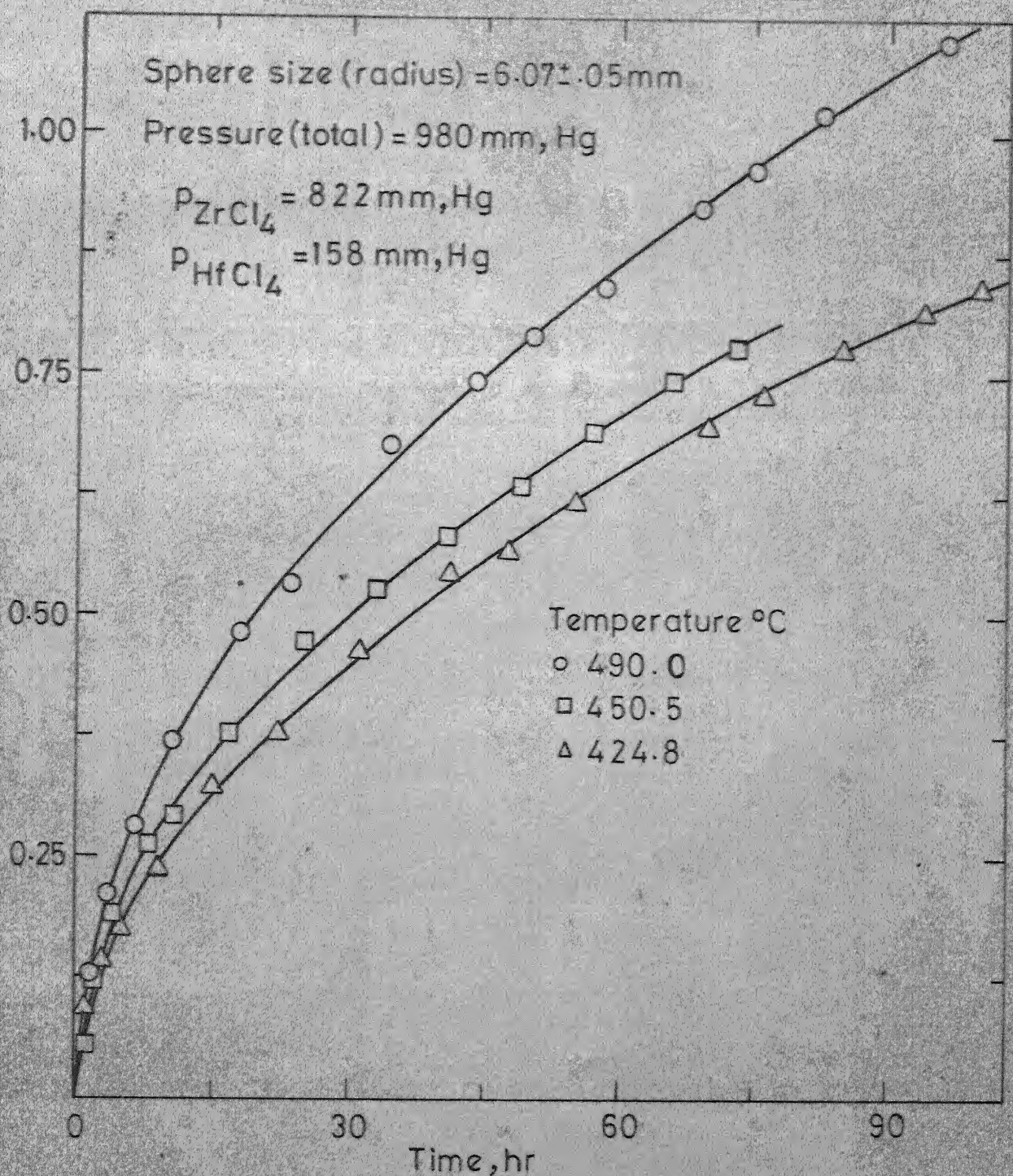


FIG. 33 EFFECT OF TEMPERATURE ON THE RATE OF FORMATION OF Na_2ZrCl_6 - Na_2HfCl_6 SOLID SOLUTIONS (reaction with gas mixture)

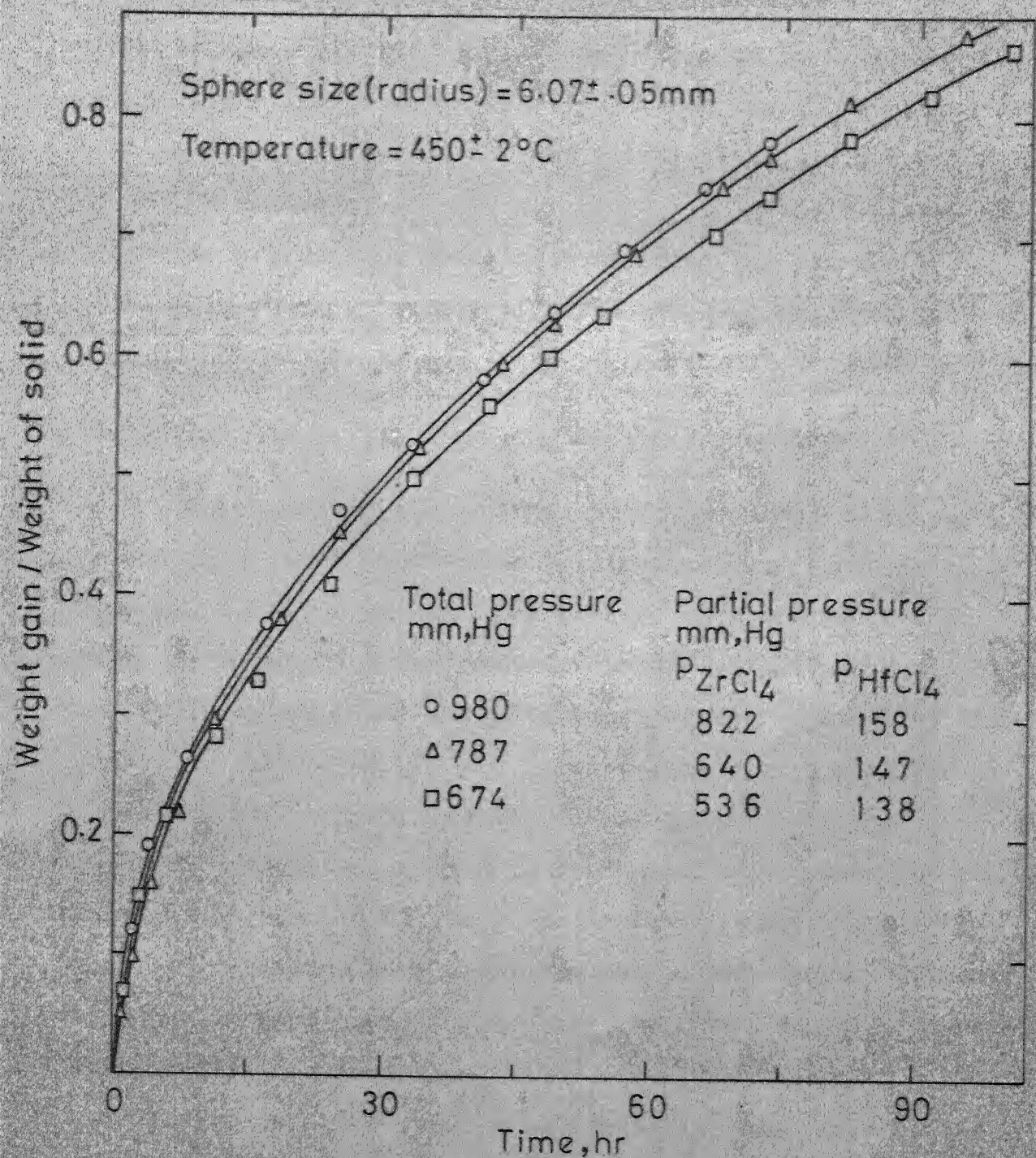


FIG. 34 EFFECT OF PRESSURE ON THE FORMATION OF Na_2ZrCl_6 - Na_2HfCl_6 SOLID SOLUTIONS (reaction with gas mixture)

numerous, concentration of V_{Na}' would not change much due to the surface reaction involving tetrachloride gas, i.e. $[V_{Na}'] \gg [V_{Cl}']$.

Therefore, from Eq. [4.19],

$$[V_{Cl}'] = \left(\frac{K'_e}{K^*P} \right)^{1/2} \quad [4.22]$$

where K^* represents a constant. The concentration of sodium ion vacancy, which remains virtually unchanged, has been incorporated in the constant K^* .

Case III Product layer contains Frenkel defects with imperfections in the chlorine lattice i.e. V_{Cl}' and Cl_i' . Arguing as in Case II, from Eq. [4.19] we obtain

$$[V_{Na}'] = \left(\frac{K'_e}{K^*P} \right)^{1/2} \quad [4.23]$$

Here K^* has significance similar to K^* above, but pertains to chlorine ion vacancy.

The applicability of the above three cases can now be tested in terms of the pressure dependence of the rate constant, K_{cv} . K_{cv} as expressed in Eq. [4.5] may be written as

$$K_{cv} = K_0 D_v C_v^R \quad [4.24]$$

where $K_0 = \frac{M_r}{r R_0^2}$, and C_v^R represents concentration of the rate controlling species (i.e. $[V_{Cl}']$ or $[V_{Na}']$) at the outer solid-gas interface. Substituting for C_v^R in Eq. [4.24] from Eqs. [4.21], [4.22] and [4.23], respectively, we get

composition distribution in the product layer, the scope of analysis of the present system is quite limited.

It would seem, however, that the present reaction system is amenable to analysis by virtually the same approach, as the one used for the single gas reactions in view of the basic kinetic similarity observed in the cases of independent formation of Na_2ZrCl_6 and Na_2HfCl_6 . In Chapter 4, it was shown that the formation of both hexachloro zirconate and hafnate is controlled by outward diffusion of sodium and chlorine ions with concurrent migration of vacancies in the opposite direction. Since, in both cases common ions Na^+ and Cl^- participated in the required transport, a similar mechanism is expected for the sodium chloride - tetrachloride mixed gas reaction resulting in the formation of a solid solution of the hexachloro compounds of zirconium and hafnium. Complete solid solubility of these two compounds was earlier shown by Flengas and Pint.¹⁰³ It is then expected that the sodium and chlorine ions migrating through the product lattice would react with the adsorbed zirconium and hafnium tetrachloride molecules on the outer solid-gas interface to form the reaction products with generation of the required vacancies. The nature of this anticipated vacancy producing surface reaction, however, is difficult to postulate at this stage.

In the following discussion the experimental data are examined in the light of the tentative hypothesis presented above. First, applicability of transport control

is examined in terms of a reaction model. The reaction model, which essentially is Carter⁴³-Valensi⁴⁴ transport control model has been rederived in terms of vacancy flux. In the present case, however, assumptions were to be made regarding product layer composition. It is assumed that product layer composition stays uniform throughout the reaction. Subsequently, an indirect evidence, which validates this assumption is presented. Nevertheless, the derivation is of general validity for reactions involving outward diffusion of matter.

5.6 Reaction model: formulation and analysis

The difficulties in modelling of mixed gas-solid reactions are compounded by the possibility of non-uniformity in composition of the product layer. It is a common practice to represent the extent of solid-gas reaction by an index concerning the reactant solid. Accordingly, in most reaction models, the fraction of solid reacted is chosen as the relevant parameter to follow the progress of the reaction. It is to be noted that, for reactions in plane geometry, weight gain data can be conveniently used for representing the progress of the reaction. But due to the change in the area of product-solid interface, weight gain data cannot be directly used for tracking progress of the reactions in spherical geometry. Consequently, fraction of solid (reactant) reacted is chosen as the reaction parameter for reactions involving spherical

solids. For mixed gas reactions, however, this parameter cannot be calculated from thermogravimetric data alone due to possible changes in the proportions of the constituents of the product layer. The fraction of solid reacted, however, can be estimated for mixed gas reactions only when the product layer composition does not change with time. In the present system, if the hypothesis presented before prevails, composition of the product layer would stay uniform. An indirect evidence, showing that this is indeed so, is presented in the next section.

At any stage of the reaction, total weight gain W can be represented as

$$W = \frac{4}{3}\pi(R_0^3 - R_1^3) \frac{\rho_{\text{NaCl}}}{M_{\text{NaCl}}} \left[\frac{\phi M_{\text{HfCl}_4} + (1-\phi)M_{\text{ZrCl}_4}}{2} \right] \quad [5.1]$$

where R_0 and R_1 stand for original and instantaneous radii of the sodium chloride sphere, respectively, and the factor ϕ denotes fraction of the total reacted sodium chloride that goes in to form sodium hexachloro hafnate. Subscripted M terms denote corresponding molecular weight while ρ_{NaCl} represents density of the NaCl sphere. If ϕ is not dependent on extent of reaction, the parameter W_α representing weight gain when the entire solid has reacted can be defined as

$$W_\alpha = \frac{4}{3}\pi R_0^3 \frac{\rho_{\text{NaCl}}}{M_{\text{NaCl}}} \left[\frac{\phi M_{\text{HfCl}_4} + (1-\phi)M_{\text{ZrCl}_4}}{2} \right] \quad [5.2]$$

Fraction of sodium chloride reacted F , now is obtained from the ratio of W and W_α . Thus

$$\frac{W}{W_\alpha} = \frac{R_0^3 - R_i^3}{R_0^3} = F \quad [5.3]$$

Since, the core radius at a particular instant (i.e. when reaction is terminated) can be measured by stripping the fragile product layer, W_α can be calculated from Eq. [5.3], using the measured radius and the known weight gain data at that instant. Fraction of sodium chloride reacted, F , at various reaction times can now be computed from the ratio of the recorded weight gains at those times and the estimated value of W_α .

Kinetic rate expression in terms of the parameter, F , is now derived by considering the volume shrinkage of the sodium chloride core arising from annihilation of vacancy pair, V_{Cl} and V_{Na} , at the product-reactant interface. It is to be noted that, volume shrinkage of the reacted solid can be equated to vacancy flux, only when vacancies reaching the product-reactant interface do not diffuse further to form voids. Annihilation of the vacancies at the interface is precondition to the following treatment based on shrinking core concept. This aspect has been elaborated earlier in Section 2.2. That the vacancies do not diffuse beyond the product-reactant interface is evidenced by the near constancy of the porosity of the core. In the course of the reaction core porosity was

found to increase by 0.01 to 0.3 per cent only. The increment is too small to affect the kinetic analysis. However, this small increase is of importance from yet another account. It was discussed earlier (cf. Section 4.7) that even such small increase in the porosity may serve to indicate occurrence of the outward diffusion. Therefore, to a first approximation the vacancy flux arriving at the product-reactant interface, can be equated to the volume rate of shrinkage of sodium chloride core.

The expression for the quasi-steady state flux of vacancies through the solid product layer is given by

$$J_v = 4\pi r^2 D_v \frac{\delta c_v}{\delta r} \quad [5.4]$$

where c_v refers to vacancy concentration of the slowest moving species, while D_v denotes diffusivity of the same. It is to be noted that c_v has the unit of number of vacancies per cm^3 .

r denotes radius of the sphere at any section. Integrating Eq. [5.4] using the boundary conditions

$$c_v = c_v^g \quad \text{at } r = R_g \text{ (outer product-gas interface)} \quad [5.5]$$

$$\text{and } c_v = c_v^i \quad \text{at } r = R_i \text{ (inner product-reactant interface)}$$

we obtain

$$J_v = 4\pi D_v \frac{R_g R_i}{R_g - R_i} [c_v^g - c_v^i] \quad [5.6]$$

For a diffusion controlled process c_v^i is negligibly small as compared to c_v^g and thus

$$J_v = 4\pi D_v \frac{R_g R_i}{R_g - R_i} c_v^g \quad [5.7]$$

The assumption leading to Eq. [5.7], however, is not essential for the kinetic model.

Since, both sodium and chlorine ion vacancies simultaneously migrate, volume flux reaching the product-reactant interface is given by

$$J_{vol} = 4\pi\sigma D_v \frac{R_g R_i}{R_g - R_i} c_v^g \quad [5.8]$$

where σ denotes volume of the vacancy pair V_{Na} and V_{Cl} . Rate of shrinkage of the solid constituent of the core volume is given by

$$\frac{dV}{dt} = -4\pi R_i^2 \frac{dR_i}{dt} \quad [5.9]$$

Equating Eqs. [5.8] and [5.9] gives

$$\frac{dR_i}{dt} = -\frac{\sigma D_v}{R_i} \left(\frac{R_g}{R_g - R_i} \right) c_v^g \quad [5.10]$$

Now, the swelling parameter, Z , can be introduced to obtain relationship between R_g and R_i . Thus

$$Z = \frac{\text{Volume of product formed}}{\text{Volume of NaCl reacted}} = \frac{R_g^3 - R_i^3}{R_o^3 - R_i^3} \quad [5.11]$$

Z can be obtained experimentally from the densities of the product and reactant solid or the measured radii. From Eq.

[5.1] we get

$$J_v = 4\pi D_v \frac{R_g R_i}{R_g - R_i} c_v^g \quad [5.7]$$

The assumption leading to Eq. [5.7], however, is not essential for the kinetic model.

Since, both sodium and chlorine ion vacancies simultaneously migrate, volume flux reaching the product-reactant interface is given by

$$J_{vol} = 4\pi\sigma D_v \frac{R_g R_i}{R_g - R_i} c_v^g \quad [5.8]$$

where σ denotes volume of the vacancy pair V_{Na}' and V_{Cl}^\bullet . Rate of shrinkage of the solid constituent of the core volume is given by

$$\frac{dV}{dt} = -4\pi R_i^2 \frac{dR_i}{dt} \quad [5.9]$$

Equating Eqs. [5.8] and [5.9] gives

$$\frac{dR_i}{dt} = -\frac{\sigma D_v}{R_i} \left(\frac{R_g}{R_g - R_i} \right) c_v^g \quad [5.10]$$

Now, the swelling parameter, Z , can be introduced to obtain relationship between R_g and R_i . Thus

$$Z = \frac{\text{Volume of product formed}}{\text{Volume of NaCl reacted}} = \frac{R_g^3 - R_i^3}{R_o^3 - R_i^3} \quad [5.11]$$

Z can be obtained experimentally from the densities of the product and reactant solid or the measured radii. From Eq.

[5.1] we get

$$R_i^3 = R_o^3 - WH \quad [5.12]$$

Combining Eqs. [5.1] and [5.11]

$$R_g^3 = R_o^3 + WH(Z-1) \quad [5.13]$$

$$\text{where } H = \frac{1}{\frac{4}{3}\pi \frac{\rho_{NaCl}}{M_{NaCl}} \left[\frac{\phi M_{HfCl_4} + (1-\phi) M_{ZrCl_4}}{2} \right]} \quad [5.14]$$

is a constant. Differentiation of Eq. [5.12] leads to

$$\frac{dR_i}{dt} = - \frac{H}{3R_i^2} \frac{dW}{dt} \quad [5.15]$$

Substituting for $\frac{dR_i}{dt}$ in Eq. [5.10], the differential rate expression becomes

$$\frac{dW}{dt} = - \frac{3\sigma R_i D_v}{H} \left[\frac{1}{\frac{R_i}{R_g} - 1} \right] c_v^R \quad [5.16]$$

Now we proceed to express the terms R_i and $\frac{R_i}{R_g}$ as functions of W and W_α . From Eq. [5.1] and [5.2]

$$R_i = R_o \left(1 - \frac{W}{W_\alpha} \right)^{1/3} \quad [5.17]$$

and from Eq. [5.12] and [5.13]

$$\frac{R_i}{R_g} = \frac{\left[1 - \frac{WH}{R_o^3} \right]^{1/3}}{\left[1 + \frac{WH(Z-1)}{R_o^3} \right]^{1/3}} \quad [5.18]$$

Combining Eq. [5.2] and [5.14]

$$W_{\alpha} = \frac{R_0^3}{H} \quad [5.19]$$

Therefore, $\frac{R_i}{R_g}$ in Eq. [5.18] can be written as

$$\frac{R_i}{R_g} = \frac{[1 - \frac{W}{W_{\alpha}}]^{1/3}}{[1 + \frac{W}{W_{\alpha}}(Z-1)]^{1/3}} \quad [5.20]$$

Substituting for R_i and R_i/R_g from Eqs. [5.17] and [5.20], respectively, into Eq. [5.16] results in

$$\frac{dW}{dt} = -\frac{3\sigma D_v}{H} R_0 \left(1 - \frac{W}{W_{\alpha}}\right)^{1/3} \left[\frac{(1 + \frac{W}{W_{\alpha}}(Z-1))^{1/3}}{(1 - \frac{W}{W_{\alpha}})^{1/3} - (1 + \frac{W}{W_{\alpha}}(Z-1))^{1/3}} \right] c_v^{R_g} \quad [5.21]$$

Since, fraction of NaCl reacted is given by $F = \frac{W}{W_{\alpha}}$ (see Eq. [5.8]), dividing throughout by W_{α} and followed by substitution of Eqs. [5.8] and [5.19], Eq. [5.21] becomes

$$\frac{dF}{dt} = -\frac{3\sigma D_v}{R_0^2} (1-F)^{1/3} \left[\frac{(1 + F(Z-1))^{1/3}}{(1-F)^{1/3} - (1 + F(Z-1))^{1/3}} \right] c_v^{R_g}$$

$$\text{or, } \frac{dF}{dt} [(1 + F(Z-1))^{-1/3} - (1-F)^{-1/3}] = -\frac{3\sigma D_v}{R_0^2} c_v^{R_g}$$

$$\text{or, } \frac{dF}{dt} [(Z + (1-Z)(1-F))^{-1/3} - (1-F)^{-1/3}] = -\frac{3\sigma D_v}{R_0^2} c_v^{R_g}$$

$$\text{or, } \frac{d(1-F)}{dt} [(1-F)^{-1/3} - (Z + (1-Z)(1-F))^{-1/3}] = -\frac{3\sigma D_v}{R_0^2} c_v^{R_g} \quad [5.22]$$

form simultaneously Na_2ZrCl_6 and Na_2HfCl_6 , it is difficult to estimate fraction of solid reacted at the outset. A method has been suggested in Section 5.6 for calculating this parameter for the present system. However, since the method is subject to certain assumption, the direct experimental parameter i.e. weight gain per unit weight of solid reactant has been plotted in Figs. 33 and 34.

5.5 Outline of the approach to the kinetic analysis

Multi-gas reaction with a solid, such as in the present case, is characterised by simultaneous formation of a number of solid compounds. The kinetic analysis, therefore, would depend on the proportion and nature of association of the product compounds. The microstructure of the product layer may comprise of dispersed phases, layered phases or a single solid solution phase. In view of the simultaneous appearance of a number of compounds, conceptual realisation of this class of reactions is considerably more difficult as compared to the reactions involving single gas and solid. Modelling difficulties accompanying such simultaneous reactions are similar to those associated with oxidation of alloys involving a single gas which also results in multi phase product layer. Even when a single solid solution phase appears, possible occurrence of non-uniformity in the product layer composition may complicate any meaningful analysis. Due to the lack of information regarding

On the other hand c_v^R , surface concentration of the rate controlling species diffusing inwards, as incorporated here, has the dimension of number of vacancies/cm³. c_v^R can be converted to molar unit i.e. moles/cm³ by introducing the Avagadro number, N_o . Thus K_m can be written as

$$K_m = \frac{D_v}{R_o^2} (\sigma N_o) \frac{c_v^R}{N_o} \quad [5.25]$$

Now σN_o represents volume per mole of sodium and chlorine vacancy pair and hence

$$\sigma N_o = \frac{M_{NaCl}}{\rho_{NaCl}} \quad [5.26]$$

$$\text{Therefore, } K_m = \frac{D_v}{R_o^2} \frac{M_{NaCl}}{\rho_{NaCl}} c_v^R = K_{cv} \quad [5.27]$$

It is to be noted that in the expression above c_v^R denotes concentration of the rate controlling species, while $\frac{M_{NaCl}}{\rho_{NaCl}}$ i.e. σN_o represents molar volume of vacancy pair. This, however, is not inconsistent at all since along with the migration of the rate controlling defect, which determines the rate of reaction, the other defect also migrates simultaneously. Condensation of both these defects leads to the shrinkage of NaCl sphere.

The experimentally obtained rate data now can be tested in terms of Eq. [5.23]. In Figs. 35 and 36 rate data have been plotted according to Eq. [5.23]. The figures show the effects of reaction temperature and total pressure, respectively. Consistently good fit of the rate equation indicates applicability

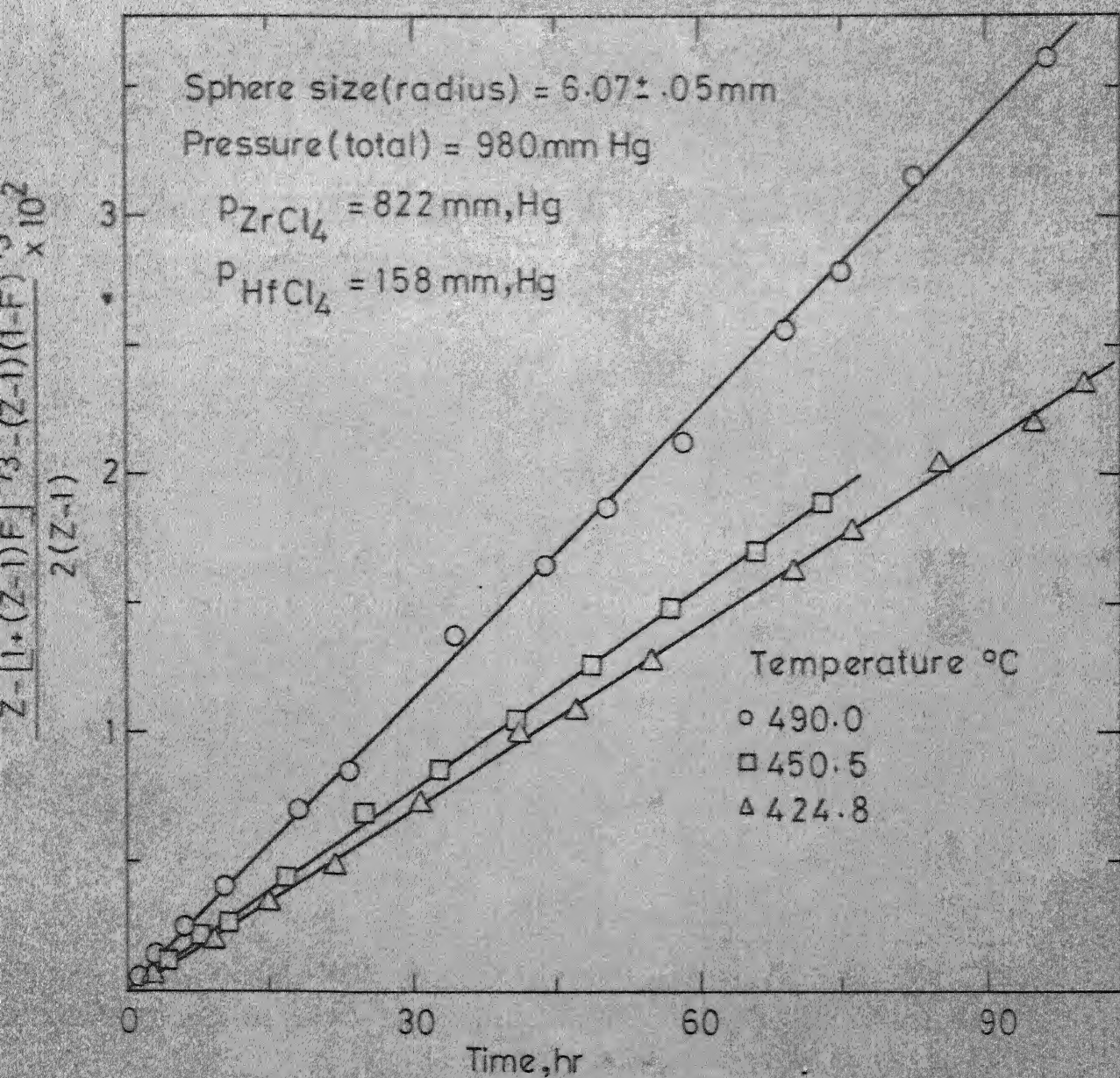


FIG. 35 CARTER-VALENSI PLOT SHOWING THE EFFECT OF TEMPERATURE ON THE RATE OF FORMATION OF Na_2ZrCl_6 - Na_2HfCl_6 SOLID SOLUTIONS

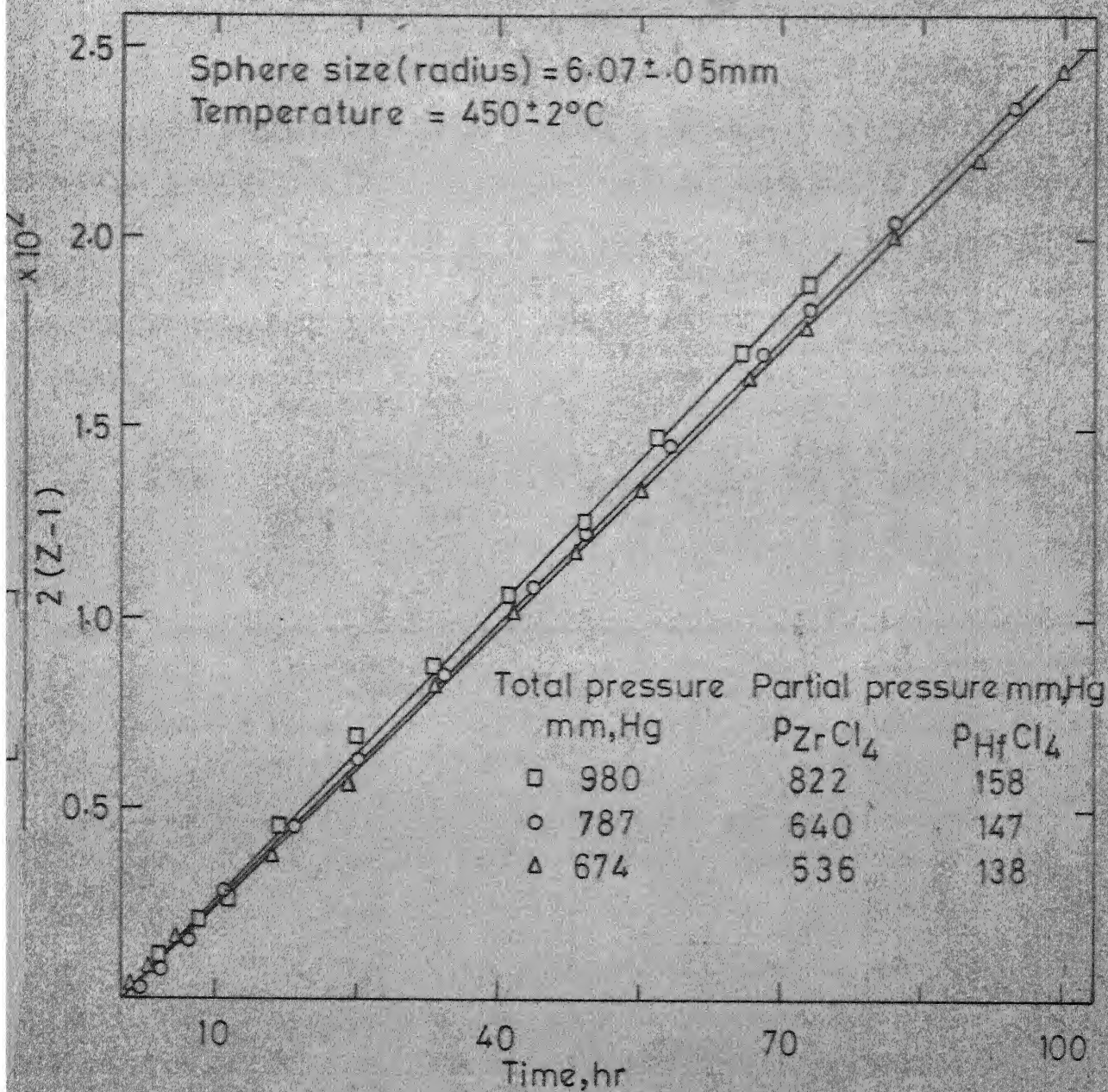


FIG. 36 CARTER-VALENSI PLOT SHOWING THE EFFECT OF PRESSURE ON THE RATE OF FORMATION OF Na_2ZrCl_6 - Na_2HfCl_6 SOLID SOLUTIONS

of the transport control hypothesis presented before. In particular, the assumption of constant ϕ in Eq. [5.1] seems justified since the Carter-Valensi model can not be derived if ϕ varies with time. Rate constants have been calculated from the slopes of these plots and is shown in Table VIII. The rate constant values found in this case was found to be greater than

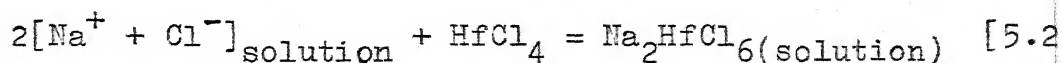
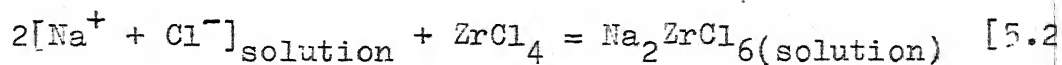
Table VIII. Carter-Valensi rate constants for the formation of Na_2ZrCl_6 - Na_2HfCl_6 solid solution.

Effect of	Sphere size (radius) mm	Total pressure mm, Hg	Partial pressure mm, Hg		Reaction temperature °C	Rate constant $K_{cv} \times 10^4$ hr ⁻¹
			P_{ZrCl_4}	P_{HfCl_4}		
Pressure	6.098	980	822	158	450.5	2.57
	6.097	787	640	147	450.0	2.49
	6.098	674	536	138	450.0	2.44
Temperature	6.115	980	822	158	490.0	3.71
	6.098	980	822	158	450.5	2.57
	6.112	980	822	158	424.8	2.30

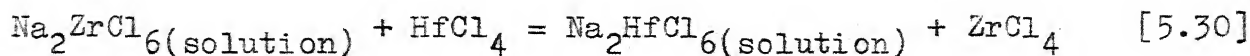
that for the formation of pure Na_2HfCl_6 but less than that for the Na_2ZrCl_6 formation.

5.7 Surface reaction

Earlier it was mentioned that the nature of the surface reaction, in particular, in relation to the vacancies generated at the outer solid-gas interface, is not known. But it seems that the compositional relation between the solid product phase and the reacting gas phase may be obtained by simpler consideration. Under the condition of outward diffusion of Na^+ and Cl^- ions, the outer reactant surface becomes the meeting point of the gaseous tetrachlorides, the hexachloro compounds and the transported sodium and chlorine ions. The product forming reaction now may be looked upon as two separate reactions i.e.



Obviously then, under equilibrium condition, relationship between the product and the gas phase would be given by combination of the two individual reactions i.e.



Equilibrium constant of the combined chemical reaction is given by

$$K'_{ss} = \frac{p_{\text{ZrCl}_4}}{p_{\text{HfCl}_4}} \cdot \frac{a_{\text{Na}_2\text{HfCl}_6}}{a_{\text{Na}_2\text{ZrCl}_6}} = \frac{p_{\text{ZrCl}_4}}{p_{\text{HfCl}_4}} \cdot \frac{x_{\text{Na}_2\text{HfCl}_6}}{x_{\text{Na}_2\text{ZrCl}_6}} \quad [5.31]$$

The hexachloro compounds are known to form ideal solid solution.¹⁰⁴ It is to be noted that if Eq. [5.31] is valid then

the product layer formed will have an uniform composition across the product layer. Since, the partial pressures of the reacting tetrachlorides remain unchanged all through the reaction, the equilibrium relation as given in Eq. [5.31] would remain constant only when concentration ratio of the hexachloro compounds also remains independent of the reaction time. To test the validity of the above postulation, the product layer composition expected from Eq. [5.31] may be compared to that obtained from actual chemical analysis of the product layers. Calculated and measured product layer compositions as shown in Table IX were found to

Table IX. Product layer composition (calculated and measured) under various reaction conditions.

Partial pressure mm, Hg		Reaction temperature °C	Composition of the product layer	
P_{ZrCl_4}	P_{HfCl_4}		%Hf	
			Calculated	Measured
822	158	450.5	25.8	25
536	138	450.0	31.4	32
822	158	424.8	25.9	29
640	147	450.0	29.1	28
822	158	490.0	25.7	26

compare well. The match may be considered good, particularly because chemical analysis data were not much accurate. Obviously, a direct evidence in this regard i.e. chemical analysis of the product layer as a function of position would have served the

purpose much better. Accordingly, electron micro probe analysis of the product layer was attempted^φ. But this could not be accomplished due to technical difficulties. It was found that the area under the electron beam gets removed in a very short time. This apparently was due to steady evolution of gases from the specimen surface.

In the light of the transport control reaction model and the equilibrium considerations presented above, it appears that the mixed tetrachloride gas- NaCl reaction is also controlled by outward diffusion of sodium and chlorine ions.

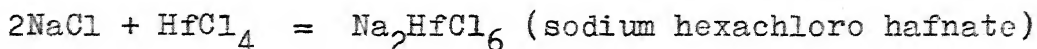
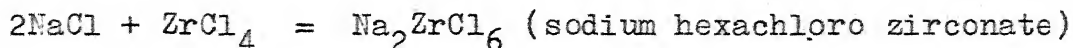
The separation efficiency of the chemical method based on the reaction between solid sodium chloride and the tetrachloride mixture now may be looked into in terms of the reaction mechanism discussed above. Earlier it was shown that the individual hexachloro compounds form at different rates; hafnium compound formation being slower. The difference in rates of Na_2ZrCl_6 and Na_2HfCl_6 formation, however, turns out to be of little use from the point of view of preferential formation of compounds and separation of zirconium from hafnium. Under all conditions, the separation factor is expected to obey the equilibrium condition of Eq. [5.31]. Thus enhancement of separation efficiency by kinetic means does not seem feasible.

^φ The trial was made at Defence Metallurgical Research Laboratory, Hyderabad.

CHAPTER 6

CONCLUSIONS

Kinetics of reaction of sodium chloride spheres with gaseous zirconium tetrachloride, hafnium tetrachloride and mixtures of these vapours have been studied thermogravimetrically under various conditions using an all glass fully closed apparatus. The overall chemical reactions can be written as



Although in the present investigation only sodium chloride was used as ~~solid~~ reactant, similar studies may be conducted on the experimental set up developed using other alkali chlorides. The main conclusions for the present studies involving zirconium tetrachloride and/or hafnium tetrachloride vapours are the following.

1. Reaction with individual tetrachlorides:

The reaction leading to the formation of the hexachloro zirconate or hexachloro hafnate are very slow. For example, in the system ZrCl_4 -NaCl, it took 86 hours to achieve 36 per cent reaction under a pressure of 381 mm, Hg and at a temperature of 451°C ; sphere radius being 6.089 mm. The reaction involving hafnium tetrachloride is even slower under identical experimental condition. The reaction rate increases with increase in

temperature and pressure while sphere size has the reverse effect.

The formation of the double salts is accompanied by appreciable swelling of the reactant size. The product layers produced are nonporous and coherent in both cases. The rate data for these solid-gas reactions consistently agree only with Carter-Valensi product phase transport control model. The model when tested for reactions involving spheres of different sizes, yielded the expected power relationship between the sphere size and the reaction rate constant. The specific rate constant varied inversely with 1.92^{th} and 2.12^{th} power of the sphere size (radius) for zirconium and hafnium reaction, respectively, in reasonable agreement with the value of two required in the Carter-Valensi model. The rate data, however, do not agree with other well known transport control models. Presumably, the swelling of the reaction product, which is quite prominent in these systems, leads to the failure of these transport control models.

Inert marker experiments showed that the diffusion of ions through the product layer occurs outward from the sodium chloride core to the surface of the product layer. The required ionic transport presumably occurs by a vacancy mechanism. It is postulated that the vacancies involved in transport are generated at the surface of the product layer by the reaction between transported sodium and chlorine ions with zirconium or hafnium tetrachloride adsorbed on the surface of the reacting

Integrating Eq. [5.21] with the initial condition; $(1-F) = 1$ at $t = 0$

$$\frac{(Z-1)[(1-F)^{2/3} - 1] + [Z + (1-Z)(1-F)]^{2/3} - 1}{2(Z-1)} = -\left[\frac{\sigma D_v}{R_o^2} c_v^R\right]t$$

or,
$$\frac{Z - (Z-1)(1-F)^{2/3} - [1 + F(Z-1)]^{2/3}}{2(Z-1)} = K_m t \quad [5.23]$$

where K_m represents the overall rate constant given by

$$K_m = \frac{\sigma D_v c_v^R}{R_o^2} \quad [5.24]$$

It can be seen that the rate equation derived here is identical to Carter-Valensi equation (Eq. [4.4]) which was employed for individual tetrachloride - sodium chloride reaction. For individual reactions ϕ is always unity and, therefore, no assumption is involved. It may be noted that the present mode of derivation is applicable to outward diffusion both by interstitial and vacancy mechanism. In the case of interstitial diffusion as ions leave the reactant lattice, it leaves vacant sites at the product-reactant interface and is amenable to analysis in the same way as presented in the foregoing derivation.

The apparent discrepancy in rate constant expression i.e. Eqs. [5.24] and [4.5] are due to different units of the concentration terms. Surface concentration terms C_v^R of the rate controlling species that appear in the expression for Carter-Valensi rate constant (Eq. [4.5]) is given by moles/cm³.

possibly due to the adsorption effect preceding the main reaction. The temperature coefficient values for reaction in the $\text{ZrCl}_4\text{-NaCl}$ system in the temperature range 425 to 500°C is 7.5 Kcal/mole at 745 mm, Hg pressure and 9.9 Kcal/mole at 1033 mm, Hg pressure. Similar data for NaCl-HfCl_4 case is available at only one pressure. Temperature coefficient for the formation of Na_2HfCl_6 (γ -phase) in the temperature range 440 to 484°C is 13 Kcal/mole; the reaction pressure being 945 mm, Hg.

2. Reaction involving mixture of tetrachloride vapours:
formation of solid solutions of hexachloro compound

The heterogeneous reaction between solid sodium chloride and gaseous mixture of zirconium tetrachloride and hafnium tetrachloride, resulting in the simultaneous formation of Na_2ZrCl_6 and Na_2HfCl_6 also conform to the outward diffusion control kinetics. The kinetic data can be fitted to the Carter-Valensi rate expression. The overall reaction is found faster than the rate of formation of Na_2HfCl_6 but slower than that of Na_2ZrCl_6 , under similar reaction conditions. The product layer composition compares well with the thermodynamic predictions based on the assumption of an equilibrium surface reaction. This is in accordance with the proposed reaction mechanism. It would seem that the product composition in this case is governed solely by the thermodynamics of the exchange reaction



The kinetic parameters apparently do not influence the composition of the solid solution.

In view of the nature of the reaction mechanism for the reaction involving gas mixture it appears that the efficiency of separation of hafnium from zirconium through reaction of tetrachloride mixtures with solid sodium chloride cannot be improved by kinetic means. Perhaps this observation can be extended to reactions with other alkali halides also.

LIST OF REFERENCES

1. J.E. Dutrizac and S.N. Flengas: 'Advances in Ext. Met.', Inst. of Min. and Met., (1968) p 572
2. T.W. Wessel: Bur. of Mines, Bull. 585 (1960) 996
3. J.E. Dutrizac and S.N. Flengas: Canadian Patent No. 863258 (1971)
4. S. Majumdar and H.S. Ray: J. Appl. Chem. Biotechnol., 4 (1972) 565
5. I.S. Morozov and Sun In-Chzhu: Russ. J. Inorg. Chem., 4 (1959) 307
6. L.J. Howell, R.C. Sommer and H.H. Kellogg: Trans. AIME, Met. Soc., 209 (1957) 193
7. I.S. Morozov and B.G. Korshunov: Russ. J. Inorg. Chem., 1 (1956) 150
8. B.G. Korshunov and N.W. Gregory: Inorg. Chem., 3 (1964) 451
9. R.L. Lister and S.N. Flengas: Can. J. Chem., 43 (1965) 2947
10. G.J. Barton, R.J. Sheil and W.R. Grimes: 'Phase Diagrams of Nuclear Reactor Materials', O.R.N.L. 2548 (1959)
11. I.S. Morozov and Sun In-Chzhu: Russ. J. Inorg. Chem., 4 (1959) 1176
12. I.S. Morozov and L. Ya. Toptygin: Bull. Acad. Sc. USSR, Div. Chem. Sc., (1959) 1834
13. T. Moeller: 'The Chemistry of the Lanthanides', Reinhold, (1963) p 38
14. J.D. Kim and D.R. Spink: J. Chem. Engg. Data, 19 (1974) 36
15. N.P. Sajin and E.A. Pepelyaeva: Int. Conf. Peaceful uses of At. Energy, 18 (1956) 559
16. W. Fisher et al: Z. Anorg. Chem. 255 (1947) 79 and 256 (1948) 277
17. M. Becker, F. Endter, W. Neugebauer and H. Renner: Int. Conf. Peaceful uses of At. Energy, 4 (1958) 276
18. J. Huro and R. Saint James: ibid, 8 (1956) 551

19. M.Y. Farah and I.S. Yamani: *ibid*, 9 (1964) 131
20. B.A.J. Lister and L.A. McDonald: A.E.R.E.C/R703
21. K. Street Jr. and G.T. Seaborg: J. Am. Chem. Soc. 70 (1948) 4268
22. J.L. Hague and L.A. Machlan: J. Res. U.S. Natl. Bur. Std., 65A (1961) 75
23. M.L. Bromberg: U.S. Patent, 2, 852, 446 (Sept. 1958)
24. A. Niselson, J.L. Sokolora and V.I. Stolayerov: Dokl. Akad. Nauk. SSSR, 183 (1966) 1107
25. A.E. van Arkel and J.E. DeBoer: Dutch Patent 15390 (Feb. 1947)
26. D.M. Gruen and J.J. Katz: J. Am. Chem. Soc., 71 (1949) 3843
27. D.C. Bradley and W. Wardlaw: J. Chem. Soc., part 1 (1951) 280
28. F. Hudswell and J.M. Hutcheon: Int. Conf. Peaceful uses of At. Energy, 8 (1956) 563
29. I.E. Newnham: J. Am. Chem. Soc., 79 (1957) 5415
30. O.D. Frampton and J. Feldman: 'Progress in Separation and Purification', Ed. E.S. Perry, Interscience, (1968)
31. C.V. Sundaram and Braham Prakash: Int. Conf. Peaceful uses of At. Energy, 8 (1956) 554
32. J. Kroll, W.F. Hergert and L.A. Yerkes: J. Electrochem. Soc., 97 (1950) 305
33. H.W. Chandler: U.S. Patent, 3, 276, 862 (1966)
34. J.E. Dutrizac and S.N. Flengas: Can. J. Chem. 45 (1967) 2317
35. P. Pint and S.N. Flengas: *ibid*, 49 (1971) 2885
36. L.T. Lacey, J.H. Bowden and S. Basden: Ind. Engg. Chem. (Fund.), 4 (1965) 275
37. M. Ishida and C.Y. Wen: AIChE Jl., 14 (1968) 311
38. G. Narsimhan: Chem. Engg. Sci., 16 (1961) 7

39. A.W.D. Hills: 'Heat and Mass Transfer in Process Metallurgy', Inst. Min. and Met., (1967) p 39
40. A.W.D. Hills: 'Heterogeneous Kinetics at Elevated Temperatures', Ed. G.R. Belton and W.L. Worrel, Plenum, (1970) p 449
41. J. Shen and J.M. Smith: Ind. Engg. Chem. (Fund.), 4 (1965) 293
42. R.H. Spitzer, F.S. Manning and W.O. Philbrook: Trans. AIME, Met. Soc., 236 (1966) 726
43. R.E. Carter: J. Chem. Phys., 34 (1961) 2010
44. G. Valensi: Compt. Rend., 201 (1935) 602
45. J. Crank: Trans. Farad. Soc. 53 (1957) 1083
46. A.M. Ginstling and B.I. Brounshtein: J. Appl. Chem. (USSR, Eng.), 23 (1959) 1327
47. R.E. Carter: 'Ultrafine Particles', Ed. W.E. Kuhn, Wiley, (1963) p 419
48. W. Jander: Z. Anorg. Allgem. Chem., 163 (1927) 1
49. H.J. Engell and F. Wever: Acta Met., 5 (1957) 695
50. R.E. Carter and F.D. Richardson: Trans. AIME, Met. Soc., 203 (1955) 336
51. S.W. Kennedy, L.W. Calvert and M. Cohen: ibid, 215 (1959) 64
52. R. Hales and A.C. Hill: Corrosion Sci., 12 (1972) 843
53. W.W. Webb, J.T. Norton and C. Wagner: J. Electrochem. Soc., 103 (1956) 107
54. E.W. Haycock: ibid, 106 (1959) 771
55. P. Kofstad, P.B. Anderson and O.J. Krudtaa: J. Less Common Metals, 3 (1961) 89
56. P. Kofstad: J. Electrochem. Soc., 110 (1963) 491
57. W.W. Smeltzer, R.R. Haering and J.S. Kirkaldy: Acta Met., 9 (1961) 880
58. J.M. Perrow, W.W. Smeltzer and J.D. Embury: ibid, 16 (1968) 1209

59. K. Hauffe: 'Oxidation of Metals and Alloys', Plenum, (1965)
60. C. Wagner: Corrosion Sci., 13 (1973) 23
61. C. Wagner: 'Diffusion in Solids, Liquids and Gases', Ed. W. Jost, Academic Press, (1952) p 71
62. G.R. Wallwork, W.W. Smeltzer and C.J. Rosa: Acta Met., 12 (1964) 409
63. W.W. Smeltzer and M.T. Simand: ibid, 5 (1957) 328
64. J.D. Gadd and E.B. Evans: Corrosion, 17 (1961) 109
65. C. Wagner: Z. Physik, Chem., B21 (1933) 25
66. P. Kofstad: 'High Temperature Oxidation of Metals', John Wiley, (1966)
67. O. Kubaschewski and B.E. Hopkins: 'Oxidation of Metals and Alloys', Butterworth, (1967)
68. C. Wagner: Corrosion Sci., 9 (1969) 91
69. P. Mayer and W.W. Smeltzer: J. Electrochem. Soc., 119 (1972) 626
70. L.D. Dalvi and W.W. Smeltzer: ibid, 121 (1974) 386
71. W.W. Smeltzer: 'Oxidation of Metals and Alloys', American Society for Metals, (1971) p 115
72. K. Fueki and J.B. Wagner Jr.: J. Electrochem. Soc., 112 (1964) 384
73. D. Tretyakov and R.A. Rapp: Trans. AIME, Met. Soc., 242 (1969) 1235
74. M.L. Volpa and J. Reddy: J. Chem. Phys., 53 (1970) 1117
75. P. Kofstad: J. Electrochem. Soc., 109 (1962) 776
76. R.L. Meussner and C.B. Birchnall: Corrosion, 13 (1957) 677t
77. M. Cagnet and J. Moreau: Acta Met., 7 (1959) 427
78. S. Mrowec and T. Werber: ibid, 8 (1960) 819
79. S. Mrowec and T. Werber: ibid, 7 (1959) 696
80. H. Rickert: Z. Physik Chem. N.F., 23 (1960) 355

81. L.B. Pfeil: J. Iron and Steel Inst., 119 (1929) 501
82. J. Barden, W.H. Brattain and W. Shockley: J. Chem. Phys., 14 (1946) 714
83. R.L. Jarry, J. Fisher and W.H. Gunther: J. Electrochem. Soc., 110 (1963) 346
84. J.B. Holt and L. Himmel: *ibid*, 116 (1969) 1569
85. J. Benard: 'Oxidation of Metals and Alloys', American Society for Metals, (1971) p 1
86. R.J. Hussey and M. Cohen: Corrosion Sci., 11 (1971) 699
87. P. Kofstad: J. Inst. Metals, 90 (1961-62) 253
88. A.G. Gourset and W.W. Smeltzer: J. Electrochem. Soc., 120 (1973) 390
89. M.G. Cowgill and J. Stringer: J. Less Common Metals, 5 (1963) 233
90. B. Chattopadhyay and S. Sadigh-Esfandiary: Corrosion Sci., 13 (1973) 747
91. P. Kofstad and S. Espevik: J. Electrochem. Soc., 112 (1965) 153
92. G. Ehrlich: J. Phys. Chem. Solids, 1 (1956) 3
93. F.S. Petit and J.B. Wagner Jr.: Acta Met., 12 (1964) 41
94. F.S. Petit, R. Yinger and J.B. Wagner: *ibid*, 8 (1960) 617
95. E.T. Turkdogan, W.M. Mckewan and L. Zwell: J. Phys. Chem., 69 (1965) 327
96. A.A. Palko, A.D. Ryon and D.W. Kuhn: *ibid*, 62 (1958) 319
97. L.A. Niselson: Russ. J. Inorg. Chem., 7 (1962) 354
98. W.M. Mckewan: Trans. AIME, Met. Soc., 212 (1958) 791
99. K.L. Luthra: 'Kinetics of the Reaction of Zirconium Tetrachloride Vapours with Solid Sodium Chloride', M.Tech. Thesis, I.I.T., Kanpur, (1972)
100. D. Caplan, A. Harvey and M. Cohen: Corrosion Sci., 3 (1963) 161

101. K.J. Laidler: 'Catalysis, Vol. 1, Part 1', Ed. P.H. Emmet, Reinhold (1954) p 75
102. S.E. Khalafalla, C.W. Schultz and T.N. Rushton: U.S. Bur. Mines, R6699 (1965)
103. S.N. Flengas and P.Pint: Can. Met. Quart., 18, p 151
104. S.N. Flengas: Private communication.

APPENDIX I

BASIC KINETIC DATA

A. Formation of Na_2ZrCl_6 Run 3Weight of the sphere = 1.77144 gm Temperature = 450.5°C Radius of the sphere = 6.087 mm Pressure (ZrCl_4) = 1013 mm, Hg

Time hr	Weight gain gm	Time hr	Weight gain gm	Time hr	Weight gain gm
0.00	0.0000	15.50	0.6569	89.50	1.6420
0.75	0.0731	19.50	0.7065	92.00	1.6500
1.25	0.1300	25.50	0.8055	102.50	1.7628
2.00	0.1950	32.25	0.9624	113.50	1.8684
2.75	0.2195	40.00	1.0614	125.50	1.9578
3.25	0.2360	48.25	1.1439	136.50	2.0391
4.00	0.2855	51.25	1.2740	140.25	2.1528
5.50	0.3763	55.25	1.3060	152.25	2.1691
7.00	0.3928	64.00	1.3780	164.75	2.2016
9.00	0.4754	72.25	1.4900	177.50	2.2427
12.00	0.5579	79.50	1.5620	189.75	2.4177
				200.75	2.4497

solid. The migration of the chlorine ion vacancy appears to be the rate controlling step. The specific reaction rate constant for hafnium and zirconium case, which are found to be proportional to $1/2.13^{\text{th}}$ and $1/1.98^{\text{th}}$ power of the tetrachloride pressure at 450°C , respectively, compare well with the postulates of the reaction mechanism.

Although over the range of the reaction conditions employed, the reaction behaviour fully conforms to the postulates of the proposed reaction mechanism, there is some evidence to suggest that the mechanism may change with temperature due to accompanying change in the polymorphic form of the reaction product. Evidence in this regard, however, is available for the NaCl-HfCl_4 system only. The difference in the pressure dependence of the reaction rate in different phase regions (γ -phase in present work and δ -phase in Pint and Flengas' work) and abrupt change in the slope of the Arrhenius type plot of the rate constant with change in the polymorphic form of the product phase, as observed during the reaction with hafnium tetrachloride, suggests possibility of change in the reaction mechanism.

In view of the superposition of a number of temperature dependent parameters in the rate constant term, no indication regarding the activation energy of the reaction could be obtained from the temperature coefficient values. However, difference in the temperature coefficient values for reactions at different pressures in the $\text{ZrCl}_4\text{-NaCl}$ system is

Run 8 (a and b)

Weight of the sphere = 1.82421 gm Temperature = 451°C

Radius of the sphere = 6.089 mm Pressure (ZrCl_4) = 381 mm, Hg
(till 86.5 hrs.
= 520 mm, Hg
(from 95.5 hrs

Time hr	Weight gain gm	Time hr	Weight gain gm	Time hr	Weight gain gm
0.0	0.0000	37.5	0.8896	111.5	1.4766
1.5	0.1210	45.5	0.9348	123.5	1.6372
2.5	0.1511	52.5	1.0407	135.5	1.7366
3.5	0.2039	63.5	1.1478	147.5	1.8054
5.5	0.2792	70.5	1.2013	159.5	1.8972
7.5	0.4149	76.5	1.2395	171.5	1.9660
11.5	0.4525	86.5	1.3160	183.5	2.0422
16.5	0.5230	Pressure changed to 520 mm, Hg		195.5	2.1106
22.5	0.6108	95.5	1.3695	206.5	2.1409
27.5	0.7238	101.5	1.4460		

Run 14

Weight of the sphere = 1.82228 gm Temperature = 500°C

Radius of the sphere = 6.089 mm Pressure (ZrCl_4) = 734 mm, Hg

Time hr	Weight gain gm	Time hr	Weight gain gm	Time hr	Weight gain gm
0.0	0.0000	10.0	0.5389	42.5	1.1629
1.0	0.0473	14.5	0.6240	50.0	1.2858
2.0	0.1891	19.5	0.7658	58.0	1.3520
4.0	0.2836	25.5	0.8604	70.5	1.4938
7.0	0.4349	33.0	1.0116	79.0	1.6262

Run 18

Weight of the sphere = 0.78306 gm Temperature = 451°C

Radius of the sphere = 4.6141 mm Pressure (ZrCl_4) = 753 mm, Hg

Time hr	Weight gain gm	Time hr	Weight gain gm	Time hr	Weight gain gm
0.0	0.0000	12.0	0.3219	56.5	0.7058
1.0	0.0330	17.0	0.3879	65.5	0.7627
2.0	0.1073	23.5	0.4539	77.5	0.8196
3.0	0.1403	33.5	0.5433	89.5	0.8846
4.0	0.1898	42.5	0.6327	101.5	0.9333
7.5	0.2641	50.5	0.6652	112.5	0.9743

Run 9

Weight of the sphere = 0.34366gm Temperature = 450°C

Radius of the sphere = 3.303 mm Pressure (ZrCl_4) = 739 mm, Hg

Time hr	Weight gain gm	Time hr	Weight gain gm	Time hr	Weight gain gm
0.0	0.0000	20.0	0.2415	77.0	0.4829
1.0	0.0436	25.0	0.2723	88.0	0.5016
2.0	0.0626	31.0	0.3138	103.5	0.5339
4.0	0.1103	40.0	0.3605	113.5	0.5612
6.0	0.1307	47.0	0.3744	125.0	0.5799
10.0	0.1767	55.5	0.4072	144.0	0.6139
13.0	0.2108	65.5	0.4453	165.5	0.6343
16.0	0.2244	74.0	0.4693	171.0	0.6462

B. Formation of Na_2HfCl_6 Run 1Weight of the sphere = 1.78302 gm Temperature = 451°C Radius of the sphere = 6.058 mm Pressure (HfCl_4) = 945 mm, Hg

Time hr	Weight gain gm	Time hr	Weight gain gm	Time hr	Weight gain gm
0.0	0.0000	25.25	0.8680	68.75	1.5182
1.50	0.1065	28.00	0.9253	82.75	1.6585
3.00	0.2866	35.50	1.0646	94.75	1.7658
9.00	0.5568	42.50	1.1633	107.50	1.8731
13.00	0.6469	49.50	1.2541	119.50	1.9804
18.25	0.7452	58.75	1.3861	127.00	2.0217
21.25	0.7861				

Run 10Weight of the sphere = 1.75789 gm Temperature = 426.5°C Radius of the sphere = 6.075 mm Pressure (HfCl_4) = 933 mm, Hg

Time hr	Weight gain gm	Time hr	Weight gain gm	Time hr	Weight gain gm
0.0	0.0000	22.0	0.6496	76.0	1.2102
2.5	0.1914	25.5	0.7064	88.5	1.3083
3.5	0.2329	30.0	0.7958	101.0	1.3984
5.5	0.3162	40.5	0.8852	113.5	1.4639
8.5	0.3814	47.5	0.9502	126.5	1.5785
12.5	0.5033	54.5	1.0396	137.5	1.6277
17.0	0.5764	63.5	1.1046	150.0	1.7178

Run 11 (a and b)

Weight of the sphere = 1.83187 gm Temperature = 475°C
 (till 80.5 hrs.)
 Radius of the sphere = 6.044 mm = 500°C
 (from 90.5 hrs.)
 Pressure (HfCl_4) = 954 mm, Hg

Time hr	Weight gain gm	Time hr	Weight gain gm	Time hr	Weight gain gm
0.0	0.0000	67.5	1.6002	133.0	2.3773
2.5	0.3127	74.0	1.7158	140.5	2.4467
7.5	0.5156	80.5	1.7818	147.0	2.5160
10.5	0.6424	Temperature changed to 500°C		156.0	2.6807
15.0	0.7523	90.5	1.8809	166.0	2.7673
23.0	0.9383	94.0	1.9469	176.5	2.8280
29.0	1.0637	103.0	2.0480	182.5	2.8713
34.5	1.1380	113.0	2.1694	188.5	2.9320
43.5	1.2783	119.5	2.2387	198.5	3.0266
50.5	1.3774	123.0	2.2820	212.0	3.0769
57.5	1.4764				

Run 13

Weight of the sphere = 0.34962 gm Temperature = 450.5°C

Radius of the sphere = 3.236 mm Pressure (HfCl_4) = 963 mm, Hg

Time hr	Weight gain gm	Time hr	Weight gain gm	Time hr	Weight gain gm
0.0	0.0000	30.0	0.3793	93.5	0.6436
1.0	0.0614	35.0	0.4085	100.5	0.6662
2.0	0.0852	41.0	0.4464	108.0	0.6867
3.5	0.1190	47.0	0.4721	116.0	0.7085
7.0	0.1647	53.0	0.4877	130.5	0.7404
10.0	0.2188	59.0	0.5223	141.0	0.7622
16.0	0.2729	68.0	0.5640	153.0	0.7857
21.0	0.3192	75.0	0.5813	159.0	0.8025
25.0	0.3381	83.0	0.6142		

Run 19

Weight of the sphere = 0.78599 gm Temperature = 450.5°C

Radius of the sphere = 4.607 mm Pressure (HfCl_4) = 939 mm, Hg

Time hr	Weight gain gm	Time hr	Weight gain gm	Time hr	Weight gain gm
0.0	0.0000	23.25	0.4956	63.5	0.8161
1.5	0.1188	27.50	0.5411	72.0	0.8801
2.5	0.1383	35.0	0.6161	79.5	0.9201
4.5	0.2114	42.0	0.6753	87.5	0.9713
7.5	0.2927	50.5	0.7393	96.5	1.0081
11.0	0.3414	55.0	0.7681	109.5	1.0492
16.0	0.3958				

Run 16 (a and b)

Weight of the sphere = 1.82356 gm Temperature = 450.5°C

Radius of the sphere = 6.085 mm Pressure (HfCl_4) = 367 mm, Hg
(till 88.5 h
= 819 mm, Hg
(from 98.0 h

Time hr	Weight gain gm	Time hr	Weight gain gm	Time hr	Weight gain gm
0.0	0.0000	42.0	0.9357	105.0	1.5308
1.0	0.1415	49.5	1.0019	116.0	1.6247
2.0	0.1983	56.5	1.0869	125.5	1.7035
4.0	0.2928	65.5	1.1720	133.0	1.7561
7.0	0.3873	77.0	1.2619	141.5	1.8218
11.0	0.4819	88.5	1.3398	150.5	1.9062
16.5	0.5859	Pressure changed to 819 mm, Hg		157.5	1.9626
26.5	0.7372	98.0	1.4557	167.0	2.0283
33.5	0.8222				

Run 21

Weight of the sphere = 1.83282 gm Temperature = 450.0°C

Radius of the sphere = 6.09 mm Pressure (HfCl_4) = 510 mm, Hg

Time hr	Weight gain gm	Time hr	Weight gain gm	Time hr	Weight gain gm
0.0	0.0000	16.0	0.6591	41.5	1.0507
1.5	0.2197	20.0	0.7324	48.5	1.0916
4.0	0.3662	27.0	0.8707	55.5	1.1735
7.0	0.4557	32.0	0.9278	65.0	1.2881
12.0	0.5729				

Run 15 (a and b)

Weight of the sphere = 1.80890 gm Temperature = 450.5°C

Radius of the sphere = 6.059 mm Pressure (HfCl₄) = 752 mm, Hg
(till 90.5 hrs.)
= 939 mm, Hg
(from 98.5 hrs.)

Time hr	Weight gain gm	Time hr	Weight gain gm	Time hr	Weight gain gm
0.0	0.0000	33.0	0.9635	106.0	1.7502
1.0	0.1568	42.5	1.0853	114.5	1.8488
2.0	0.2476	49.5	1.1910	127.5	1.9463
4.0	0.3384	57.0	1.2885	138.0	2.0438
7.0	0.4622	67.0	1.4035	145.0	2.0844
11.0	0.5365	79.0	1.5273	153.0	2.1250
16.0	0.6851	90.5	1.6098	163.0	2.2144
21.0	0.7924	Pressure changed to 939 mm, Hg		175.5	2.3200
27.0	0.8822			186.5	2.3688

C. Reaction with gas mixture

Run 26

Weight of the sphere = 1.83384 gm Temperature = 450.5°C

Radius of the sphere = 6.098 mm Pressure (total) = 980 mm, Hg

 $W_{\alpha} = 3.982$ gm $P_{ZrCl_4} = 822$ mm, Hg $P_{HfCl_4} = 158$ mm, Hg

Time hr	Weight gain gm	Time hr	Weight gain gm	Time hr	Weight gain gm
0.0	0.0000	11.0	0.5327	49.0	1.1632
1.0	0.1042	17.0	0.6887	57.0	1.2683
2.0	0.2200	25.0	0.8640	66.0	1.3618
4.0	0.3474	33.0	0.9645	73.0	1.4319
8.0	0.4818	41.0	1.0697		

Run 27

Weight of the sphere = 1.82403 gm Temperature = 450°C

Radius of the sphere = 6.098 mm Pressure (total) = 674 mm, Hg

 $W_{\alpha} = 3.847$ gm $P_{ZrCl_4} = 536$ mm, Hg $P_{HfCl_4} = 138$ mm, Hg

Time hr	Weight gain gm	Time hr	Weight gain gm	Time hr	Weight gain gm
0.0	0.0000	24.0	0.7472	67.0	1.2826
1.0	0.1266	33.0	0.9143	73.0	1.3394
3.0	0.2745	41.5	1.0205	82.0	1.4305
6.0	0.3934	48.0	1.0934	91.0	1.4988
11.0	0.5184	54.5	1.1633	100.0	1.5747
16.0	0.6130				

W_{α} = Weight of solid reactant when entire solid has reacted
(See Eq. [5.2])

Run 4

Weight of the sphere = 1.81433 gm Temperature = 475.3°C

Radius of the sphere = 6.075 mm Pressure (ZrCl_4) = 753 mm, Hg

Time hr	Weight gain gm	Time hr	Weight gain gm	Time hr	Weight gain gm
0.00	0.0000	35.00	1.0553	118.5	1.9633
1.00	0.2127	39.50	1.1862	129.5	2.0533
2.50	0.2945	49.00	1.2353	136.0	2.0861
4.00	0.3927	60.25	1.4071	143.0	2.1597
7.00	0.4826	66.25	1.4807	153.75	2.2169
10.00	0.5726	73.00	1.5380	165.5	2.2987
14.00	0.6872	83.00	1.6525	177.5	2.3724
20.00	0.7853	91.75	1.7611	192.5	2.4951
26.00	0.9244	102.50	1.8325	203.5	2.5196

Run 5

Weight of the sphere = 1.76568 gm Temperature = 450°C

Radius of the sphere = 6.041 mm Pressure (ZrCl_4) = 257 mm, Hg

Time hr	Weight gain gm	Time hr	Weight gain gm	Time hr	Weight gain gm
0.00	0.0000	25.50	0.6377	90.50	1.2074
0.75	0.0607	30.50	0.6909	102.00	1.3138
1.75	0.1594	39.50	0.7820	114.00	1.3821

(Continued)

Run 30

Weight of the sphere = 1.82231 gm Temperature = 490°C

Radius of the sphere = 6.115 mm Pressure (total) = 980 mm, Hg

 $W_{\alpha} = 4.018$ gm $P_{ZrCl_4} = 822$ mm, Hg $P_{HfCl_4} = 158$ mm, Hg

Time hr	Weight gain gm	Time hr	Weight gain gm	Time hr	Weight gain gm
0.0	0.0000	18.0	0.8779	58.5	1.5354
1.5	0.2355	23.5	0.9702	69.0	1.6861
3.5	0.3824	34.5	1.2340	75.0	1.7558
6.5	0.5162	44.0	1.3527	82.5	1.8651
10.5	0.6688	50.5	1.4412	96.5	1.9970

APPENDIX II

Data and calculation: change in pore volume

Run no.	Sphere weight gm		Sphere radius mm		Pore volume, cm ³			Increase in pore volume per cent
	Initial	Unreacted core	Initial	Unreacted core	Initial	Unreacted core	Reacted layer + unreacted core	
21 (Hf)	1.83282	1.15377	6.0902	5.2832	0.09964	0.08477	0.01488	0.09965
16 (Hf)	1.82356	1.04244	6.0851	5.1623	0.10151	0.09478	0.00697	0.10175
20 (Zr)	1.84200	0.83629	6.0830	4.8412	0.09202	0.08906	0.00324	0.09230
24 (Zr)	1.80560	1.25754	6.0970	5.4642	0.11539	0.10259	0.01293	0.11552
19 (Hf)	0.78599	0.40608	4.6075	3.7803	0.04667	0.03871	0.00810	0.04681
27(Mixt.)	1.82403	1.07377	6.0987	5.1850	0.10769	0.08796	0.01975	0.10771
28(Mixt.)	1.85304	1.11877	6.1127	5.2350	0.10087	0.08423	0.01666	0.10089
29(Mixt.)	1.85072	1.10839	6.0971	5.2020	0.09458	0.07776	0.01685	0.09461
30(Mixt.)	1.82231	0.91248	6.1155	4.9310	0.11635	0.08078	0.03562	0.11640

Pore Volume = Volume x Porosity

$$\text{Porosity} = 1 - \frac{\text{Density (actual)}}{\text{Density (theoretical)}}$$

Sodium chloride density (theoretical,
used for porosity calculation) = 2.164 gm/cm³

Run 28

Weight of the sphere = 1.85304 gm Temperature = 424.8°C

Radius of the sphere = 6.112 mm Pressure (total) = 980 mm, Hg

 $W_{\alpha} = 3.927$ gm $p_{\text{ZrCl}_4} = 822$ mm, Hg $p_{\text{HfCl}_4} = 158$ mm, Hg

Time hr	Weight gain gm	Time hr	Weight gain gm	Time hr	Weight gain gm
0.0	0.0000	22.0	0.6989	70.0	1.2923
1.0	0.1820	31.0	0.8595	76.0	1.3519
3.0	0.2630	41.0	1.0078	85.0	1.4406
5.0	0.3242	47.0	1.0506	94.0	1.5125
9.0	0.4420	55.0	1.1424	100.5	1.5553
15.0	0.5918				

Run 29

Weight of the sphere = 1.85072 gm Temperature = 450°C

Radius of the sphere = 6.097 mm Pressure (total) = 787 mm, Hg

 $W_{\alpha} = 4.0221$ $p_{\text{ZrCl}_4} = 640$ mm, Hg $p_{\text{HfCl}_4} = 147$ mm, Hg

Time hr	Weight gain gm	Time hr	Weight gain gm	Time hr	Weight gain gm
0.0	0.0000	18.5	0.7022	58.0	1.2697
1.0	0.1044	25.0	0.8310	68.0	1.3737
2.0	0.1803	34.0	0.9672	73.0	1.4210
4.0	0.2941	43.5	1.0957	82.0	1.5060
7.0	0.4023	49.0	1.1657	95.0	1.6100
11.0	0.5409				